Detailed Kinetic Modelling of the Oxidation and Combustion of Large Hydrocarbons Using an Automatic Generation of Mechanisms

I N A U G U R A L - D I S S E R T A T I O N

zur
Erlangung der Doktorwürde
der
Naturwissenschaftlich – Matematischen
Gesamtfakultät
der
Ruprecht – Karls – Universität
Heidelberg

Vorgelegt von
Master Eng. Yuswan Muharam
aus Makasar, Indonesien

Tag der mündlichen Prüfung: 18.11.2005

Detailed Kinetic Modelling of the Oxidation and Combustion of Large Hydrocarbons Using an Automatic Generation of Mechanisms

Gutachter: Prof. Dr. Dr. h.c. Jürgen Warnatz
Prof. Dr. Olaf Deutschmann

ABSTRACT

A mechanism generator code to automatically generate mechanisms for the oxidation and combustion of large hydrocarbons has been successfully modified in this work. The modification was through:

(1) improvement of the existing rules such as cyclic-ether reactions and aldehyde reactions,
(2) inclusion of some additional rules to the code, such as ketone reactions, hydroperoxy cyclic-ether formations and additional reactions of alkenes,
(3) inclusion of small oxygenates, produced by the code but not included in the handwritten C_1-C_4 sub-mechanism yet, to the handwritten C_1-C_4 sub-mechanism.

In order to evaluate mechanisms generated by the code simulation of observed results in different experimental environments has been carried out. The simulation of auto-ignition of n-pentane in a rapid-compression machine shows good agreement with experimental results. Experimentally derived and numerically predicted ignition delays of n-heptane/air and n-decane/air mixtures in high-pressure shock tubes in a wide range of temperatures, pressures and equivalence ratios agree very well. Concentration profiles of the main products and intermediates of n-heptane, iso-octane and n-decane oxidation in jet-stirred reactors at a wide range of temperatures and equivalence ratios are generally well reproduced. Sensitivity and reaction flow analyses were performed for shock tube and jet-stirred reactor environments, respectively, in an attempt to identify the most important reactions under the relevant conditions of study. In addition, the ignition delay times of different normal alkanes was numerically studied.

Zusammenfassung

Ein Computerprogramm zum automatischen Erzeugen von Mechanismem für die Oxidation und Verbrennung von großen Kohlenwasserstoffen wurde in dieser Arbeit erfolgreich modifiziert. Zu den Veränderungen zählen:

(1) Verbesserung der existierenden Reaktionsregeln für z. B. Reaktionen von zyklischen Ethern und Aldehyden
(2) Implementierung von zusätzlichen Regeln in den Code, z. B. für Reaktionen der Ketone, für die Bildung von zyklischen Hydroperoxiethern und für zusätzliche Alkenereaktionen
(3) Ergänzung des C_1-C_4 Untermechanismus durch Einbeziehung kleiner oxygenierte Kohlenwasserstoffe, die vom neuen Programm automatisch erzeugt werden, bisher aber nicht im manuell erstellten C_1-C_4 Untermechanismus enthalten waren.

Zur Evaluierung der von diesem Code erzeugten Mechanismen wurden Ergebnisse aus verschiedenartigen Experimenten simuliert. Die Simulation der Selbstzündung von n-Pentane in einer schnellen Kompressionsmaschine zeigt eine gute Übereinstimmung mit den experimentellen Ergebnissen. Experimentell abgeleitete und numerisch vorhergesagte Zündverzögerungszeiten von n-Heptane/Luft und n-Dekan/Luft Mischungen in Hochdruckstoßrohren über einen weiten Temperatur- und Druckbereich sowie Mischungsverhältnis stimmen gut überein. Konzentrationsprofile der Haupt- und Zwischenprodukte der n-Heptane, iso-Oktan und n-Dekan Oxidation in Rührreaktoren werden über einen großen Temperatur- und Mischungsbereich gut wiedergegeben. Es wurden zudem Sensitivitäts- und Reaktionsflußanalysen für Stoßwellenmessungen und Rührreaktoren durchgeführt, um die wichtigsten Reaktionen unter den Bedingungen dieser Arbeit zu identifizieren. Zusätzlich wurden Zündverzögerungszeiten für verschiedene n-Alkane numerisch untersucht.

TABLE OF CONTENT

Chapter 1

INTRODUCTION

1.1 Background

Combustion includes a chemical reaction between substances and is usually accompanied by the generation of heat and light in the form of a flame. The rate at which the reactants react is high. This is because of the nature of the chemical reaction itself, and because more energy is generated than escaped into the surrounding medium, resulting in the temperature of the reactants is raised to accelerate the reaction.

The combustion of hydrocarbons is a complex process, which proceeds through a large number of elementary steps. The initial molecules of a hydrocarbon fuel react to yield a variety of reaction intermediates, which then undergo chemical transformations, and finally give the final products, i.e. carbon dioxide (CO_2) and water (H_2O). The overall mechanism of hydrocarbon combustion is complicated by the diversity of molecules and radicals involved.

The combustion process develops according to the chain mechanism of radicals. The chain branching is the main feature of the combustion process which is able to make the process self-accelerated. The behavior of the intermediates highly depends on the temperature. Therefore, the evolution of the combustion process is different at different temperatures. The operating chemical kinetic mechanism changes continuously with temperature.

Many practical combustion systems, such as spark-ignition, Diesel and gas turbine engines, operate in a wide range of operating condition. In the ignition process in a spark-ignition engine, for instance, the fuel/air charge enters the cylinder at nearly ambient condition, and in a transient process is compressed to 10 bar - 40 bar and unburned gas temperature of 1000 K - 1200 K.

There is continued interest in developing a better understanding of the oxidation and combustion of large hydrocarbons, which are more representative for practical fuels used in automotive engines, for a wide range of operating conditions. This interest is motivated by the need to improve the efficiency and performance of currently operating combustion systems, the fuel economy, and the need to reduce pollutant emission.

Detailed chemical kinetic models can be used to predict and analyse the formation of a wide spectrum of observed products, and to control physical processes such as flame speed and autoignition time.

A mechanism is a system consisting of a number of elementary chemical reactions with their rate coefficients determined by fundamental kinetic experiments or theoretical treatment. Detailed mechanisms are a centre feature of chemical kinetic models and developed as response to and validated by a set of experimental measurements. Consequently, the range of this experimental data set limits the range of applicability of the mechanisms. Extrapolation of detailed mechanisms from one regime to others is difficult and frequently inaccurate. For instance, due to the fact that the chain branching reactions and many pathways are different in the two regimes, the mechanisms for a shock tube model are not correct if applied for hydrocarbon oxidation at low temperatures. The best solution is that the range of mechanism validation is expanded to a maximum practical level by comparing it to a number of experimental data sets that permits to apply the so-called comprehensive mechanism in a wider range, providing a further knowledge that is not possible if directly obtained from experimental results.

Three regimes of combustion and oxidation of large hydrocarbons have been defined. The first regime occurs at low temperatures, including slow combustion, cool flames and the negative temperature coefficient (NTC) between 650 K and 750 K, in which the overall rate of the combustion process decreases with increasing temperature. The end of the NTC area is defined as the beginning of the intermediate regime. The third regime is combustion at higher temperatures, accompanied by hot flames. Ignition in two stages is characteristic for large hydrocarbons combustion, in which a cool flame stage yielding readily oxidizable products precedes a hot flame stage. It is important to have a detailed model that can predict the combustion and oxidation of hydrocarbons in all temperature regimes due to the fact that practical combustion systems operate at a wide range of conditions.

1.2 The Status of Chemical Kinetic Models for Large Hydrocarbons

Recent modeling studies of premixed systems such as stirred reactors and shock tubes have helped in the development of detailed chemical kinetic mechanisms describing the oxidation of large hydrocarbons as the primary reference fuels such as n-heptane and iso-octane, or as practical fuel models used in automotive engines.

1.2.1 Pentane

Ribaucour et al. [1] have developed a detailed mechanism of 975 reactions and 193 species based on a common skeleton scheme, which was used to simulate their experimental measurements on autoignition of n-pentane and 1-pentene in a rapid-compression machine between 600 K and 900 K at a pressure of 7.50 bar. This mechanism gives reasonable results for delay times.

Numerical simulations of the experiments in a rapid-compression machine for the autoignition of n-pentane were carried out using a detailed chemical kinetic reaction mechanism by Westbrook et al. [2]. The results are interpreted in terms of a low-temperature oxidation mechanism involving the addition of molecular oxygen to alkyl and hydroperoxyalkyl radicals.

Experiments in a rapid-compression machine were used by Ribaucour et al. [3] to examine the influence of variations in fuel molecular structures on the autoignition of all three possible isomers of pentane (neopentane, 2-methylbutane and n-pentane). Numerical simulations of the same experiments were carried out using a detailed chemical kinetic reaction mechanism.

An intermediate temperature combustion study of neopentane by Curran et al. [4] modelled the concentration profiles obtained during the addition of neopentane to slowly reacting mixtures of $H_2 + O_2 + N_2$ in a closed reactor at 753 K and 0.67 bar.

A detailed chemical kinetic reaction mechanism consisting of 1875 reactions among 390 species for the oxidation of neopentane was applied by Wang et al. [5] to reproduce experimental measurements taken in a flow reactor operating at a pressure of 8 bar in a temperature range of 620 K - 810 K.

Dagaut and Cathonnet [6] have studied the oxidation of neopentane experimentally and numerically in a perfectly stirred reactor operating at steady state at 1, 5 and 10 bar for equivalence ratios ranging from 0.25 to 2 and temperatures of 800 K - 1230 K. The mechanism consists of 746 reversible reactions and 115 species and gives good agreement between the experimental data and the modelling results.

Taconnet et al. [7] have modelled their experimental results on the oxidation of neopentane and iso-pentane in a jet-stirred reactor at 0.85 bar and 873 K by developing a generalized mechanism.

1.2.2 Hexane

Curran et al. [8] have studied the chemistry of all five isomers of hexane by comparing a detailed kinetic model with measurements of exhaust gases from a motored engine operated at a compression ratio just less than that required for autoignition. The relative ordering of the isomers with regard to critical compression ratios for ignition and the major intermediates produced are well reproduced by the model.

A chemical kinetic model comprising 386 reactions and 61 species has been used by Burcat et al. [9] to model their measurements of ignition delay times and product distributions in preignited n-hexane/O_2/Ar mixtures from 1020 K to 1725 K and 1 bar – 7 bar. The calculated results give moderate agreement with the experimental ones.

The ignition of 2-methyl-pentane has been modelled and compared to experiments of the ignition delay time in a shock tube by Burcat et al. [10] using 2-methyl-pentane in mixtures with oxygen diluted by argon.

1.2.3 Heptane

Westbrook et al. [11] have proposed a detailed mechanism consisting of 212 species and 765 elementary reactions to describe the oxidation of n-heptane, iso-octane and their mixtures over a wide range of operating conditions.

Chevalier et al. [12] have generated a mechanism consisting of 620 species and 2400 reactions by means of a computer program to calculate ignition delay times of the stoichiometic n-heptane/air mixture in a temperature range of 600 K - 1500 K. The results were in good agreement with the experimental measurements.

Chakir et al. [13] have extended a chemical kinetic reaction mechanism from previous studies on smaller hydrocarbons up to C_6 and C_7 species and used it to reproduce experimental data on the oxidation of n-heptane in a jet-stirred reactor in a temperature range of 950 K - 1200 K at atmospheric pressure for equivalence ratios ranging from 0.2 to 2.0.

Lindstedt and Maurice [14] have assembled a 659 reaction, 109 species mechanism for the combustion of n-heptane. The data from species profiles in counterflow diffusion flames [15], stirred reactors [13] and burning velocities in premixed flames [16] have been used to validate that mechanism.

A semi-detailed kinetic scheme for n-heptane oxidation has been developed by Ranzi et al. [17]. Both the low and high temperature primary mechanisms were reduced to a lumped kinetic model involving only a limited number of intermediate steps. This primary reaction scheme is flexible enough to predict accurately the intermediate components, the heat release and also ignition delay times.

Nehse et al. [18] have used a computer code to automatically generate the chemical kinetic mechanisms for n-heptane and n-decane to reproduce experimental measurements in high-pressure shock tubes for n-heptane oxidation [19] and n-decane oxidation [20].

Come et al. [21] have used a computer package to automatically generate the chemical kinetic mechanisms for n-heptane and iso-octane. The predictions of the models were compared with experimental results obtained in perfectly stirred reactors in the low- and high-temperature ranges [13, 22, 23].

A detailed chemical kinetic mechanism has been developed and used by Curran et al. [24] to study the oxidation of n-heptane in flow reactors [25, 26], a jet-stirred reactor [23, 27], shock tubes [19, 28, 29] and a rapid-compression machine [30].

Doute et al. [31] have elaborated a detailed reaction mechanism for n-heptane combustion and compared computed mole fraction profiles with observed ones in four premixed flames stabilized on a flat-flame burner at 0.06 bar in a wide range of equivalence ratios (0.7–2.0) [32].

A detailed reaction mechanism has been evaluated by El Bakali et al. [33] by comparison of computed species mole fraction profiles with experimental ones measured in a rich n-heptane/O_2/N_2 flame stabilized at atmospheric pressure. Good agreement was obtained for most molecular species, especially intermediate olefins, dienes and alkynes.

Seiser and co-workers [34] have studied extinction and autoignition of n-heptane in a counterflowing non-premixed system where transport processes are important, and modelled the results with a truncated version (consisting of 770 reversible reactions and 159 species) of a detailed model consisting of 2540 reactions and 555 species [24]. The truncated model was able to give a satisfactory reproduction of the data showing that high-temperature chemistry dominates the autoignition process in the counterflow flame.

High-temperature detailed chemical kinetic reaction mechanisms have been developed by Westbrook et al. [35] for all nine chemical isomers of heptane, following techniques and models developed previously for other smaller alkane hydrocarbon species. These reaction

mechanisms were tested by computing shock-tube ignition delay times for stoichiometric heptane/oxygen mixtures diluted by argon [36].

1.2.4 Octane

Come et al. [21] have used a computer package to automatically generate the chemical kinetic mechanisms for n-heptane and iso-octane. The predictions of the models were compared with experimental results obtained in perfectly stirred reactors in the low- and high-temperature ranges [13, 22, 23].

A semi-detailed kinetic scheme for iso-octane has been developed by Ranzi and coworkers [37]. This model was used to simulate the studies in a turbulent flow reactor [38], stainless steel and quartz jet-stirred reactors [23], rapid-compression machine and shock tube [39] covering the range from 550 to 1500 K and up to 40 bar.

A detailed chemical kinetic mechanism has been developed and used by Curran et al. [40] to study the oxidation of iso-octane in a jet-stirred reactor [23], flow reactors [26, 41], shock tubes [42] and in a motored engine [43].

Detailed modelling of the oxidation of n-octane and n-decane in the gas phase was performed by Glaude and coworkers [44] using computer-designed mechanisms. For n-octane, the predictions of the model were compared with experimental results obtained by Dryer and Brezinsky [38] in a turbulent plug flow reactor at 1080 K and 1 bar. The agreement between the computed and the experimental values is satisfactory both for conversions and for the distribution of the products.

A detailed chemical kinetic mechanism consisting of approximately 850 species and 3570 reactions was used by Chen et al. [41] to calculate their experiment results on the lean oxidation of iso-octane in the intermediate temperature regime at elevated pressures in a flow reactor.

1.2.5 Decane

Dagaut et al. [45] have modelled the oxidation of n-decane in a jet-stirred reactor at 10 bar from 550 to 1150 K at residence time of 0.5 and 1 s and for equivalence ratios of between 0.5 and 1.5. Their detailed mechanism gives a good description for species profiles at temperatures over 800 K, but does not match the data in the intermediate- to low-temperature regions.

A computer code has been used by Nehse et al. [18] to automatically generate the chemical kinetic mechanisms for n-heptane and n-decane. For n-decane the predictions of the model were compared with experimental results obtained by Pfahl et al. [20] in a high-pressure shock tube.

Doute et al. [46] have computed the chemical structure of a premixed n-decane/O_2/N_2 flame for an equivalence ratio of 1.7. The consumption of fuel molecule by H-atom abstraction and the reactions of decyl radicals are described in detail. The mechanism comprises 78 species involved in 638 reactions.

Detailed modelling of the oxidation of n-decane was carried out by Glaude et al. [44] with an automatically generated mechanism and compared with the jet-stirred reactor species profiles data of Bales-Gueret [47] obtained at temperatures of 922 K – 1033 K, residence times of 0.1 s – 0.25 s and atmospheric pressure.

Battin-Leclerc and co-workers [48] have simulated n-decane experiments performed in a jet-stirred reactor [47] and in a premixed laminar flame [49] from 550 to 1600 K. Their mechanism, generated automatically, included a massive 7920 reactions.

Zeppieri et al. [50] have developed a partially reduced mechanism for the oxidation and pyrolysis of n-decane validated against flow reactor, jet-stirred reactor [47] and n-decane/air shock tube ignition delay [20].

A chemical kinetic mechanism for the combustion of n-decane has been compiled and validated by Bikas and Peters [51] for a wide range of combustion regimes. Validation has been performed by using measurements on a premixed flame of n-decane, O_2 and N_2, stabilized at 1 bar on a flat-flame burner [46] as well as from experiments in shock waves [20], in a jet-stirred reactor [45] and in a freely propagating premixed flame [52]. The reaction mechanism features 600 reactions and 67 species including thermal decomposition of alkanes, H-atom abstraction, alkyl radical isomerization and decomposition for the high temperature range, and a few additional reactions at low temperatures.

1.2.6 Hexadecane

Ristori et al. [53] have reported a modeling study of gas-phase oxidation of n-hexadecane or cetane. This study was based on experiments performed in a jet-stirred reactor at 1 bar pressure at temperatures ranging from 1000 K to 1250 K and for equivalence ratios of 0.5, 1 and 1.5. The kinetic model features 242 species and 1801 reactions and gives reasonable

agreement with species profiles except for the parent fuel itself whose reactivity is underestimated.

Fournet et al. [54] have presented a detailed kinetic model, which was automatically generated by using a computer package. Their study was based on experiments performed in a jet-stirred reactor at temperatures ranging from 1000 K to 1250 K, 1 bar pressure, a constant mean residence time of 0.07 s and high degree of nitrogen dilution (0.03 mol-% of fuel) for equivalence ratios equal to 0.5, 1 and 1.5. The long linear chain of this alkane necessitates the use of a detailed secondary mechanism for the consumption of the alkenes formed as a result of primary parent fuel decomposition. This high temperature mechanism includes 1787 reactions and 265 species, featuring satisfactory agreement for the formation of products but still does not adequately account for the consumption of hexadecane.

1.3 Automatic Generation of Chemical Kinetic Mechanisms

To write detailed chemical kinetic mechanisms for the oxidation and combustion of large hydrocarbons for a wide range of temperatures and equivalent ratios, hundreds of elementary reactions have to be considered. Such large mechanisms have become difficult to write manually. Therefore, it is a convenient and rigorous way to write such large mechanisms by means of an automatic procedure, as showed by Tomlin et al. [55].

The Nancy group [21] has developed a system, named EXGAS, to generate automatically mechanism and relevant kinetic and thermochemical data to model the gas-phase oxidation and combustion of normal and branched alkanes, ethers and alkenes. The system provides reaction mechanisms made of three parts:

- A reaction base, including all the unimolecular or bimolecular reactions containing less than three carbon atoms (C_0-C_2 reaction base) and reactions of C_3-C_4 unsaturated hydrocarbons.
- A comprehensive primary reaction where only the initial organic molecule or mixture, oxygen and free radicals that appear in the mechanism are considered as reactants. The primary mechanism includes only elementary steps.
- A lumped secondary mechanism whose reactants are the lumped molecular products formed from the primary mechanism. The reactions of these lumped molecules are not elementary, but rather global reactions that produce molecules or radicals whose reactions are included in the C_0-C_2 reaction base. The secondary mechanism includes: degenerate branching reactions occurring first by breaking the bond between the two oxygen atoms of hydroperoxydes

and followed by subsequent decomposition of free radicals formed; reactions of aldehydes, alkanes, alcohols and epoxides, occurring first by an H-abstraction followed by subsequent decomposition; reactions of cyclic ether involving first an H-abstraction to give lumped radicals that can either decompose or react with oxygen; and additions of H, OH, CH_3 or HO_2 to alkenes.

Validation has been performed for the reference species like n-heptane [21], iso-octane [21], n-octane and n-decane [44] and n-hexadecane [54], but none of these had the success that might have been expected at temperatures lower than 900 K.

Green et al. [56] have developed computer methods to construct chemical kinetic models for the combustion, oxidation and pyrolysis of hydrocarbons including the generated reactions, the molecular properties and the rate parameters by a variety of quantum- and group-additivity based techniques. They also have developed computer methods for modelling the pressure dependence (fall-off and chemical activation) of gas-phase reactions.

A computer code named MOLEC, which can generate automatically mechanisms for the combustion and oxidation of large hydrocarbons, has been developed in the Warnatz group [57, 64]. This system is based on simple rules, which appear from a very limited number of different types of reactions in the combustion and oxidation of large hydrocarbons. The most important types of reactions are:

- decomposition of hydrocarbons (e.g. alkanes, alkenes),
- H-atom abstraction by reactive radicals (e.g. O, H, OH, HO_2, CH_3),
- β-scission of radicals,
- internal H-atom abstraction (isomerization),
- addition to molecular oxygen,
- O-O bond scission,
- radical addition to a double bond.

The rate coefficients of these types of reactions for hydrocarbons with more than four carbon atoms can be classified. They depend on

- the radicals abstracting a H atom from alkanes, alkenes, aldehydes, ketones or cyclic ethers (e.g. O, H, OH, HO_2, CH_3),
- the type of H atom being abstracted (primary, secondary or tertiary),
- the number of available equivalent H atoms,
- the size of the intermediate ring structures (5-, 6-, 7- or 8-membered).

Starting from elementary reactions between molecular reactants (fuel and oxygen), the decompositions, rearrangements and additions, which generate new species, are automatically evaluated. Due to the fact that the reaction mechanisms for the C_1-C_4 hydrocarbons already exists and that the rate coefficients of small species strongly depend on the chain length, the code considers only the reactions of species larger than C_4. The method of the MOLEC program is based on representation of molecules as binary trees and pattern matching. As a supporting system LISP is used because of its flexibility concerning the data structure, algorithm development and availability of a user interface design.

The C_5-C_{fuel} sub-mechanism produced automatically by the code has to be coupled to the handwritten C_1-C_4 sub-mechanism to compose a detailed mechanism for fuel oxidation, which is then solved numerically.

1.4 Objectives

It is obvious that MOLEC can give a very detailed chemical kinetic mechanism since no simplification of the secondary mechanism (as defined by the Nancy Group) is considered. However, mechanisms provided by MOLEC were only able to reproduce experimental flame speeds and ignition delay times [12, 18]. Therefore, the main objective of this work is to modify the code so that the formation of a wide spectrum of observed products can be predicted and analyzed. The way to achieve this objective was through:

(1) improvement of the existing rules such as cyclic-ether reactions and aldehyde reactions,
(2) inclusion of some additional rules to the code, such as ketone reactions, hydroperoxy cyclic-ether formations and additional reactions of alkenes,
(3) inclusion of small oxygenates, produced by the code but not included in the handwritten C_1-C_4 sub-mechanism yet, to the handwritten C_1-C_4 sub-mechanism.

The additional objectives of this work are to use mechanisms automatically generated by this code to reproduce experimental measurements in a rapid-compression machine [1], jet-stirred reactors [23, 27, 45], shock tubes [19, 20, 29], to predict and analyze the ignition delay times of C_5-C_{10} normal alkanes and to carry out sensitivity and reaction flow analyses on each set of experimental results.

1.5 The Outline of the Dissertation

This dissertation consists of seven chapters. An introduction concerning the background, the status of chemical kinetic models and the automatic generation of chemical kinetic mechanism is given in Chapter 1.

Chapter 2 describes the chemical kinetics of combustion processes. Chapter 3 discusses all reaction rules known to be pertinent to both low- and high- temperature kinetics and considered in the MOLEC code.

Chapter 4 describes briefly the implementation of rule-oriented programming to automatically generate reaction mechanisms. And finally, prior to the conclusion chapter, Chapters 5 and 6 discuss the mechanism validation and the mechanism analyses, respectively.

Chapter 2

CHEMICAL KINETICS

Chemical reactions occur when molecules of one species collide with molecules of another species and, for some of these collisions, one or more new molecules will be created. In the chemical reaction the atoms of reacting molecules are redistributed in the new molecules. To achieve this, the reacting molecules must have sufficient kinetic energy so that their chemical bonds can be broken during the impact and other bonds can be formed. As the energy of these bonds depends on the nature of the atoms and on geometrical factors, the energy content of the products of the collision may be different from the energy content of the colliding molecules. This is the basis for heat being released or absorbed in chemical reactions [58].

For the combustion reaction of methane (CH_4), the following reaction occurs:

$$CH_4 + 2O_2 \rightarrow CO_2 + 2H_2O. \qquad 2.1$$

This equation indicates that the process of combustion of 1 mol of CH_4 and 2 moles of O_2 will produce, if complete, 1 mol of CO_2 and 2 mol of H_2O. However, this is an overall process or a global reaction. In actual molecular collisions, the number of molecules of reactants colliding at the same time to produce the number of molecules of products is not the same as indicated by the global reaction. In an actual combustion process, many bonds have to be broken (e.g. between C and H in the CH_4 molecule) and many bonds have to be formed (e.g. between H and O in H_2O). The colliding molecules will not have enough kinetic energy to achieve that much bond reshuffling required by Equation 2.1. However, the following three reactions occur at a molecular level,

$$CH_4 + O \rightarrow CH_3 + OH \qquad 2.2$$
$$CH_4 + H \rightarrow CH_3 + H_2 \qquad 2.3$$
$$CH_4 + OH \rightarrow CH_3 + H_2O. \qquad 2.4$$

For example, Reaction 2.2 involves breaking one C-H bond and forming an O-H bond. These reactions, 2.2 to 2.4, are examples of elementary reactions, i.e., reactions that can occur in the event of a molecular collision. The overall combustion process will consist of

hundreds or thousands of such elementary reactions and many species and radicals appear. The series of elementary reactions that comprises the overall reaction process is called a reaction mechanism or a detailed chemical mechanism.

Only a brief overview of the aspects of chemical kinetics is summarised in this chapter. Detailed descriptions can be found in literature [58-62].

2.1 Rate Laws of Global Reactions

All chemical reactions take place at a definite rate which depends on the conditions of the system. The most important of these conditions are the concentration of the reactants, the temperature and the presence of a catalyst or inhibitor. The rate of reaction may be expressed in terms of the concentration of any of the reacting substances or of any reaction product; i.e., the rate may be expressed as the rate of decrease of the concentration of a reactant or the rate of increase of a reaction product. For an arbitrary global reaction

$$\mathrm{A + B + C + \ldots \xrightarrow{k} D + E + F + \ldots,} \qquad 2.5$$

where A, B, C, … denote the different species involved in the reaction, a rate law describes an empirical formulation of the reaction rate, i.e., the rate of formation or consumption of a species in a chemical reaction. Looking at the consumption of species A, the reaction rate can be expressed as

$$\frac{\mathrm{d[A]}}{\mathrm{d}t} = -k[\mathrm{A}]^a[\mathrm{B}]^b[\mathrm{C}]^c \ldots\ldots \qquad 2.6$$

Here [A], [B], [C], … are the concentrations of species A, B, C, …, respectively, in mol/cm^3, with a, b, c, … being reaction orders with respect to those species and k being the reaction rate coefficient. The sum of all exponents is the overall reaction order. The amount of the products does not affect $\mathrm{d[A]}/\mathrm{d}t$. The reaction rate coefficient k is specific to the global reaction. It is not a function of the reactant concentrations.

In some cases, one or more species exist in excess in a reaction system so that their concentrations do not change noticeably. If, for instance, [B], [C], … remain approximately constant during the reaction, an effective rate coefficient can be generated

from the rate coefficient and the near constant concentrations of the species in excess. Using $k_{\mathrm{eff}} = k[\mathrm{B}]^b[\mathrm{C}]^c \ldots$, a simplified version of Equation 2.6 can be obtained

$$\frac{\mathrm{d}[\mathrm{A}]}{\mathrm{d}t} = -k_{\mathrm{eff}}[\mathrm{A}]^a . \qquad 2.7$$

The temporal change of the concentration of species A can be calculated by integrating this differential equation, as it will be shown next for some typical cases.

For first-order reactions (a = 1), integration of Equation 2.7 yields the first-order time behavior

$$\ln \frac{[\mathrm{A}]_t}{[A]_0} = -k_{\mathrm{eff}}(t - t_0), \qquad 2.8$$

where $[\mathrm{A}]_0$ and $[\mathrm{A}]_t$ denote the concentration of species A at time t_0 and t, respectively.

Similarly, for second-order reactions (a = 2) the temporal behaviour below can be obtained

$$\frac{1}{[\mathrm{A}]_t} - \frac{1}{[\mathrm{A}]_0} = k_{\mathrm{eff}}(t - t_0). \qquad 2.9$$

For third-order reactions (a = 3) the temporal behaviour is

$$\frac{1}{[\mathrm{A}]_t^2} - \frac{1}{[\mathrm{A}]_0^2} = 2k_{\mathrm{eff}}(t - t_0). \qquad 2.10$$

If the time behaviour is measured, the reaction order can be determined. Logarithmic plots of the concentrations versus time for first-order reactions lead to linear dependences with the slope $-k_{\mathrm{eff}}$ and plots of $1/[\mathrm{A}]_t$ versus time for second-order reactions lead to linear dependences with the slope k_{eff}, as shown in Fig. 2.1. A similar treatment is possible for other integer reaction orders a.

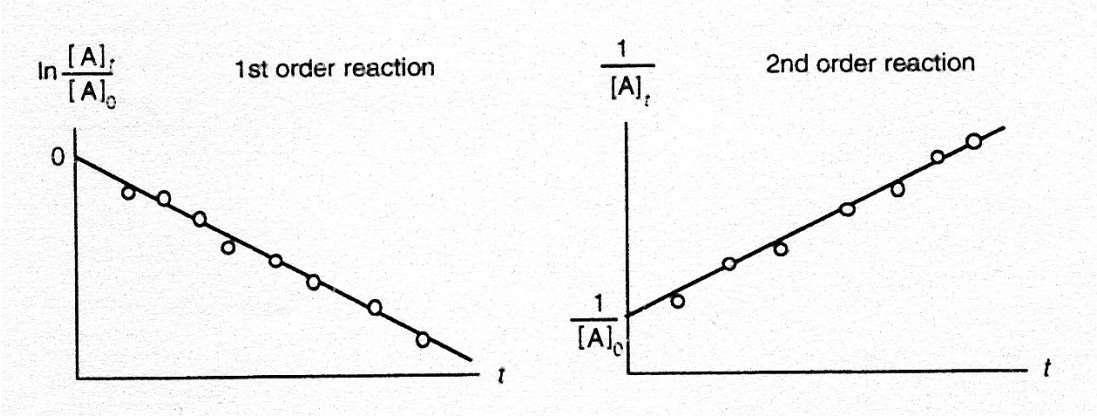

Fig. 2.1. Time behaviour of the concentration for first- and second-order reactions [59]

Very complicated rate laws are frequently found in chemical kinetics. The reaction orders are usually not integers. They can be negative, depending on time and reaction conditions. An extrapolation to conditions where no experimental measurements exist is not reliable or even be completely wrong. In many cases, a mechanistic interpretation of non-elementary rate laws is not possible.

2.2 Elementary Reactions

As has been described above, an elementary reaction occurs at a molecular level exactly in the way described by the chemical reaction equation.

2.2.1 The law of mass action

The law of mass action states that the rate of disappearance of a chemical species is proportional to the product of the concentrations of the reacting chemical species, where each concentration is raised to a power equal to the corresponding stoichiometric coefficient. It is valid only for elementary reactions. Consider a generic elementary reaction

$$a_1R_1 + a_2R_2 + a_3R_3 + ... + a_mM \rightarrow b_1P_1 + b_2P_2 + b_3P_3 + ... + b_MM \qquad 2.11$$

between reactants R_1, R_2, R_3, …, from which products P_1, P_2, P_3, …, are formed. M is an example of species that appears on both sides. The rates of reactant consumption and product formation are given by:

$$\frac{\mathrm{d}[\mathrm{R}_1]}{\mathrm{d}t} = -a_1 r, \quad \frac{\mathrm{d}[\mathrm{R}_2]}{\mathrm{d}t} = -a_2 r, \quad \frac{\mathrm{d}[\mathrm{R}_3]}{\mathrm{d}t} = -a_3 r, \ldots \qquad 2.12$$
$$\frac{\mathrm{d}[\mathrm{P}_1]}{\mathrm{d}t} = b_1 r, \quad \frac{\mathrm{d}[\mathrm{P}_2]}{\mathrm{d}t} = b_2 r, \quad \frac{\mathrm{d}[\mathrm{P}_3]}{\mathrm{d}t} = b_3 r, \ldots$$
$$\frac{\mathrm{d}[M]}{\mathrm{d}t} = b_M r - a_M r$$

with r being the reaction rate

$$r = k[\mathrm{R}_1]^{a_1}[\mathrm{R}_2]^{a_1}[\mathrm{R}_3]^{a_3}\ldots. \qquad 2.13$$

The parameter k is the reaction rate coefficient and $[R_1]$, $[R_2]$, $[R_3]$, … are the concentrations of reactant R_1, R_2, R_3, …, respectively in mol/cm^3. Equation 2.11 is a statement of the stoichiometry of the reaction: every a_1 mol of R_1 is joined by a_2 mol of R_2, a_3 mol of R_3 etc., to produce simultaneously b_1 mol of P_1, b_2 mol of P_2, b_3 mol of P_3 etc.. So the amount of R_1 that has reacted is related to how much R_2, R_3 etc. have reacted and Equation 2.12 describes this relationship. If a species M appears in both the reactants and the products, then the multiplicity of r is the difference (b_M-a_M). If $b_M = a_M$, then M is called a third body. It may not be altered, but its presence is crucial for the success of the reaction, as it provides energy to, or takes energy away from, the collisions between the reactants.

2.2.2 Types of elementary reactions

Elementary reactions can be classified according to the number of reactant molecules participating. For a generic elementary reaction

$$a_1\mathrm{R}_1 + a_2\mathrm{R}_2 + a_3\mathrm{R}_3 + \ldots + a_\mathrm{m}\mathrm{M} \rightarrow b_1\mathrm{P}_1 + b_2\mathrm{P}_2 + b_3\mathrm{P}_3 + \ldots + b_\mathrm{M}\mathrm{M} \qquad 2.11$$

the reaction is of overall order (a_1+a_2+a_3+…), while it is of order a_1 with respect to reactant R_1, etc. The overall order is also called molecularity. Depending on the molecularity, we have the following types of elementary reactions:

1. Unimolecular reactions:

$$\mathrm{R}_1 \rightarrow b_1\mathrm{P}_1 + b_2\mathrm{P}_2 + \ldots \qquad 2.14$$

This reaction is an idealization, since molecules normally do not disintegrate spontaneously. For that to happen, a collision with another molecule is necessary (which, by the way, makes the reaction effectively second-order). The rate is first-order and is given by $r = -k[\mathrm{R}_1]$, and k has units (1/s).

2. Bimolecular reactions:

$$\mathrm{R}_1 + \mathrm{R}_2 \rightarrow b_1\mathrm{P}_1 + b_2\mathrm{P}_2 + \ldots \qquad 2.15$$

This is the most common reaction in combustion since the collision probability where there are only two molecules present is highest. The rate is second-order and given by $r = -k[\mathrm{R}_1][\mathrm{R}_2]$, where k has units $(\mathrm{mol/cm^3})^{-1}\ \mathrm{s^{-1}}$.

3. Trimolecular reactions:

$$\mathrm{R}_1 + \mathrm{R}_2 + \mathrm{R}_3 \rightarrow b_1\mathrm{P}_1 + b_2\mathrm{P}_2 + \ldots \qquad 2.16$$

The probability that three molecules will collide simultaneously is small, but nevertheless third-order reactions are very important. Radical recombination reactions, for example, between OH and H to produce water, will take place only if a third body, M, participates in the collision and hence these are third-order reactions. A third body is needed because recombination reactions are exothermic and the third body must absorb some of this energy. The reaction rate is third-order and is given by $r = -k[\mathrm{R}_1][\mathrm{R}_2][\mathrm{R}_{31}]$, where k has units $(\mathrm{mol/cm^3})^{-2}\ \mathrm{s^{-1}}$.

2.2.3 Forward and backward reactions

Many elementary reactions can proceed in both directions, i.e. to the right and to the left. Hence the products can become reactants and vice versa. The specific reaction rates will, in general, be very different. Elementary reaction equations that are both forward and backward are written with a two-direction arrow. For example, the reaction

$$a_1R_1 + a_2R_2 \overset{k}{\longleftrightarrow} b_1P_1 + b_2P_2 \qquad 2.17$$

means that this is equivalent to the mechanism

$$a_1R_1 + a_2R_2 \xrightarrow{k_f} b_1P_1 + b_2P_2 \qquad 2.18$$

$$b_1 P_1 + b_2 P_2 \xrightarrow{k_b} a_1 R_1 + a_2 R_2 \qquad 2.19$$

that gives

$$\frac{\mathrm{d}[\mathrm{R}_1]}{\mathrm{d}t} = -a_1 k_f [\mathrm{R}_1]^{a_1} [\mathrm{R}_2]^{a_2} + a_1 k_b [\mathrm{P}_1]^{b_1} [\mathrm{P}_2]^{b_2} . \qquad 2.20$$

Both reaction rate coefficients (k_f and k_b) must be prescribed, but they are related through the equilibrium constant of the reaction.

2.3 Temperature Dependence of Rate Coefficients

The reaction rate coefficient is given by the Arrhenius law

$$k = A' \exp\left[-\frac{E_a}{RT} \right] \qquad 2.21$$

where A' is the pre-exponential factor and E_a is the activation energy. These quantities come from experiments or from statistical mechanics calculations. As mentioned above, not all molecular collisions will result in reaction, but only those with kinetic energy higher than the energy needed to break the bonds of the reactant molecules. This energy barrier is the activation energy. Its maximum value corresponds to the bond energies in the molecule. In dissociation reactions, for instance, the activation energy is approximately equal to the bond energy being broken. The value of activation energy may also be much smaller or even zero. The proportion of collisions occurring between molecules that have kinetic energy higher than E_a is given by $\exp(-E_a/RT)$.

Since most elementary binary reactions exhibit Arrhenius behaviour over modest ranges of temperature, the temperature dependence can usually be incorporated with sufficient accuracy into the exponential alone. However, for the large temperature ranges found in combustion, “non-Arrhenius” behaviour of the rate coefficient tends to occur, particularly for processes that have a small energy barrier. Therefore, it is necessary to adopt a modified Arrhenius form which expresses the impact of temperature on the rate coefficient

$$k = AT^n \exp\left[-\frac{E_a}{RT}\right] \qquad 2.22$$

where the power of T accounts for a temperature dependence of the pre-exponential factor, A'.

2.4 Pressure Dependence of Rate Coefficients

The apparent dependence of rate coefficient of dissociation (unimolecular) and recombination (bimolecular) reactions on pressure is an indication that these reactions are not elementary. They are, in fact, a sequence of reactions. In the simplest case, the pressure dependence can be understood using the Lindemann model. According to this model, a unimolecular decomposition is only possible if the energy in the molecule is sufficient to break the bond. Therefore, it is necessary that, for the decomposition reaction to proceed, energy must be added to the molecule by collision with other molecules, M (e.g., for the excitation of the molecular vibrations). The excited molecule may then, depending on the strength of the excitation, decompose into the products, or it may subsequently deactivate through a second collision,

$$\mathrm{A} + \mathrm{M} \xrightarrow{k_a} \mathrm{A}^* + \mathrm{M} \qquad \text{(activation)} \qquad 2.23$$

$$\mathrm{A}^* + \mathrm{M} \xrightarrow{k_{-a}} \mathrm{A} + \mathrm{M} \qquad \text{(deactivation)} \qquad 2.24$$

$$\mathrm{A}^* \xrightarrow{k_u} \mathrm{P(roducts)} \qquad \text{(unimolecular reaction)} \qquad 2.25$$

where A* is the excited molecule, k_a, k_{-a} and k_u are the rate coefficients of the activation, deactivation and unimolecular reactions, respectively. The rates of these sequences of reactions are

$$\frac{\mathrm{d}[\mathrm{P}]}{\mathrm{d}t} = k_u[\mathrm{A}^*] \qquad 2.26$$

and

$$\frac{\mathrm{d}[\mathrm{A}^*]}{\mathrm{d}t} = k_a[\mathrm{A}][\mathrm{M}] - k_{-a}[\mathrm{A}^*][\mathrm{M}] - k_u[\mathrm{A}]. \qquad 2.27$$

Assuming that the concentration of the reactive intermediate A* is in a quasi-steady state

$$\frac{\mathrm{d}[\mathrm{A}^*]}{\mathrm{d}t} \approx 0\,, \tag{2.28}$$

one can obtain

$$[\mathrm{A}^*] = \frac{k_\mathrm{a}[\mathrm{A}][\mathrm{M}]}{k_{-\mathrm{a}}[\mathrm{M}] + k_\mathrm{u}} \tag{2.29}$$

and

$$\frac{\mathrm{d}[\mathrm{P}]}{\mathrm{d}t} = \frac{k_\mathrm{u} k_\mathrm{a}[\mathrm{A}][\mathrm{M}]}{k_{-\mathrm{a}}[\mathrm{M}] + k_\mathrm{u}}\,. \tag{2.30}$$

Two extremes of reaction, at very low and at very high pressure, can be distinguished from Equation 2.30. In the low-pressure range, the concentration of the collision partners M is very small and $k_{-\mathrm{a}}[\mathrm{M}] << k_\mathrm{u}$. Therefore, an apparent second-order rate law is obtained

$$\frac{\mathrm{d}[\mathrm{P}]}{\mathrm{d}t} = k_\mathrm{a}[\mathrm{A}][\mathrm{M}]. \tag{2.31}$$

The reaction rate is now proportional to the concentrations of species A and the collision partner M, because the activation is slow (i.e. rate limiting) at low pressures.

In the high-pressure range, the concentration of the collision partner M is large and $k_{-\mathrm{a}}[\mathrm{M}] >> k_\mathrm{u}$. This gives an apparent first order rate law

$$\frac{\mathrm{d}[\mathrm{P}]}{\mathrm{d}t} = \frac{k_\mathrm{u} k_\mathrm{a}}{k_{-\mathrm{a}}}[\mathrm{A}] = k_\infty[\mathrm{A}]. \tag{2.32}$$

Here the reaction rate does not depend on the concentration of the collision partners, because at high pressures collision occurs very often and, thus, the decomposition of the activated molecule A* is rate-limiting instead of the activation.

The Lindemann mechanism illustrates the fact that reaction orders of complex (non-elementary) reactions depend on the conditions chosen. However, the Lindemann mechanism itself is a simplified model.

If the rate law of a unimolecular reaction is written as $\mathrm{d}[\mathrm{P}]/\mathrm{d}t = k_\mathrm{a}[\mathrm{A}]$, then the rate coefficient k depends on pressure and temperature. The theory of unimolecular reactions yields fall-off curves, which describe the pressure dependence of k for different temperatures. The logarithm of the rate coefficient is usually plotted versus the logarithm of the pressure.

Typical fall-off curves are shown in Fig. 2.2. At very high pressures, $k = k_\mathrm{u}k_\mathrm{a}[\mathrm{M}]/(k_{-\mathrm{a}}[\mathrm{M}] + k_\mathrm{u})$ tends to the limit k_∞, i.e., the rate coefficient becomes independent of the pressure. At very low pressure, the rate coefficient k is proportional to [M] = p/RT, resulting in a linear dependence. Similarly, if the effective activation energy is low, the reaction rate coefficient k will decrease with temperature.

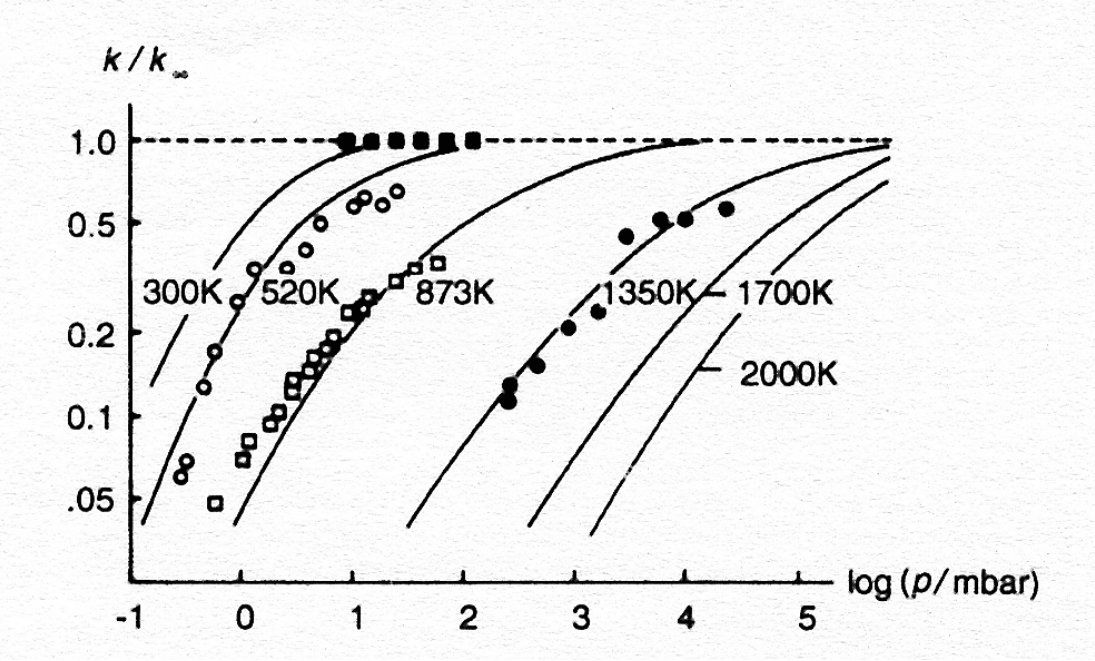

Fig. 2.2. Fall-off curves for unimolecular reaction $C_2H_6 \rightarrow CH_3 + CH_3$ [60].

Figure 2.2 shows that the fall-off curves for unimolecular reactions highly depend on temperature, and that the rate coefficients show different temperature dependence at different values of the pressure.

2.5 Thermodynamics and Kinetics

In a reaction proceeding in both forward and backward directions, equilibrium is dynamic. The rates of both directions are the same so that the equilibrium concentrations are maintained. For the following arbitrary reaction

$$A + B \leftrightarrow C + D, \tag{2.33}$$

this relationship occurs at equilibrium

$$\frac{r_f}{r_b} = \frac{k_f [A]_{eq} [B]_{eq}}{k_b [C]_{eq} [D]_{eq}} = 1, \tag{2.34}$$

where r_f and r_b are the rates of the forward and backward reactions and the subscript eq refers to equilibrium. Therefore

$$\frac{k_f}{k_b} = \frac{[C]_{eq} [D]_{eq}}{[A]_{eq} [B]_{eq}}, \tag{2.35}$$

$$\frac{k_f}{k_b} = K_{11}, \tag{2.36}$$

where K_{11} is the equilibrium constant.

A reaction rate is sometimes easier to measure in one direction than another. For example, the recombination of methyl radicals to form ethane

$$CH_3 + CH_3 \xrightarrow{k_2} C_2H_6, \tag{2.37}$$

has been studied over a wide range of temperatures and pressures. The backward decomposition reaction is important in high temperature processes, such as combustion, and there is considerable interest in the value of k_{-2}. The decomposition rate has been measured, but it is difficult to make such measurements over a wide range of temperatures. The rate coefficients are constant (at a given T and P) and do not change as equilibrium is approached. Therefore, it is possible to use the measured values of k_2 and the equilibrium constant K_2 to calculate the value of the dissociation rate coefficient k_{-2}.

$$k_{-2} = \frac{k_2}{K_2}. \qquad 2.38$$

Generally, the rate coefficients have concentration units so that K_2 in Equation 2.38 is K_c. This K_c can be converted to K_p (a equilibrium constant which is expressed in term of equilibrium pressures) through

$$K_c = \frac{K_p}{p^{\mathrm{O}} RT}, \qquad 2.39$$

where p^{O} is a standard pressure, and Equation 2.38 becomes

$$k_{-2} = \frac{k_2}{\left(\frac{K_P}{p^{\mathrm{O}} RT}\right)}. \qquad 2.40$$

Using the relationship between K_p / p^{O} and the change in standard Gibbs energy of reaction, ΔG^{O}

$$\Delta G^{\mathrm{O}} = -RT \ln \frac{K_p}{p^{\mathrm{O}}} \qquad 2.41$$

and the relationship between ΔG^{O} and the change in standard enthalpy and entropy of reaction, ΔH^{O} and ΔS^{O}

$$\Delta G^{\mathrm{O}} = \Delta H^{\mathrm{O}} - T\Delta S^{\mathrm{O}}, \qquad 2.42$$

the following equation can be obtained

$$k_{-2} = k_2 RT \exp\left(\frac{\Delta H_T^{\mathrm{O}}}{RT}\right) \exp\left(-\frac{\Delta S_T^{\mathrm{O}}}{R}\right). \qquad 2.43$$

where ΔH_T^{O} and ΔS_T^{O} are the standard enthalpy and entropy of reaction at temperature T:

$$\Delta H_T^{\mathrm{O}} = \Delta H_{fT}^{\mathrm{O}}(\mathrm{C_2H_6}) - 2\Delta H_{fT}^{\mathrm{O}}(\mathrm{CH_3}) \qquad 2.44$$

$$\Delta S_T^{\mathrm{O}} = S_T^{\mathrm{O}}(\mathrm{C_2H_6}) - 2S_T^{\mathrm{O}}(\mathrm{CH_3}) \qquad 2.45$$

where $\Delta H_{fT}^{\mathrm{O}}$ and S_T^{O} are the molar standard enthalpy of formation and the molar third law entropy of the respective species at temperature *T*.

2.6 Reaction Mechanisms

If many elementary reactions take place, the net amount of reactant consumed or product produced will come from adding the contribution of each elementary reaction. For a mechanism composed of elementary reactions 2.2 to 2.4 above, the rate of consumption of CH_4 and the rate of formation of CH_3 are

$$\frac{\mathrm{d}[\mathrm{CH_4}]}{\mathrm{d}t} = -k_1[\mathrm{CH_4}][\mathrm{O}] - k_2[\mathrm{CH_4}][\mathrm{H}] - k_3[\mathrm{CH_4}][\mathrm{OH}] \qquad 2.46$$

$$\frac{\mathrm{d}[\mathrm{CH_3}]}{\mathrm{d}t} = k_1[\mathrm{CH_4}][\mathrm{O}] + k_2[\mathrm{CH_4}][\mathrm{H}] + k_3[\mathrm{CH_4}][\mathrm{OH}] \qquad 2.47$$

In general, species will participate in some reactions as reactants and in others as products. The overall consumption or production rate will be the net outcome of all the elementary reactions.

For a mechanism composed of *R* elementary reactions of *S* species, which is given by

$$\sum_{s=1}^{S} \nu_{rs}^{(\mathrm{e})} \mathrm{A}_s \xrightarrow{k_r} \sum_{s=1}^{S} \nu_{rs}^{(\mathrm{p})} \mathrm{A}_s \,, \qquad 2.48$$

where $r = 1, 2, \ldots, R$, $\nu_{rs}^{(\mathrm{e})}$ and $\nu_{rs}^{(\mathrm{p})}$ denote stoichiometric coefficients of reactants and products, respectively, the rate of formation of a species *i* is given by addition over the total of the rate equations in where species *i* is involved,

$$\left(\frac{\partial c_i}{\partial t}\right)_{\mathrm{chem}} = \sum_{r=1}^{R} k_r \left(\nu_{ri}^{(\mathrm{p})} - \nu_{ri}^{(\mathrm{e})}\right) \prod_{s=1}^{S} c_s^{\nu_{rs}^{(\mathrm{e})}} \,, \qquad 2.49$$

where $i = 1, 2, \ldots, S$.

2.6.1 Chain reactions

Hydrocarbon combustion occurs through chain reactions, i.e., processes of yielding products that initiate further processes of the same kind, a self-sustaining sequence. The reactions below are examples of chain reactions.

$$H_2 + M \rightarrow H + H + M \quad (2.50)$$
$$O_2 + H \rightarrow O + OH \quad (2.51)$$
$$HO_2 + H \rightarrow OH + OH \quad (2.52)$$
$$H + OH + M \rightarrow H_2O + M \quad (2.53)$$

Reaction 2.50 is a chain-initiating reaction, in which a reactive intermediate is formed through the action of an agent such as heat or molecular oxygen. Reaction 2.51 is a chain-branching reaction producing more radicals. Reaction 2.52 is a chain-propagating reaction, in which the radicals may change identity, but the number of radicals does not change. Reaction 2.53 is a chain-terminating reaction, in which the radicals are consumed and the chain terminates.

Chain reactions are crucial for combustion. Flames would not be self-sustaining if the chemistry did not have this property. With chain reactions, the reaction rate may grow exponentially and this may lead to explosions. In a normal flame, this does not happen because heat is removed from reaction zone by diffusion or convection, and due to consumption of the fuel.

2.6.2 Analysis of reaction mechanisms

Detailed reaction mechanisms for hydrocarbon combustion may consist of several thousand elementary reactions. However, many of these reactions are unimportant and can be neglected. Thus, analysis methods, which eliminate negligible reactions, are of interest. Several methods can be used. Sensitivity analysis identifies the rate-limiting reaction steps. Reaction flow analysis determines the characteristic reaction paths. The information obtained by these methods can be used to eliminate unimportant reactions and thus generate a simplified, or reduced, reaction mechanism.

1. Sensitivity analysis

The rate laws for a reaction mechanism consisting of R reactions among S species can be written as a system of first order ordinary differential equations,

$$\frac{\mathrm{d}c_i}{\mathrm{d}t} = F_i(c_1, ..., c_S; k_1, ..., k_R),\ i = 1, 2, ..., S \qquad 6.54$$
$$c_i = c_i^0 \text{ at } t = t_0$$

The time t is the independent variable, the concentration c_i of species i are the dependent variables, and k_r, the parameters of the system; c_i^0 denotes the initial condition.

Here only the rate coefficients of the chemical reactions taken into account are considered as parameters of the system; nevertheless, initial concentration, pressure, etc. can also be treated as system parameters, if desired. The solution of the differential equation system 6.54 depends on the initial conditions as well as on the parameters.

For many elementary reactions, a change in the parameters of the system (the rate coefficients) has nearly no effect on the time-dependent solution. Even if the reaction is included explicitly in the mechanism, it does not need a highly accurate rate coefficient. On the other hand, for a few of the elementary reactions, changes in the rate coefficients have really large effects on the outcome of the system. Accordingly, accurate rate coefficients are demanded. These few important reaction steps are rate-determining steps or rate-limiting steps.

The dependence of the solution c_i on the parameters k_r is called sensitivity. Absolute sensitivity ($E_{i,r}$) and relative sensitivity ($E_{i,r}^{\mathrm{rel}}$) can be defined as

$$E_{i,r} = \frac{\partial \mathrm{c}_i}{\partial k_r} \text{ and} \qquad 6.55$$

$$E_{i,r}^{\mathrm{rel}} = \frac{k_r}{c_i}\frac{\partial \mathrm{c}_i}{\partial k_r} = \frac{\partial \ln c_i}{\partial \ln k_r} \qquad 6.56$$

2. Reaction flow analysis

Reaction flow analysis calculates the percentage of the contributions of different reactions to the formation or consumption of chemical species. An example of a reaction flow analysis is given in Table 2.1.

Table 2.1. Schematic illustration of the output of a reaction flow analysis

Reaction	Species					
	1	**2**	**3**	**…**	***S*-1**	***S***
1	20%	3%	0	…	0	0
2	0	0	0	…	0	0
3	2%	5%	0	…	100%	90%
.	.	.	.		.	.
.	.	.	.		.	.
.	.	.	.		.	.
***R*-1**	78%	90%	100%	…	0	5%
R	0	2%	0	…	0	0

In this example, 20% of the formation of species 1 can be attributed to Reaction 1, 2% to Reaction 3 and 78% to Reaction *R*-1. The total percentage of all contribution has to be 100%. Such a table allows the construction of instructive reaction flow diagrams.

Chapter 3

REACTION RULES

Although detailed chemical kinetic mechanisms of large hydrocarbons contain several hundred species taking part in thousands of elementary reactions, only a very limited number of different types of reactions appear. Building on this observation, it is possible to formulate all possible reactions taking place in the combustion and oxidation of large hydrocarbons along with their rate coefficients using simple rules. Each rule represents a particular type of reaction. Due to lack of data, we use the same reaction rate coefficients for analogous occurrences in different molecules. Thus, the rate coefficients for abstraction of a tertiary H atom by OH radical will be exactly the same for 2-methyl butane, 2-methyl pentane, 3-methly pentane or iso-octane, because all of the molecules contain a tertiary H atom (Fig. 3.1).

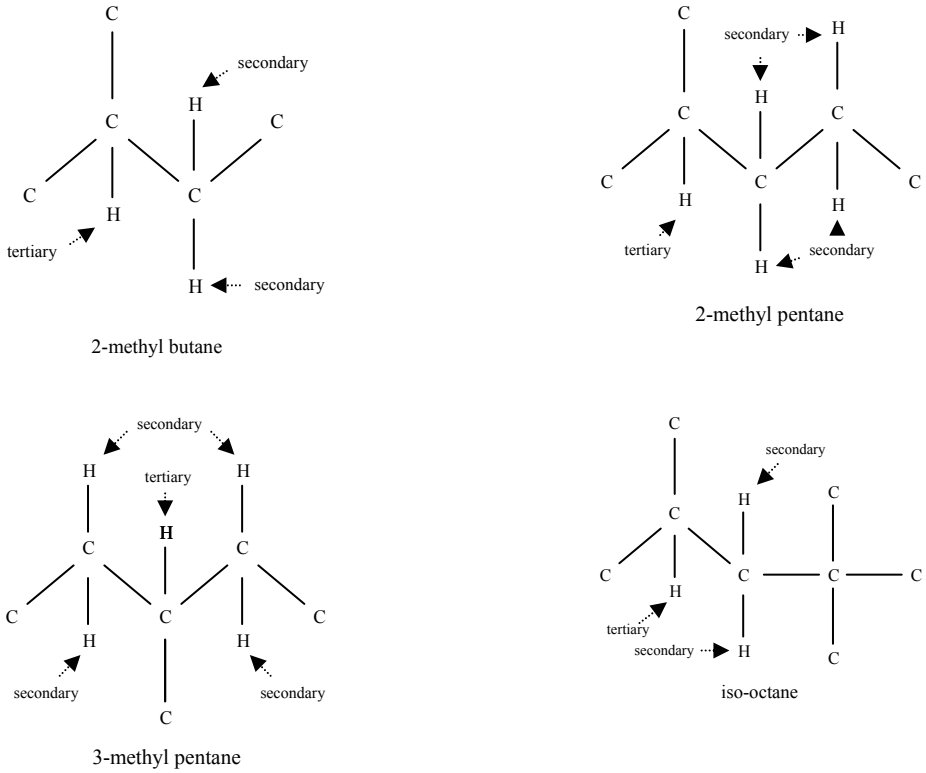

Fig. 3.1. Secondary and tertiary H atoms of 2-methyl butane, 2-methyl pentane, 3-methyl pentane and iso-octane.

In the same line, the total rate coefficient of secondary H-atom abstraction by OH radical in 2-methyl pentane and 3-methyl pentane is twice those of 2-methly butane and iso-octane, since 2-methyl pentane and 3-methyl pentane contain 4 H atoms at secondary sites, while 2-methly butane and iso-octane contain just 2 of such H atom.

We organize the reaction into two groups: low-temperature and high-temperature reactions. The naming conventions and the arrow symbols used in the description of each rule below are as follow:

- R denotes alkyl radicals or C_nH_{2n+1} structures,
- R' denotes C_nH_{2n} species or structures,
- R″ denotes C_nH_{2n-1} species or structures,
- $\rightarrow$ denotes irreversible reactions and
- $\leftrightarrow$ reversible reaction.

All rate coefficients of each type of reaction and the corresponding references are summarized in Appendix 1.

3.1 High-Temperature Reactions

Reaction rules 3.1.1-3.1.19 are sufficient to simulate many high temperature applications of the oxidation and combustion of alkanes and alkenes.

3.1.1 Unimolecular decomposition of alkanes

Unimolecular decomposition of an alkane serves as initiation reaction and consists of two reaction rules, one producing two alkyl radicals and another yielding one alkyl radical and one H atom,

$$RH \rightarrow R^{\bullet} + R^{\bullet}, \qquad 3.1$$

$$RH \rightarrow R^{\bullet} + H^{\bullet}. \qquad 3.2$$

The rate coefficients are taken from previous studies [12, 18].

These reactions describe the breaking of a covalent bond to form two radicals, and they are kinetically sensitive to the stability of the radicals involved, because the highly exothermic

reverse reaction, i.e. radical-radical combination, is not kinetically activated (in the absence of steric effects), i.e. $E_{\text{reverse}} = E_{\text{c}} \approx 0$.

Since multiple paths are available for this type of reaction, the path that involves cleavage of the weakest chemical bond is expected to be the fastest path. In this light, C-H bonds are typically stronger than C-C bonds, and the relative strength of C-H and C-C bonds is in the order primary > secondary > tertiary.

3.1.2 Abstraction of H atoms from alkanes

Abstraction of an H atom is one of the types of elementary radical reaction in which one radical is consumed while another is formed. This reaction is a cleavage of a C-H bond by hydrogen transfer to an abstracting radical. At both low and high temperature, H-atom abstraction from alkanes takes place, leading to the formation of alkyl radicals,

$$RH + X \rightarrow R^{\bullet} + XH, \qquad 3.3$$

where X represents active radicals.

The rate coefficients depend on the abstracting radicals, the type of H atom being abstracted (primary, secondary or tertiary) and the number of equivalent H atoms in the fuel. Tertiary, secondary, primary H atom is the energetically favoured sequence, since the tertiary C-H bond energy is lower than that of secondary C-H, which in turn is lower than that of primary C-H atoms.

Besides small active radicals such as H, O, OH, HO_2 and CH_3, we consider also alkylperoxy radicals, whose formation will be discussed in 3.2.1, as radical capable to abstract H atoms from alkanes. The code includes all alkylperoxy radicals produced during the course of reaction. It covers primary, secondary and tertiary sites of the peroxy group. In our kinetic models for hydrocarbon oxidation, however, we consider only alkylperoxy radicals having fuel structure, since at lower temperatures their concentration is fairly high to affect the overall reaction rate.

The code considers also H-atom abstraction by large alkyl radicals as suggested by Curran et al. [24] and Fournet et al. [54]. Three types of alkyl radicals, i.e. primary, secondary and tertiary alkyl radicals, are included. For the same reason as discussed above, only the radicals with fuel structure are taken into account in all our models.

H-atom abstraction from a fuel molecule via molecular oxygen attack serves as initiation reaction. At low temperature, this reaction is rather slow because of the fairly high activation energy (> 167 kJ/mol). However, since the radical R will start a chain, an initiation reaction occurs.

3.1.3 Decomposition of alkyl radicals

Decomposition of alkyl radicals occurs by breaking a bond in β position to the radical site (β scission) to regenerate the abstracting radicals and to produce molecules with a double bond involving the carbon atom that had been the radical centre. Two pathways are considered in our code; the first producing alkenes and H atoms, and the second yielding smaller alkenes and small alkyl radicals,

$$R^{\bullet} \rightarrow R' + H, \qquad 3.4$$

$$R^{\bullet} \rightarrow \text{small } R' + \text{small } R^{\bullet}. \qquad 3.5$$

Decomposition of alkyl radical is only important at relatively high temperatures (T > 900 K), as at low temperature addition of alkyl radicals to molecular oxygen is faster than β scission. This is because the decomposition of alkyl radicals has a relatively high activation energy, while addition of alkyl radicals to molecular oxygen has no energy barrier.

3.1.4 Isomerization of alkyl radicals

Isomerization of alkyl radicals is one of several possible pathways for alkyl radical reactions. In this reaction, the alkyl radical transfers an H atom from one site to the radical site, yielding a new radical site at the position at which the transferred H atom was initially located,

$$R_1^{\bullet} \rightarrow R_2^{\bullet}. \qquad 3.6$$

The rate coefficients depend on the ring strain energy barrier involved, described in terms of the number of atoms in the transition state ring structure (including H atoms), the type of H atom being abstracted (primary, secondary or tertiary) and the number of available equivalent H atoms.

3.1.5 Oxidation of alkyl radicals to form alkenes

Reaction of an alkyl radical with oxygen proceeds through many reaction channels. Most of these channels can be represented by addition of alkyl radicals to molecular oxygen to produce alkylperoxy radicals (Rule 3.2.1), which has no energy barrier. Rule 3.1.5 is effectively irreversible and has a significant activation energy to lead to the formation of conjugate alkenes and HO_2 radicals,

$$R^{\bullet} + O_2 \rightarrow R' + HO_2. \qquad 3.7$$

The rate coefficients depend on the type of H atom transferred to molecular oxygen and the number of available equivalent H atoms.

With increasing temperature within an intermediate regime ($750 < T < 900$), reaction of alkyl radicals with O_2 to produce alkylperoxy radicals proceeds in the reverse direction and that to produce alkenes accelerates, so that alkene yields increase.

3.1.6 Decomposition of alkenes

Decomposition of alkenes occurs through many reaction pathways. Due to its relatively low activation energy (approximately 290 kJ/mol), however, only decomposition leading to the formation of allylic radicals has been considered,

$$R' \rightarrow \text{allylic } R'' + \text{small } R^{\bullet}. \qquad 3.8$$

The rate coefficients have been taken from previous studies [12, 18].

3.1.7 Abstraction of allylic H atoms

Abstraction of H atoms from alkenes is a new reaction included in our code. Three types of H-atom abstraction from alkenes, which depend on the type of abstractable H atoms (Fig. 3.2), are considered. The first one is abstraction of allylic H atoms. Hydrogen atoms, which are connected to a carbon atom next to a double bond, are called allylic H atoms. They can be primary, if connected to a carbon atom linked to two other H atoms, secondary, if connected to a carbon atom linked to one other H atom and tertiary, if connected to a carbon atom linked to no other H atom. Abstraction of an allylic H atom leads to the formation of a resonance-stabilized radical. This radical undergoes β scission to yield, for instance, 1-3-butadiene,

$$R' + X \rightarrow \text{allylic } R'' + XH, \qquad 3.9$$

where X represents active radicals.

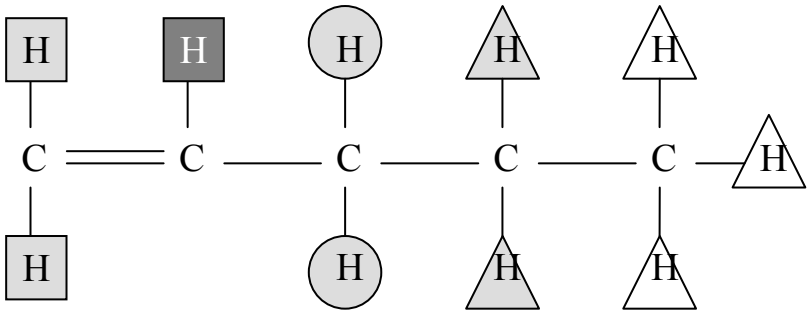

Fig. 3.2. *Different types of abstractable H atoms in the 1-pentane molecule. Triangles represent alkylic H atoms, circles allylic H atoms and square vinylic H atoms; white backgrounds indicate primary H atoms, grey backgrounds secondary H atoms, and black backgrounds tertiary H atoms.*

.

The rate coefficients depend on the type of allylic H atom and the number of available equivalent H atoms.

3.1.8 Abstraction of vinylic H atoms

Vinylic H atoms are hydrogen atoms connected to a carbon atom of a double bond. There are only two types of vinylic H atom: secondary if connected to a carbon atom linked to one other H atom, tertiary if connected to a carbon atom linked to no other H atom. Abstraction of a vinylic H atom leads to the formation of a vinylic radical, which in turn will undergo decomposition to produce, for instance, acetylene or allene. This H-atom abstraction is more difficult than the previous one,

$$R' + X \rightarrow \text{vinylic } R'' + XH. \qquad 3.10$$

The rate coefficients depend on the type of vinylic H atom and the number of available equivalent H atoms.

3.1.9 Abstraction of alkylic H atoms

This is the third type of H-atom abstraction from alkenes. H atoms connected to a carbon atom linked to two other H atoms are primary. H atoms connected to a carbon atom linked

to one other H atom are secondary. If no other H atom is linked to a carbon atom, to which an H atom is connected, that H atom is called tertiary. This H-atom abstraction plays a significant role in case of long alkenes and leads to the formation of specific products observed experimentally, such as dialkene (e.g. C_5H_8),

$$R' + X \rightarrow \text{alkenyl } R'' + XH. \qquad 3.11$$

Since alkylic H atoms are at the site far from a double bond, the double bond affects only a small portion of the molecule, the rest of which remains paraffinic in character. Thus, the rate coefficients related to H-atom abstraction from alkanes will be used in case of H-atom abstraction from alkenes to form alkenyl radicals and depend on the type of H atom being abstracted and the number of available equivalent H atoms.

3.1.10 Addition of H atoms to double bonds

Radical addition to double bonds is significantly exothermic. We consider addition of H atoms to a double bond as the reverse reaction of alkyl radical decomposition at the β position to the radical site (Rule 3.1.3),

$$R' + H \rightarrow R^{\bullet}. \qquad 3.12$$

3.1.11 Addition of CH_3 radicals to double bonds

Addition of a CH_3 radical to a double bond in alkenes is considered as the reverse reaction of alkyl radical decomposition (Rule 3.1.3),

$$R' + CH_3 \rightarrow R^{\bullet}. \qquad 3.13$$

3.1.12 Addition of O atoms to double bonds

Addition of an O atom to a double bond in alkenes is a new reaction in our code. This reaction leads to the formation of a ketyl radical and a small alkyl radical,

$$R' + O \rightarrow \text{ketyl radical} + \text{small } R^{\bullet}. \qquad 3.14$$

3.1.13 Addition of OH radicals to double bonds

A like 3.1.12, addition of an OH radical to a double bond in alkenes is a new reaction in our code. This reaction leads to the formation of an aldehyde or a ketone,

$$R' + O \rightarrow \text{aldehyde or ketone + small } R^{\bullet}. \qquad 3.15$$

3.1.14 Addition of HO_2 radicals to double bonds

Addition of HO_2 to a double bond in an alkene leads to the formation of a hydroperoxy alkyl radical, R′OOH, which in turn will decomposes to form a cyclic ether, an aldehyde or a ketone,

$$R' + HO_2 \rightarrow R'OOH. \qquad 3.16$$

3.1.15 Retro-ene reactions

A retro-ene reaction, which is a 1,5-hydrogen shift reaction followed by dissociation, is a new reaction included in our code. It leads to the formation of two small alkenes,

$$R' \rightarrow \text{small } R' + \text{small } R'. \qquad 3.17$$

An example of this reaction is of the reaction of 1-heptene which will produce 1-butene and propene.

The rate coefficients based on the results presented by Richard et al. [63] are used for this reaction.

3.1.16 Isomerization of alkenyl radicals

Isomerization of alkenyl radicals, which is a new reaction in our code, gives resonance-stabilized allylic radicals. The fastest isomerization is that involving cyclic transition states containing five or six atoms [54]. At 1100 K the isomerization of alkenyl radicals to give allylic radicals is about 5-10 times faster than β scission,

$$\text{alkenyl } R'' \rightarrow \text{allylic } R''. \qquad 3.18$$

3.1.17 Decomposition of allylic radicals

Decomposition of allylic radicals occur by breaking a bond in β position to the radical site (β scission). This leads to the formation of dialkenes, for instance, 1,3-butadiene and 1,3-pentadiene,

$$\text{allylic } R'' \rightarrow \text{dialkene.} \qquad 3.19$$

3.1.18 Decomposition of vinylic radicals

Decomposition of vinylic radicals occur through two pathways: breaking a bond in β position to the radical site (β scission) to produce dialkenes, or to yield alkynes,

$$\text{vinylic } R'' \rightarrow \text{dialkene or alkyne.} \qquad 3.20$$

3.1.19 Decomposition of alkenyl radicals

Besides isomerization, another alkenyl radical reaction is its decomposition. The decomposition becomes significant if isomerization of the alkenyl radical is not possible, because, e.g., the alkene is short. This decomposition occurs through β scission giving dialkenes and alkyl radicals, or alkenes and smaller alkenyl radicals,

$$\text{Alkenyl } R'' \rightarrow \text{dialkene} + \text{small } R^{\bullet}, \text{ or} \qquad 3.21$$

$$\text{Alkenyl } R'' \rightarrow \text{small } R' + \text{smaller alkenyl } R''. \qquad 3.22$$

All reaction pathways at high temperature are schematically summarized in Fig. 3.3.

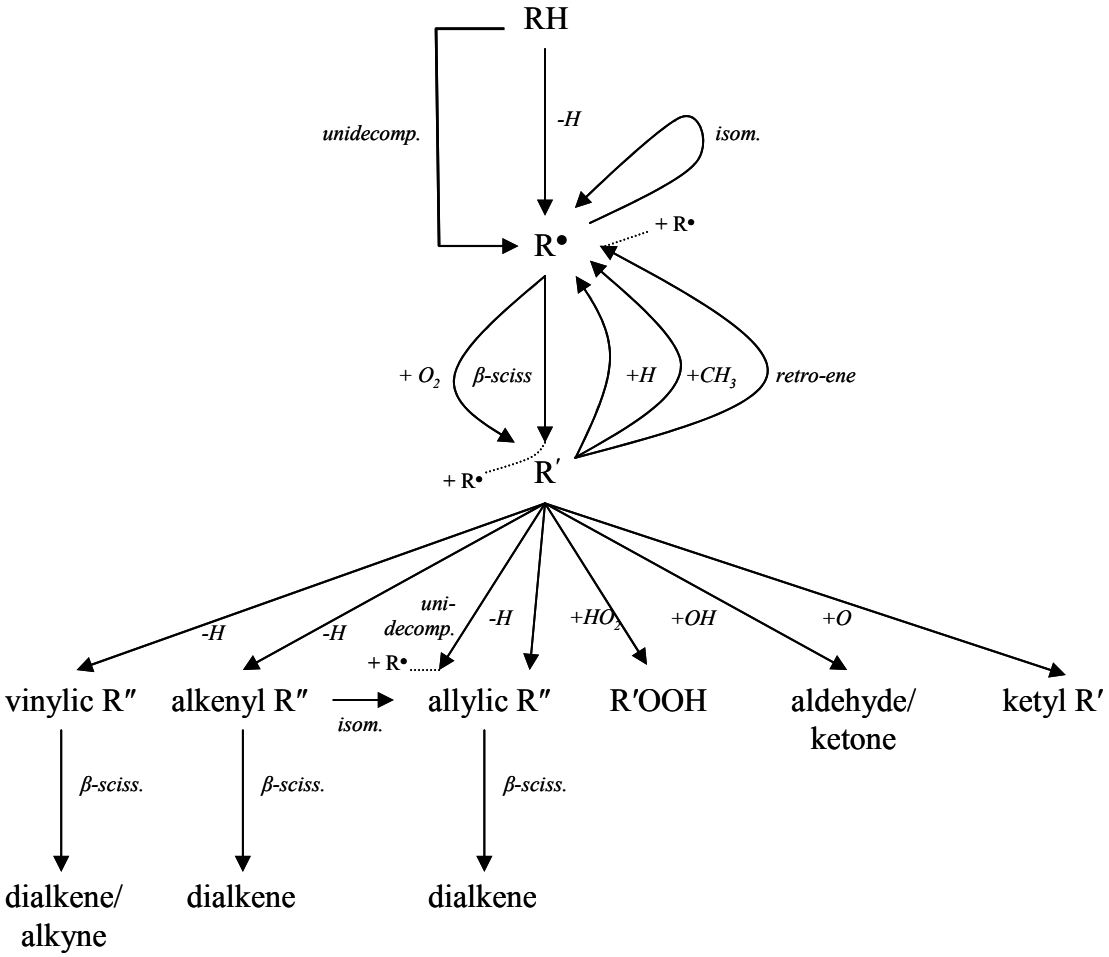

Fig. 3.3. The scheme of high-temperature reaction pathways.

3.2 Low-Temperature Reactions

At low temperature there is a so-called degenerate chain branching characterized by the fact that a main precursor of chain branching (here $RO_2^\bullet$ radicals) is decomposed at higher temperature (T > 800 K), leading to an inverse temperature dependence (the negative temperature coefficient, NTC) of the reaction rate.

3.2.1 Addition of alkyl radicals to molecular oxygen

At low temperature the high activation energies (113-167 kJ/mol) associated with the β scission of alkyl radicals and internal H-atom abstraction reaction make these processes

rather slow. The most important reaction for alkyl radicals is their addition to molecular oxygen,

$$R^{\bullet} + O_2 \leftrightarrow RO_2^{\bullet}. \qquad 3.23$$

This reaction is known to be exothermic and reversible and to have very low activation energy (practically zero). With increasing temperature, this reaction is shifted to the left. Alkylperoxy radical, $RO_2^{\bullet}$, dissociates rapidly and the concentration of $RO_2^{\bullet}$ is very small.

3.2.2 Isomerization of alkylperoxy radicals

An alkylperoxy radical produced by addition of the corresponding alkyl radical to molecular oxygen undergoes isomerization through internal H-atom transfer (1,4-, 1,5-, 1,6- and 1,7-isomerization) to form a hydroperoxy alkyl radical. This reaction is formulated as reversible reaction,

$$RO_2^{\bullet} \leftrightarrow R'OOH^{\bullet}. \qquad 3.24$$

The rate coefficients depend on the ring strain energy barriers involved, described in term of the number of atoms in the transition state ring structure (5-, 6-, 7- and 8-membered rings including H atoms), the type of H atom abstracted (primary, secondary, or tertiary) and the number of available equivalent H atoms at that site.

3.2.3 Abstraction of H atoms from alkanes by alkylperoxy radicals

The fate of alkylperoxy radicals could be to propagate the chain by abstracting H atoms from fuel leading to the formation of hydroperoxides and alkyl radicals,

$$RO_2^{\bullet} + RH \rightarrow ROOH + R'. \qquad 3.25$$

The rate coefficients depend on the type of H atom being abstracted and the number of available equivalent H atoms.

3.2.4 Reaction of alkylperoxy radicals with HO_2

In this work, this reaction was included in the code. The reaction products are hydroperoxides and oxygen,

$$RO_2^{\bullet} + HO_2 \rightarrow ROOH + O_2. \qquad 3.26$$

It should be noted that this reaction is bimolecular, the rate of reaction depending on the concentrations of $RO_2^{\bullet}$ and HO_2. The concentration of the HO_2 radical, although high relative to other radical species in the oxidation process, will typically be of the order of 10^{-6} mol cm^{-3} or less [24]. This shows that the unimolecular isomerization of alkylperoxy radicals will be much faster than this bimolecular reaction. However, the balance between OH and other radicals is often of great importance in these problems so that this reaction is included in the code.

3.2.5 Reaction of alkylperoxy radicals with H_2O_2

This is an interesting reaction converting one stable species and a peroxy radical into another stable species and another peroxy radical,

$$RO_2^{\bullet} + H_2O_2 \rightarrow ROOH + HO_2. \qquad 3.27$$

The peculiarity in this reaction and its influence on the overall reaction sequences is due to the differences in the temperatures at which the ROOH and H_2O_2 species decompose [24]. ROOH decomposes at a lower temperature than H_2O_2. Conversion of H_2O_2 to ROOH leads to an enhanced overall reactivity at lower temperatures.

3.2.6 Homolytic O-O scission of hydroperoxides

Hydroperoxides can undergo homolytic cleavage of the peroxidic bond to produce alkoxy radicals,

$$ROOH \rightarrow RO^{\bullet} + OH. \qquad 3.28$$

This reaction is a branching process since it generates two radicals, which are quite active. At slow oxidation, hydroperoxyde molecules are mostly produced through abstraction of H atoms from alkanes via alkylperoxy radical attack (Rule 3.2.3) so that this reaction is important.

3.2.7 Decomposition of alkoxy radicals

The unstable alkoxy radical tends to decompose quite readily. Large alkoxy radicals can decompose into smaller stable oxygenated species, i.e., aldehydes or ketones and small alkyl radicals,

$$RO^{\bullet} \rightarrow \text{aldehyde or ketone} + \text{small } R^{\bullet}. \qquad 3.29$$

3.2.8 Addition of hydroperoxy alkyl radicals to molecular oxygen

The second addition to molecular oxygen in reaction sequences included in our code is addition of hydroperoxy alkyl radicals to form peroxy hydroperoxy alkyl radicals,

$$R'OOH^{\bullet} + O_2 \leftrightarrow OOR'OOH^{\bullet}. \qquad 3.30$$

The rate coefficients of this reaction are taken from previous studies [12, 18].

3.2.9 β scission of hydroperoxy alkyl radicals formed by the (1,4) isomerization

Hydroperoxy alkyl radicals possessing a radical site in β position to the hydroperoxy group can undergo C-O scission or C-C scission to yield conjugate alkenes and HO_2, or hydroperoxyalkenes and small alkyl radicals, respectively,

$$R'OOH^{\bullet} \rightarrow \text{alkene} + HO_2, \text{ or} \qquad 3.31$$

$$R'OOH^{\bullet} \rightarrow \text{hydroperoxyalkene} + \text{small } R^{\bullet}. \qquad 3.32$$

The first reaction in this rule has proven to be quite sensitive and is responsible for a large part of the NTC behaviour in n-heptane oxidation kinetics [24].

3.2.10 Homolytic C-C scission of hydroperoxy alkyl radicals formed by the (1,5) isomerization

A hydroperoxy alkyl radical, produced by the isomerization of an alkylperoxy radical involving a 6-membered intermediate ring structure, can undergo β scission in two pathways: to produce an alkene and a small hydroperoxy alkyl radical with the radical site

at the carbon atom linked to an oxygen atom (breaking the β bond at Fig. 3.4), or to yield a hydroperoxyalkene and a small alkyl radical,

$$R'OOH^{\bullet} \rightarrow \text{small alkene} + \text{small } R'OOH^{\bullet}\text{, or} \qquad 3.33$$

$$R'OOH^{\bullet} \rightarrow \text{hydroperoxyalkene} + \text{small } R^{\bullet}. \qquad 3.34$$

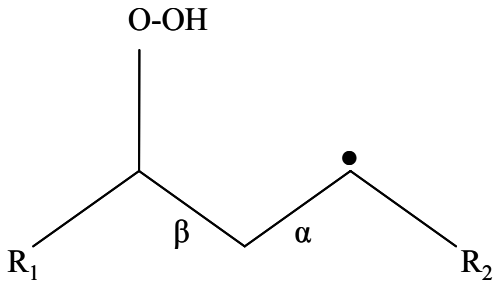

Fig. 3.4. Hydroperoxy alkyl radical formed by the (1,5) isomerization

The first path is probably faster than the second, since the C-C bond being broken in a hydroperoxy alkyl radical in the first path is probably weakened by the presence of an O atom.

3.2.11 Homolytic C-C scission of hydroperoxy alkyl radicals formed by the (1,6) and (1,7) isomerization

A hydroperoxy alkyl radical, produced by the isomerization of an alkylperoxy radical with an intermediate ring structure of seven and eight atoms, can undergo β scission in two pathways: to produce an alkene and a small hydroperoxy alkyl radical, or to yield a hydroperoxyalkene and a small alkyl radical,

$$R'OOH^{\bullet} \rightarrow \text{small alkene} + \text{small } R'OOH^{\bullet}\text{, or} \qquad 3.35$$

$$R'OOH^{\bullet} \rightarrow \text{hydroperoxyalkene} + \text{small } R^{\bullet}. \qquad 3.36$$

3.2.12 Homolytic O-O scission of hydroperoxy alkyl radicals with the radical site at a carbon atom linked to oxygen atom

A hydroperoxy alkyl radical, produced from the first path of 3.2.10, can decompose to produce an aldehyde or a ketone,

$$R'OOH^{\bullet} \rightarrow \text{aldehyde of ketone} + OH. \qquad 3.37$$

3.2.13 Oxidation of hydroperoxy alkyl radicals

Our code includes another pathway of the reaction of hydroperoxy alkyls with molecular oxygen. This reaction occurs via the transfer of an H atom at the β position from the radical site to oxygen,

$$R'OOH^{\bullet} + O_2 \rightarrow \text{hydroperoxyalkene} + HO_2. \qquad 3.38$$

3.2.14 Formation of cyclic ethers from hydroperoxy alkyl radicals

This reaction sequence involves the breaking of the O-O bond, followed by the formation of a cyclic ether with the remaining O atom being part of it. The activation energy for this reaction depends on the size of the cyclic ring being formed. Oxirane, oxetane, tetrahydrofurane and tetrahydropyrane are produced from hydroperoxy alkyl radicals, the radical site being in β, γ, δ, ε, respectively position to the carbon atom linked to the hydroperoxy group,

$$R'OOH^{\bullet} \rightarrow \text{cyclic ether} + OH. \qquad 3.39$$

3.2.15 Isomerization of peroxy hydroperoxy alkyl radicals

Isomerization of a peroxy hydroperoxy alkyl radical occurs through an internal transfer of H atoms connected to a carbon atom linked to a hydroperoxy group,

$$OOR'OOH^{\bullet} \leftrightarrow HOOR''OOH. \qquad 3.40$$

Figure 3.5 depicts an example of isomerization of a peroxy hydroperoxy alkyl radical.

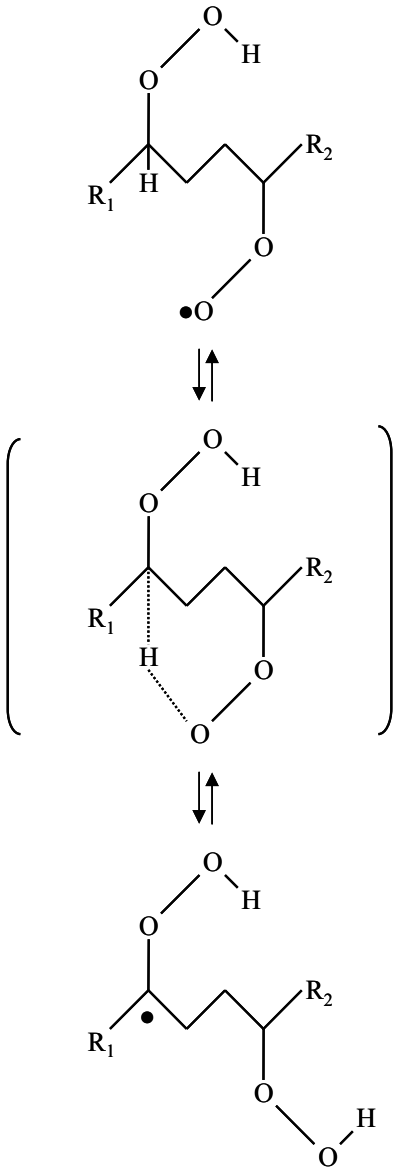

Fig. 3.5. Isomerization of a peroxy hydroperoxy alkyl radical

The rate coefficients of this reaction depend on the intermediate ring structure, the type of H atom being transferred (secondary, tertiary) and the number of available equivalent H atoms.

3.2.16 Homolytic O-O scission of dihydroperoxy alkyl radicals

This reaction leads to the formation of a ketohydroperoxyde and a hydroxyl radical,

$$HOOR''OOH \rightarrow O=R''OOH + OH. \quad 3.41$$

3.2.17 Formation of hydroperoxy cyclic ethers from dihydroperoxy radicals

This reaction sequence involves the breaking of the O-O bond, followed by the formation of a hydroperoxy cyclic ether. The activation energy depends on the size of the cyclic ring being formed,

$$HOOR''OOH \rightarrow \text{hydroperoxy cyclic ether} + OH. \quad 3.42$$

3.2.18 Decomposition of ketohydroperoxides

A ketohydroperoxide can undergo decomposition leading to the formation of two radicals, a carbonyl radical and a hydroxyl radical, providing chain branching as it produces two radicals from one stable species,

$$O=R''OOH \rightarrow O=R''O^{\bullet} + OH. \quad 3.43$$

3.2.19 Decomposition of O=R''O•

This carbonyl radical can decompose to form an aldehyde and a ketyl radical,

$$O=R''O^{\bullet} \rightarrow \text{aldehyde} + \text{ketyl radical}. \quad 3.44$$

3.2.20 Abstraction of H atoms from cyclic ethers

Since we consider only hydrocarbons larger than C_4 in our code, cyclic ether species involved have large structures. Our treatment for such large cyclic ethers is exactly the same as in Curran at al. [24]. Cyclic ether reaction sequences are assumed to occur through

H-atom abstraction by active radical species, followed by immediate ring opening, leading to the formation of ketyl radicals,

$$\text{cyclic ether} + X \rightarrow \text{ketyl radical} + XH, \qquad 3.45$$

where X is an active radical.

Similar to the H-atom abstraction from alkanes, the easiness of H-atom abstraction from cyclic ethers will be in the following order: tertiary > secondary > primary. In addition, a hydrogen atom bound to a carbon atom linked to the oxygen atom in the ring structure will be easier abstracted.

3.2.21 Decomposition of hydroperoxy cyclic ethers

A hydroperoxy cyclic ether can decompose into an aldehyde or a ketone and a ketyl radical,

$$\text{hp cyclic ether} \rightarrow \text{adehyde or ketone} + \text{ketyl radical} + OH. \qquad 3.46$$

3.2.22 Abstraction of H atoms from aldehydes or ketones

Aldehydes and ketones formed during low temperature oxidation are H-atom donors in hydrocarbon oxidation. Their H atoms are more readily abstractable than those of the fuel,

$$\text{Aldehyde or ketone} + X \rightarrow \text{ketyl radical} + XH. \qquad 3.47$$

The rate coefficients depend on the type of the H atom being abstracted and the number of available equivalent H atoms. In addition, H atoms bound to a carbon atom linked to the oxygen atom are more easily abstracted.

3.2.23 Decomposition of ketyl radicals

Ketyl radicals can undergo β scission to form stable alkenals or alkenons and smaller alkyl radicals, or smaller ketyl radicals and smaller dialkenes,

$$\text{Ketyl radical} \rightarrow \text{alkenal or alkenon} + \text{small } R^{\bullet}, \text{ or} \qquad 3.48$$

$$\text{Ketyl radical} \rightarrow \text{small ketyl radical} + \text{small } R'. \qquad 3.49$$

The reactions for alkenals, alkenons, hydroperoxy alkenes, oxo-hydroperoxy alkenes, alkoxy radicals, hydroperoxy alkyl radicals and other species with C-C double bonds are treated to be analogous to those with C-C single bonds. All reaction pathways at low temperatures are summarized schematically in Figure 3.6.

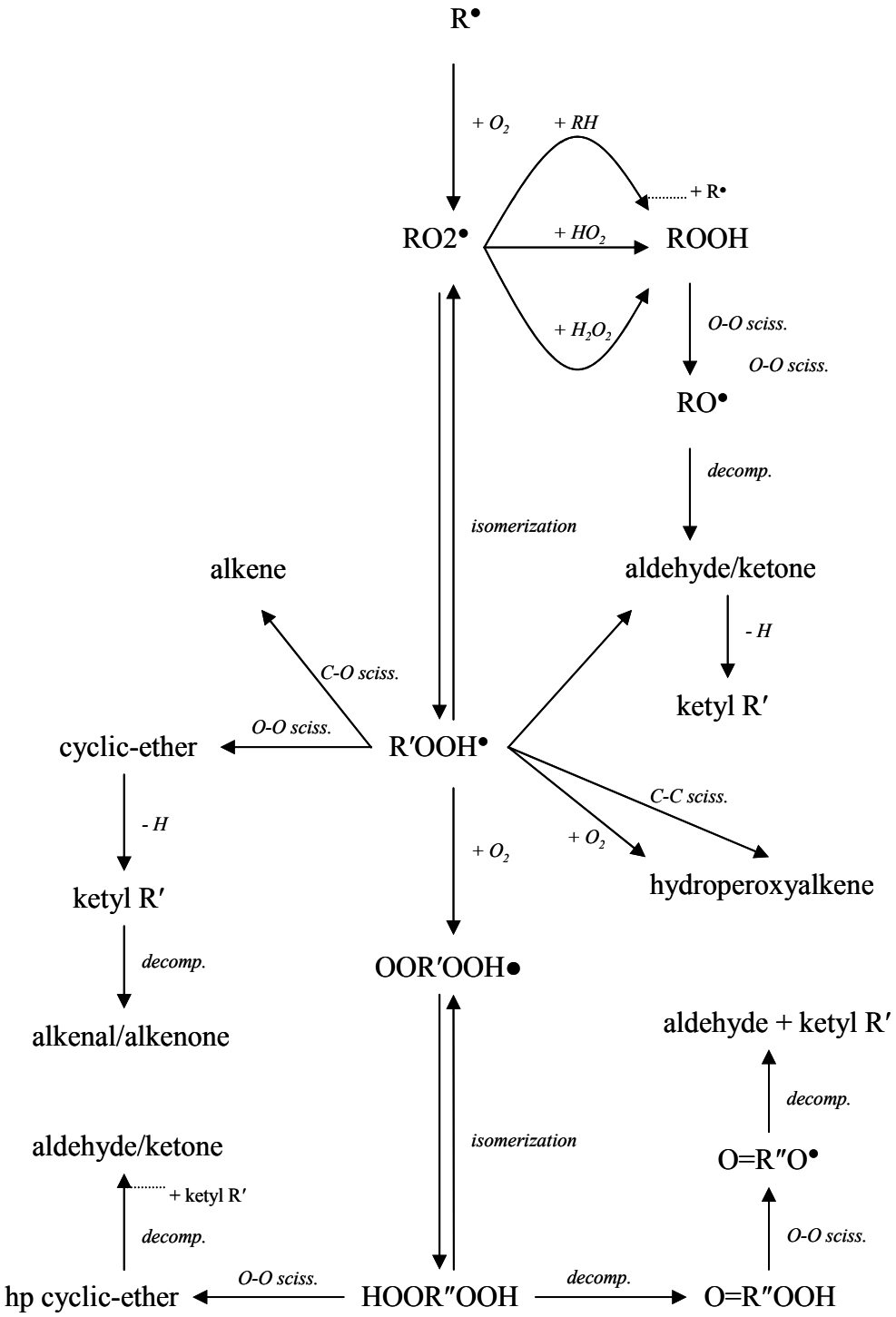

Fig. 3.6. Scheme of low-temperature reaction pathways.

Chapter 4

AUTOMATIC GENERATION OF REACTION MECHANISMS

1. Rule-Oriented Programming

As already discussed in detailed by Chevalier et al. [64], for the implementation of rule-oriented programming techniques from several areas of computer science were used, mainly from artificial intelligence (rule paradigm, tree structures) and computer algebra (canonical form techniques). As a supporting system LISP is used because of its flexibility concerning the data structure, algorithm development and availability of a user interface design.

In the artificial intelligence research several programming paradigms, which facilitate the representation of complex knowledge context, were developed. As the chemical reactions are an area with "exact" knowledge, which mostly is encoded in rules written in natural language, the usage of the rule-oriented program paradigm is mostly adequate.

The knowledge is formally coded in production rules of the following type:

Rn If P_1 and P_2 and P_3 and …
then C_1 and C_2 and …

The rule has a name (here "Rn"), which later will be used for identification. A set of premises (here P_1, P_2 …) is linked by logical conjunction (and, or, not). The premises are expressions testing the objects for certain properties. If all tests are positive, the conclusions (here C_1, C_2 …) are activated (the rule "fires"). An example of this is

R2 If (is alkane(x))
then (reaction: beta scission(x)).

Most of the rules are formulated in a manner independent from each other; so it is possible to activate, deactivate, add and withdraw rules without recompilation.

At the moment the rules act on two semantic levels:

- On the production level reactions are deduced from new or generated species. A general inference machine activates each production rule for any relevant object or combination of objects exactly once.
- On a reformation level each newly generated species is investigated for necessary reformations. Here, for example, two neighbored radical positions are converted into a double bound.

In the course of the development a third level of rules was introduced, which plays the role of a meta rule: “rule Rx should be activated only if Ry did not yet fire”. These meta rules define a unique sequence of dependency. They sometimes facilitate the description, but they create an additional dependency among the rules, which reduces the flexibility.

2. Data structures

It is most convenient to represent molecules as graphs, where the atoms are nodes and the molecular links are edges. As complex analysis procedures are required, the sorted tree (ST) was selected among the different possible graph structures. A tree is a directed graph where one node plays the special role of a root. There are zero or more branches (links) from the root to the other parts of the tree, which then form sub-trees. The branches are sorted lexicographically based on the atom weight. A branch b1 is considered “heavier” then b2, if the first (leftmost) different atom in b1 is heavier then that in b2. Double or higher bounds are kept as labels of the links, and they are integrated in the lexicographical ordering.

In order to get a completely unique representation, one selects among the different possible ST’s of a molecule that one as “canonically sorted tree” (CST), which has an atom of the heaviest element class as root and which is the most important under the lexicographical ordering. The CST is canonical in the sense of computer algebra, as

- for a given molecule (ST) the corresponding CST can be computed by a straightforward (recursive) algorithm,
- two molecules are chemically equivalent if and only if their CST’s are identical.

The CST is the most important means for the identification of generated molecules.

All molecules are represented as formally saturated. Open bounds are saturated by an artificial “element” named @. This representation offers several advantages:

- The detection of radicals and radical points in a molecule is simple by looking for an explicit @.
- The open bound can play the role of the root in a ST. That ability is often used as a radical point, which often is the origin of chemical activity.
- The formal correctness of a molecule can be simply verified by counting the links of a node and comparing it with the valence of the atom. Missing links are not implicitly recorded as radicals.

Practical considerations have led to a different handling of "missing" links. In most situations H atoms automatically fill them, as in the context of hydrocarbons this approach facilitates encoding of molecules.

3. 2-Dimensional structural input

It is hard to generate tree structures by hand. Thus, a technique that allows to draw molecules in two dimensions with ASCII characters was developed. Two examples of the 2-dimensional structural input are

```
"          H      H      H          "
"          |      |      |          "
"   H------C------C------C------H    "
"          |      |      |          "
"          H   H-C-H   H          "
```

and, with the convention of omitted H atoms,

```
"          C------C------C          "
"                 |                 "
"                 C                 "
```

4. Pattern Matching

In the rules for the automatic generation of combustion reactions the following types of tests in the premises are used:

- Classification of molecules by collecting and/or counting their atoms (e.g., hydrocarbon(x) $\leftrightarrow$ x contains only H and C).

- Classification of molecules by looking for special branches (e.g., has_branches_O-O-H(x) ↔ x contains a –O–O–H group).
- Classification of very specific shapes of parts of molecules.

While the first two types are coded as an enlargeable set of test functions, which operate directly on the ST of a molecule, the implementation of the third one is much more complicated. Here a very general pattern matching technique is used. The local shape is described by a pattern, which is encoded as an ST like for a complete molecule. However, here some of the branches can be variables. If now a molecule m is compared with a pattern p, first all ST variants of m with the same root as p are computed, giving m_1, m_2, …. In the next step each m_i is compared with p separately. Constants (atoms, link labels) must match identically, while variables match anything. If there is no contradiction, the pattern fits.

Example:

```
(mrule H1 (m)
        (prog (res)
                (mpmatch ONCE m
                        "                &1      &4        "
                        "                |       |        "
                        "          @------C-------C------@  "
                        "                |       |        "
                        "                &2      &3       "
                (setq res (mpgen
                        "                &1      &4       "
                        "                |       |        "
                        "                C= = = C         "
                        "                |       |        "
                        "                &2      &3       "
)))
(value res)
```

In this rule the first group of strings defines a pattern, which contains two adjacent C atoms, which both have an open link, and four variable links. This pattern, for instance, fits for the molecule

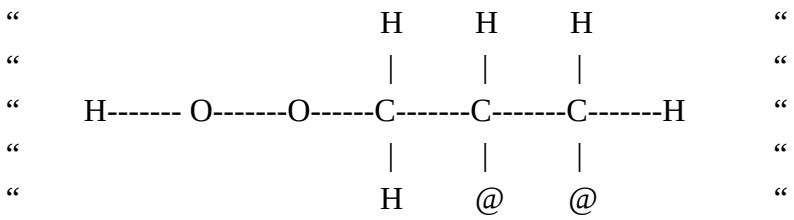

where &1 is bound to the left part of the molecule, while all remaining variables are bound to an H atom. In the second part of the rule, a new molecule is constructed by the components bound in the variables, which here results in

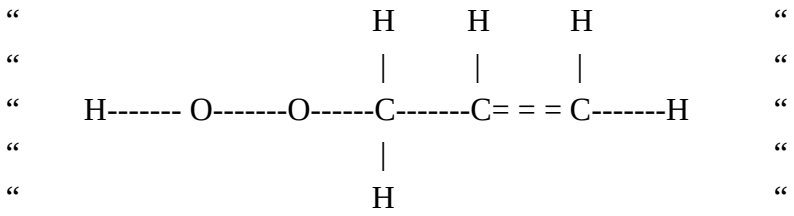

This is one of the rules on the reformation level.

There are several modes of pattern matching:

- ONCE : only the first pattern fit is regarded,
- ALL : all possible pattern fits are regarded, and the rule body is executed for each fit separately.

A specific difficulty is the control the multiplicities. Here different formalisms were implemented for different question types; for example, multiple matches are reduced, but their multiplicity is available as a number, or equivalent matches are counted explicitly. The last case is especially important, if reactions concerning H atoms are handled. Here one in general has multiplicities, which enter the final rate calculation.

Chapter 5

MECHANISM VALIDATION

This chapter discusses mechanism validation carried out for several reference fuels: n-pentane, n-heptane, iso-octane and n-decane. Experimental results of those fuels from a rapid-compression machine, shock tubes and jet-stirred reactors will be used for this purpose.

A mechanism validation was performed by comparing calculation results to experimental measurements available in literature. A common part of the mechanisms is the handwritten C_0-C_4 sub-mechanism built from 950 elementary reactions. In order to reduce CPU time, we did not take into account types of reactions involving species containing hydroperoxy groups and C-C double bonds in all of our mechanisms. The simulations were accomplished using the HOMREA code [65], which has been developed in the Warnatz group.

5.1 N-pentane

Autoignition of n-pentane was studied by Ribaucour et al. [1] in a rapid-compression machine (RCM) between 600 K and 900 K, pressures of 6 bar - 9 bar and an equivalence ratio of 1. N-pentane shows all typical features under rapid compression: an ignition limit around 650 K, a two-stage ignition with a cool flame decreasing in intensity between 650 K and 850 K, and a large zone of negative temperature coefficient extending from 760 K to 860 K. The first-stage ignition occurs at lower temperatures and approaches the total ignition with decreasing temperature.

To simulate these experimental results, a mechanism for n-pentane consisting of 185 species and 1186 elementary reactions has been automatically generated by MOLEC. Figure 5.1 shows the autoignition delay times of a stoichiometic n-pentane/air mixture numerically calculated together with experimentally observed. The calculation results are in good agreement with the experimental ones for both ignition delay times. The lower ignition limit and the negative temperature coefficient (NTC) are correctly reproduced.

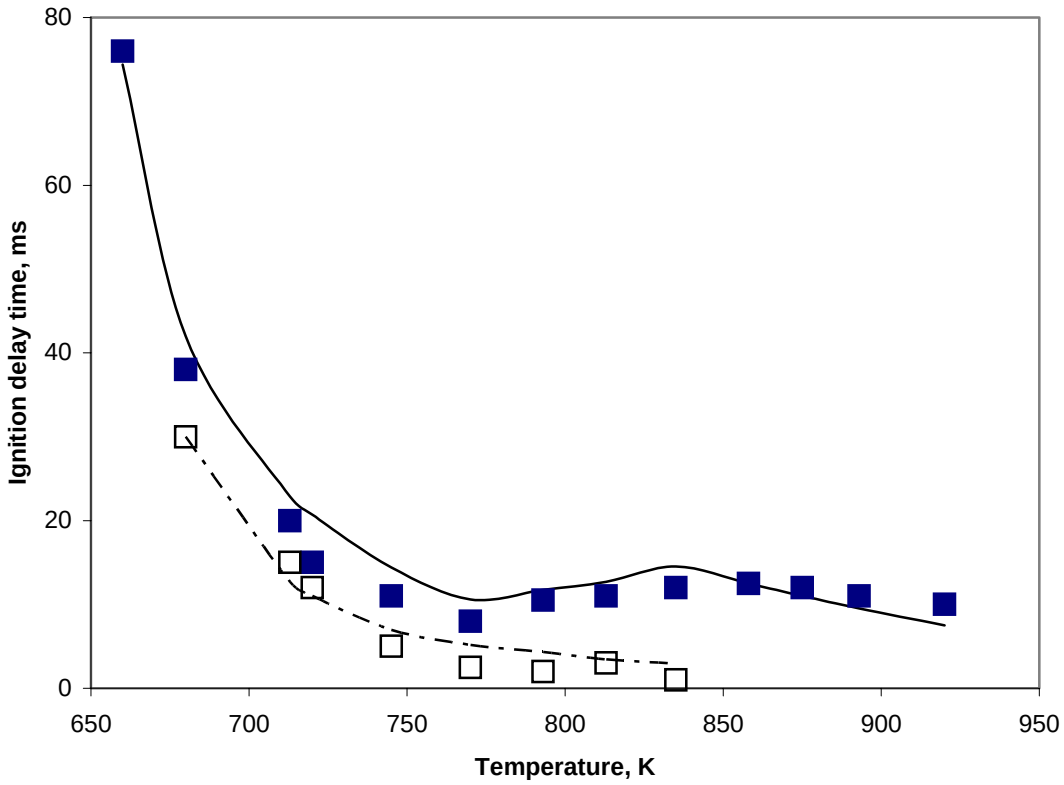

Fig. 5.1: Ignition delay times of stoichiometric n-pentane/air mixtures versus core gas temperature at pressures of 6 bar - 9 bar. Open symbols indicate experimental first-stage ignition delay times; closed symbols, total ignition delay times; lines, calculated delay times.

5.2 N-heptane

The C_5-C_7 sub-mechanisms generated by MOLEC were coupled with the handwritten C_0-C_4 sub-mechanism to build a detailed chemical kinetic mechanism for n-heptane oxidation consisting of 486 species taking part in 2008 elementary reactions. This mechanism is used to reproduce experimental results on n-heptane oxidation in a shock tube and in a jet-stirred reactor.

5.2.1 Shock tube

A study on ignition delay times of n-heptane/O_2/Ar mixtures behind reflected shock waves for equivalence ratios ranging from 0.5 to 4.0 in a temperature range of 1300 K - 2000 K has been carried out by Coats and Williams [29]. The experimental ignition delays together

with the calculated ones are presented in Fig. 5.2. As can be seen in this figure, good agreement between the experimental and calculated results is achieved for the stoichiometric and fuel-lean mixtures. However, the model rather overestimates the ignition delays of the fuel-rich mixtures. The fuel-lean mixtures burn more easily than the stoichiometric and fuel-rich mixtures under this pyrolysis condition. This trend is well reproduced by the model.

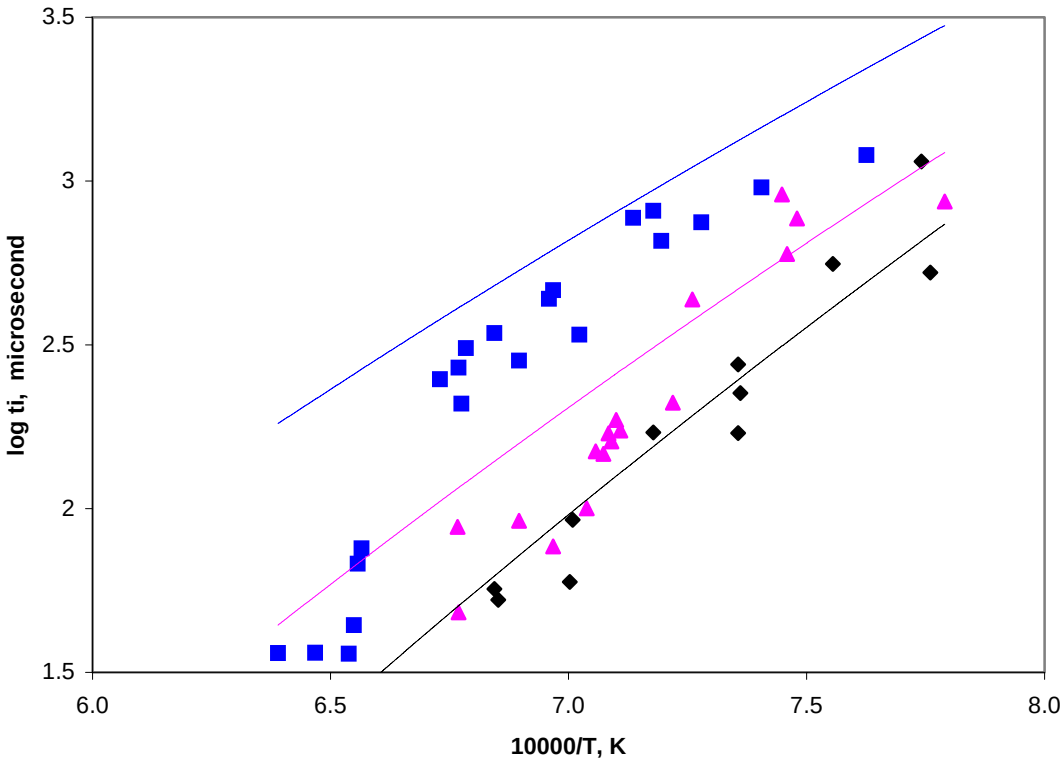

Fig. 5.2: Ignition delay times of n-heptane/O_2/Ar versus the inverse of the initial temperature behind the reflected shock wave. Diamond symbols indicate equivalence ratio = 0.5; triangle, equivalence ratio = 1.0; square, equivalence ratio = 2.0.

Ciezki and Adomeit [19] have experimentally investigated specific aspects of auto-ignition of n-heptane in a high pressure shock tube at pressures ranging from 3.2 bar to 42 bar, but at rather lower temperatures ranging from 660 K - 1350 K for various mixture compositions. The ignition delay times observed together with numerically predicted are presented in Figs. 5.3 to 5.5.

In Fig. 5.3 the ignition delay times of stoichiometic n-heptane/air mixtures is plotted logarithmically versus the inverse of the initial temperature behind the reflected shock wave at various initial pressures. In general, the calculations show excellent agreement with the experimental measurements. The decrease in the corresponding global activation energies with increasing pressure is well reproduced by the model within the investigated temperature range.

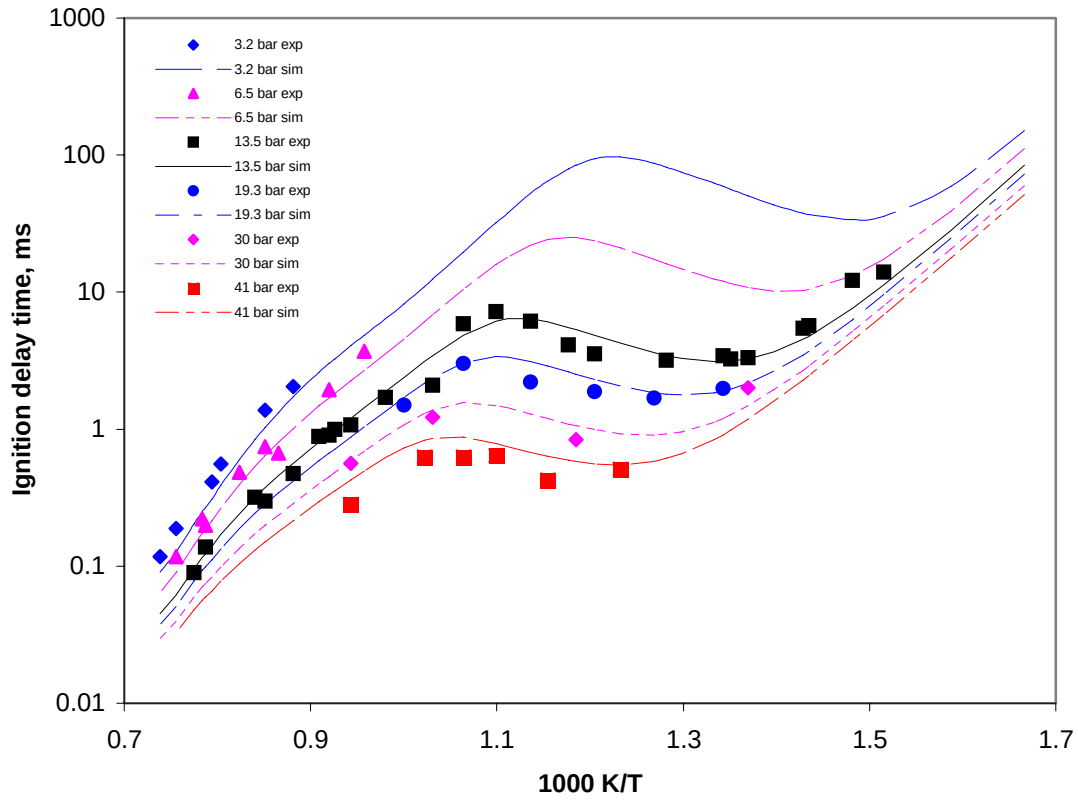

Fig. 5.3: Ignition delay times of stoichiometric n-heptane/air versus the inverse of the initial temperature behind the reflected shock wave. Symbols indicate the experimental results; lines, calculations.

A somewhat linear temperature dependence of the ignition delay time in the Arrhenius plot is reproduced by the kinetic model in the high-temperature region. The S-shaped curves with maximum and minimum values are observed experimentally and computationally in the intermediate temperature region. At a pressure of 13.5 bar, for example, this non-linear temperature dependence of the ignition delay time occurs between 950 K and 750 K and possesses a negative temperature coefficient. The magnitude of each NTC region at various pressures is accurately reproduced by the reaction mechanism. Furthermore, the shift of the NTC region towards higher temperatures with increasing pressure is also correctly reproduced. Linear lines can express the temperature dependence of the ignition delay time in the low-temperature region.

The experimental fact that the influence of pressure on the ignition delay is most pronounced in the NTC region is well reproduced by the model. In the low-temperature region pressure has the smallest influence on the ignition delay times. In the high-temperature region pressure has a varying degree of influence on the ignition delay times and the dependence becomes smaller with increasing temperature.

The effect of the composition of n-heptane/air mixture on the ignition delay time at 13.5 bar and 41 bar is plotted in Fig. 5.4 and 5.5, respectively. The model can reproduce very well the ignition delay times for various equivalence ratios at 13.5 bar, but it shows a lower overall reactivity than the experiments at 41 bar. As can be seen in Fig. 5.4, at the constant initial pressure 13.5 bar and up to 1250 K the fuel-rich mixtures autoignite more easily than the lean-fuel mixtures. Above 1250 K, the contrary trend occurs: The fuel-lean mixtures burn faster than the fuel-rich mixtures, as shown in Fig. 5.2. At the constant initial pressure 41 bar the temperature point at which the contrary trend occurs is shifted towards a higher temperature, as seen in Fig. 5.5. The dependence of the ignition delay time on the equivalence ratio in the high-temperature region is small, but increases towards lower temperatures. In the transition region the dependence of the ignition delay time on the equivalence ratio reaches its maximum.

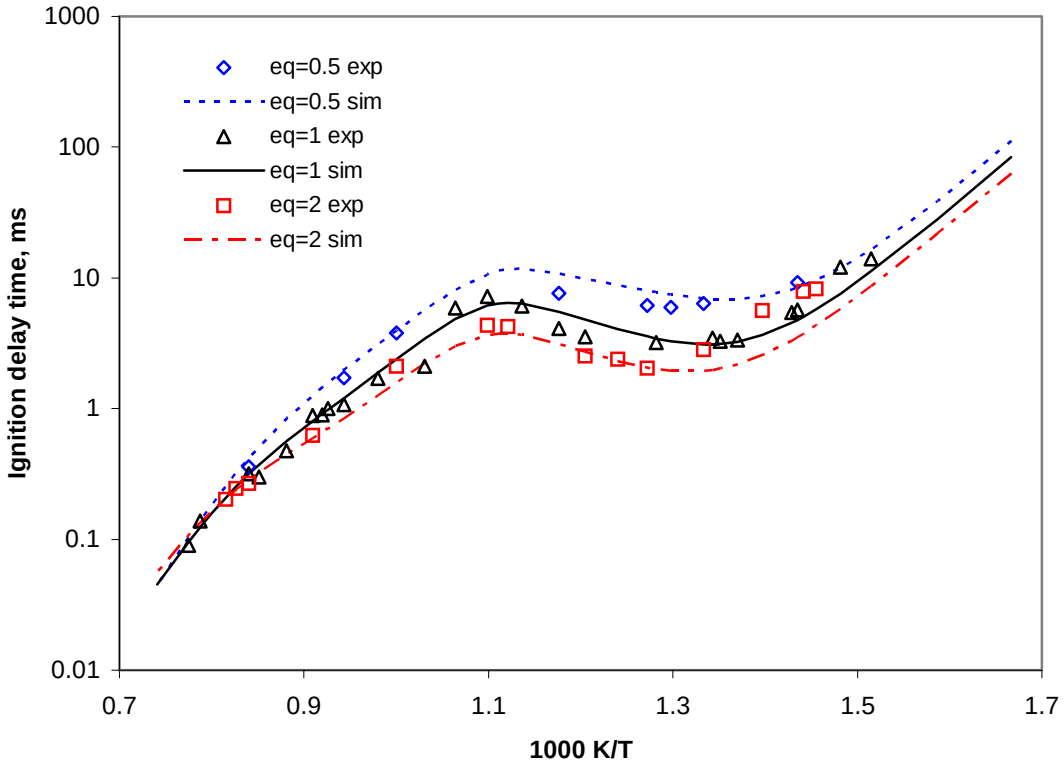

Fig. 5.4: Ignition delay times of n-heptane with various equivalence ratios at 13.5 bar.

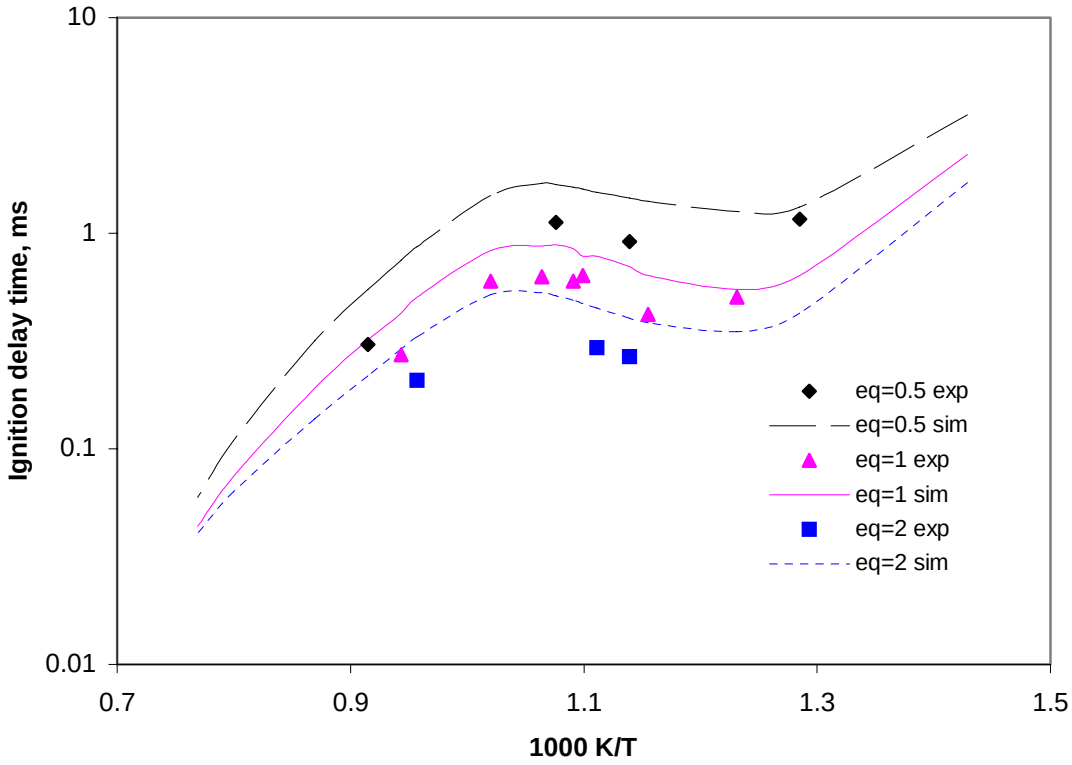

Fig. 5.5: Ignition delay times of n-heptane with various equivalence ratios at 41 bar

5.2.2 Jet-stirred reactor

N-heptane oxidation in a high-pressure jet-stirred reactor was investigated experimentally by Dagaut et al. [23, 27]. The experimental conditions covered are the low- and high-temperature regimes (550 K - 1150 K), a wide range of pressure (1 bar - 40 bar), equivalence ratios of 0.3-1.5 and 99 vol.-% dilution by nitrogen. Reactants, intermediates and final products were measured for the cool flame, the NTC region and the high-temperature combustion, providing a valuable set of data to better characterize those specific aspects of linear hydrocarbon oxidations.

Figure 5.6 shows a comparison between the experimentally derived and numerically predicted conversion of n-heptane at 10 bar and a contact time of 1 s for three different equivalence ratios (0.5, 1.0 and 1.5). Numerical calculations were carried out under isothermal, constant pressure conditions. In general, the kinetic model can reproduce the experiments within the investigated temperature range. Three kinetic regimes typical of n-alkane oxidation are reproduced. In the low-temperature regime slow combustion and cool flame regions, observed by the experiments below 640 K, are correctly predicted, but with a lower overall reactivity than seen in the experiments. In the high-temperature regime a fast oxidation of n-heptane takes place. From 640 K - 750 K, a transition or NTC region is also reproduced for all equivalence ratios, suggesting that the effect of equivalence ratio can be disregarded in practice. As seen in this figure, the fuel-lean mixture shows a higher overall reactivity. The dependence of the overall reactivity on the mixture composition is highest in the transition region.

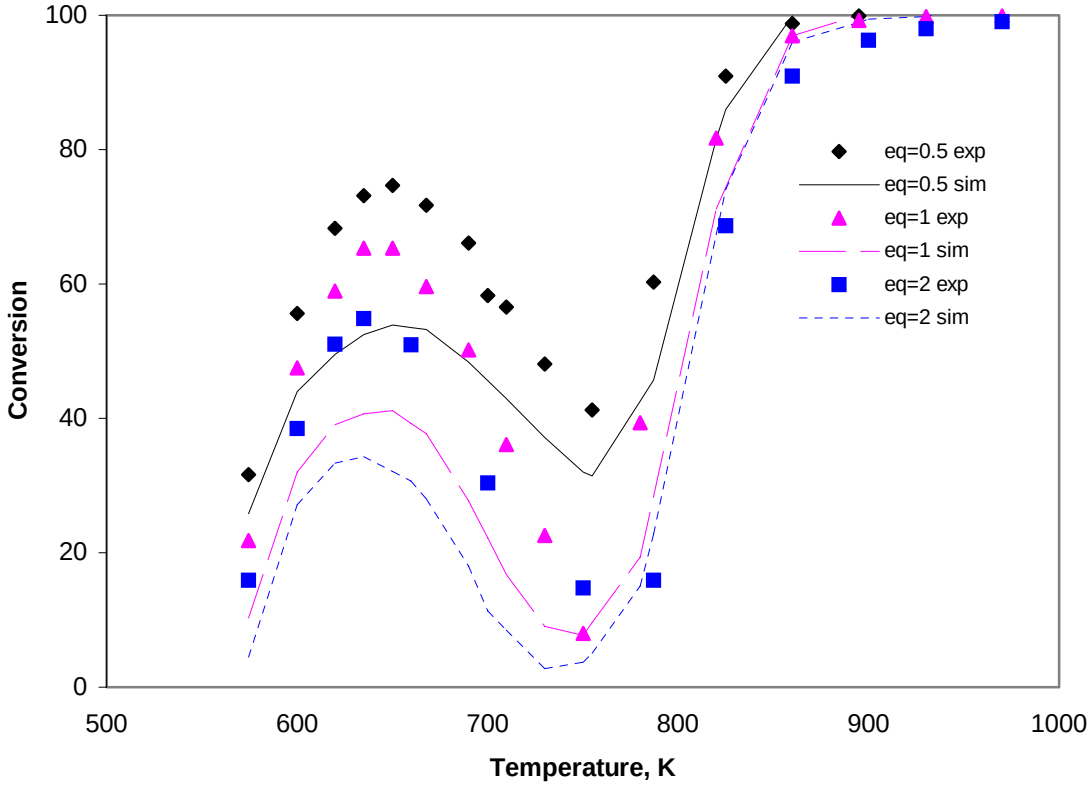

Fig. 5.6: Oxidation of 0.1 % n-heptane in a jet-stirred reactor at 10 bar and a contact time of 1 s. Comparison between experimental and calculated conversion of n-heptane.

A set of comparisons between the experimental and predicted concentrations of the main product CO_2 and the major intermediate CO are given in Fig. 5.7 for various equivalence ratios. In general, the model agrees well with the experimental results for both species. Unsatisfactory under-predictions of the concentration of these species in the low-temperature regime are a consequence of lower conversion levels of n-heptane predicted by the model, as seen in Fig 5.6. The predominance of CO production over CO_2 in the low-temperature regime makes it evident that the oxidation proceeds through the formation of oxygenated intermediates, which are cool-flame-chemistry constituents. The numerical calculations show the trend that in the low-temperature regime CO formation increases as the amount of oxygen in the initial mixtures increases. Above 750 K, the oxidation occurs faster with the fast formation of both molecules. It can be seen from this figure that by increasing the amount of oxygen in the initial mixture, the rate of CO oxidation to form CO_2 becomes faster, the CO_2 concentration increases more exponentially with increasing temperatures, and the drop of the CO concentration is shifted towards lower temperatures.

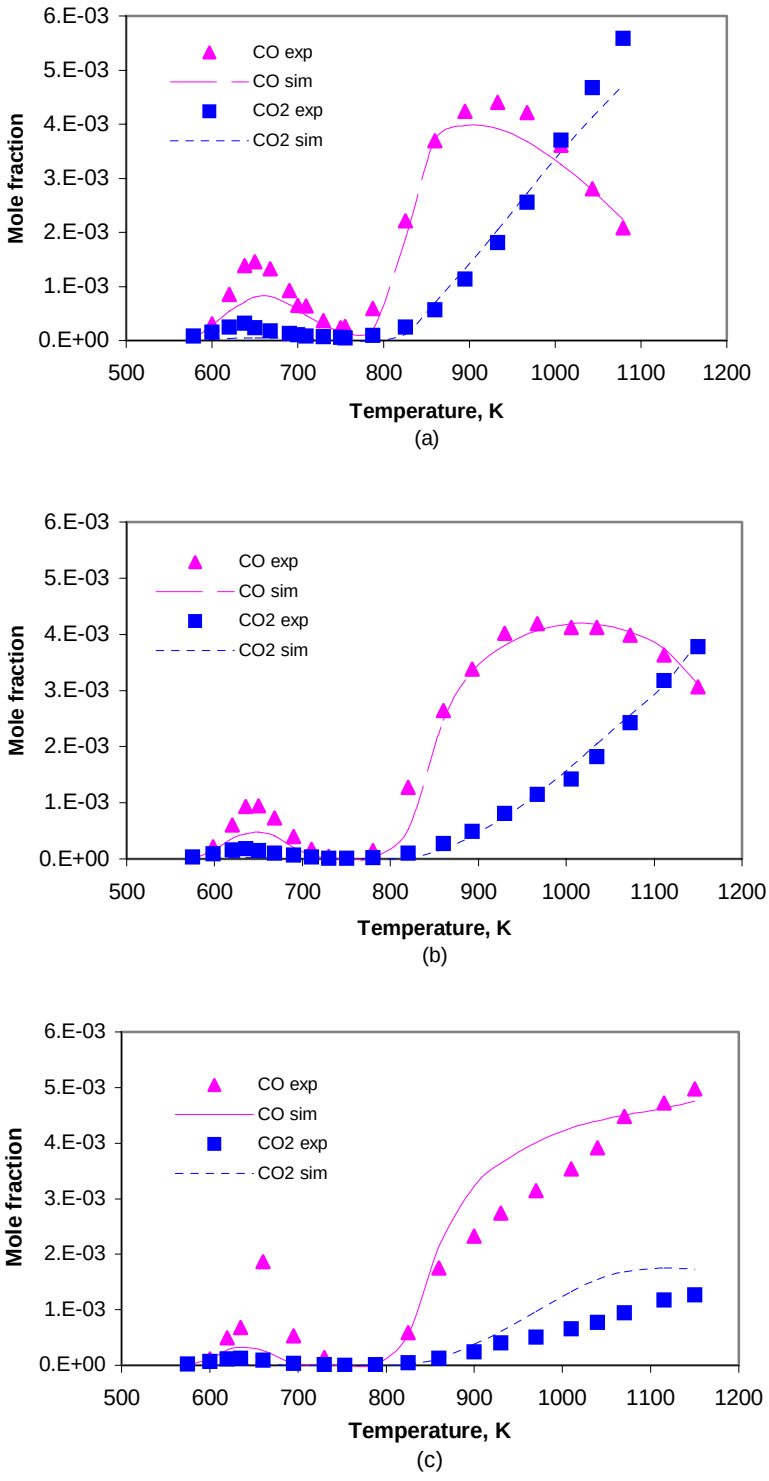

Fig. 5.7: Oxidation of 0.1 % n-heptane in a jet-stirred reactor at 10 bar and a contact time of 1 s. Comparison between experimental and calculated concentrations of CO and CO_2. Equivalence ratio = 0.5 (a); 1.0 (b); 1.5 (c).

Further sets of comparisons between the experimental and predicted concentrations of paraffinic intermediates (methane and ethane) are given in Fig. 5.8, of olefinic intermediates (ethylene, propene and 1-butene) in Fig. 5.9 and of other oxygenated intermediates (formaldehyde, acetaldehyde and ethylaldehyde) in Fig. 5.10. In general, the chemical kinetic mechanism agrees with the experiments for those molecules in the investigated temperature range.

For methane and ethane, the model gives excellent predictions. Very small amounts of methane and ethane in the low-temperature regime, followed by a fast increase above 750 K and then a decrease at higher temperatures are exhibited both by the experiment and the model. As seen in Fig. 5.8, it is clear that the maximum value of the methane concentration is shifted towards a higher temperature with decreasing the amount of oxygen in the initial mixture. The trend that the maximum value of methane concentration in the fuel-rich mixture is higher than those in the stoichiometric and fuel-lean mixtures is also well reproduced.

The ethylene profile is predicted well above 750 K, but overestimated in the low-temperature regime. The propene profile is underpredicted by the order of 2, while the 1-butene profile is overestimated by the order of 2. Ethylene is a major intermediate product in the low- and high temperature regimes.

Following carbon monoxide, formaldehyde is a major oxygenated intermediate in both low- and high-temperature regimes, followed by acetaldehyde and propylaldehyde. Their profiles are well reproduced by the model. The experimental and calculated results are evidences that, together with carbon monoxide, formaldehyde is responsible for engine knocking at low temperatures. The fuel-rich mixture better suppresses oxygenated intermediates than the stoichiometric and fuel-lean mixtures in the low-temperature regime.

The overall result of these calculations indicates that below 750 K the oxidation occurs via a low-temperature mechanism leading to the formations of CO, CO_2, formaldehyde, acetaldehyde, propylaldehyde and ethylene. Above 750 K, the oxidation takes place through a high-temperature mechanism with the fast production of CO, CO_2, formaldehyde, ethylene and methane.

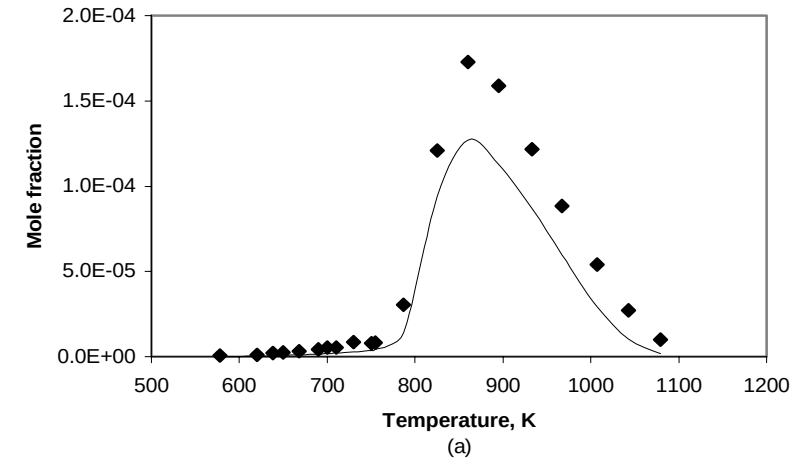

(a)

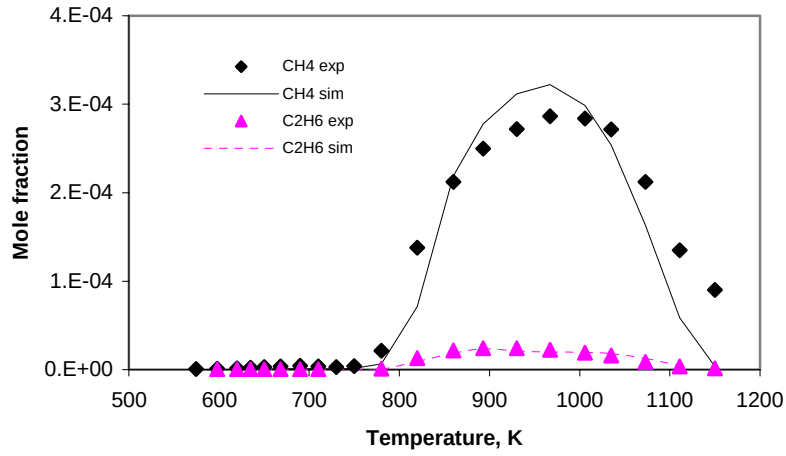

(b)

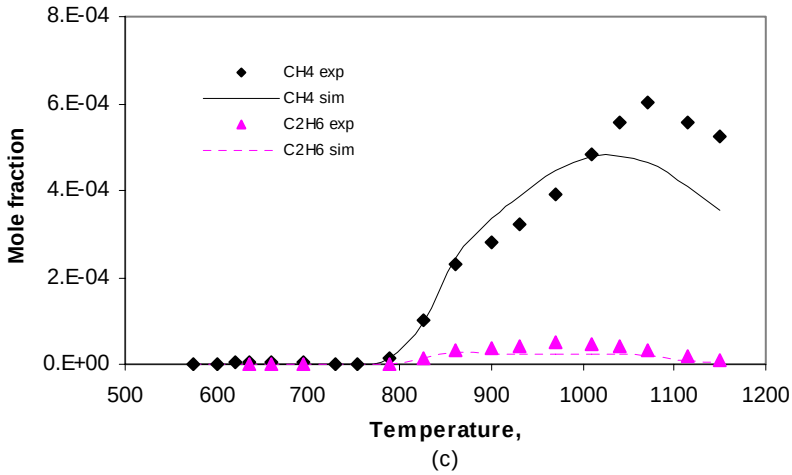

(c)

Fig. 5.8: Oxidation of 0.1 % n-heptane in a jet-stirred reactor at 10 bar and a contact time of 1 s. Comparison between experimental and calculated concentrations of CH_4 and C_2H_6. Equivalence ratio = 0.5 (a); 1.0 (b); 1.5 (c).

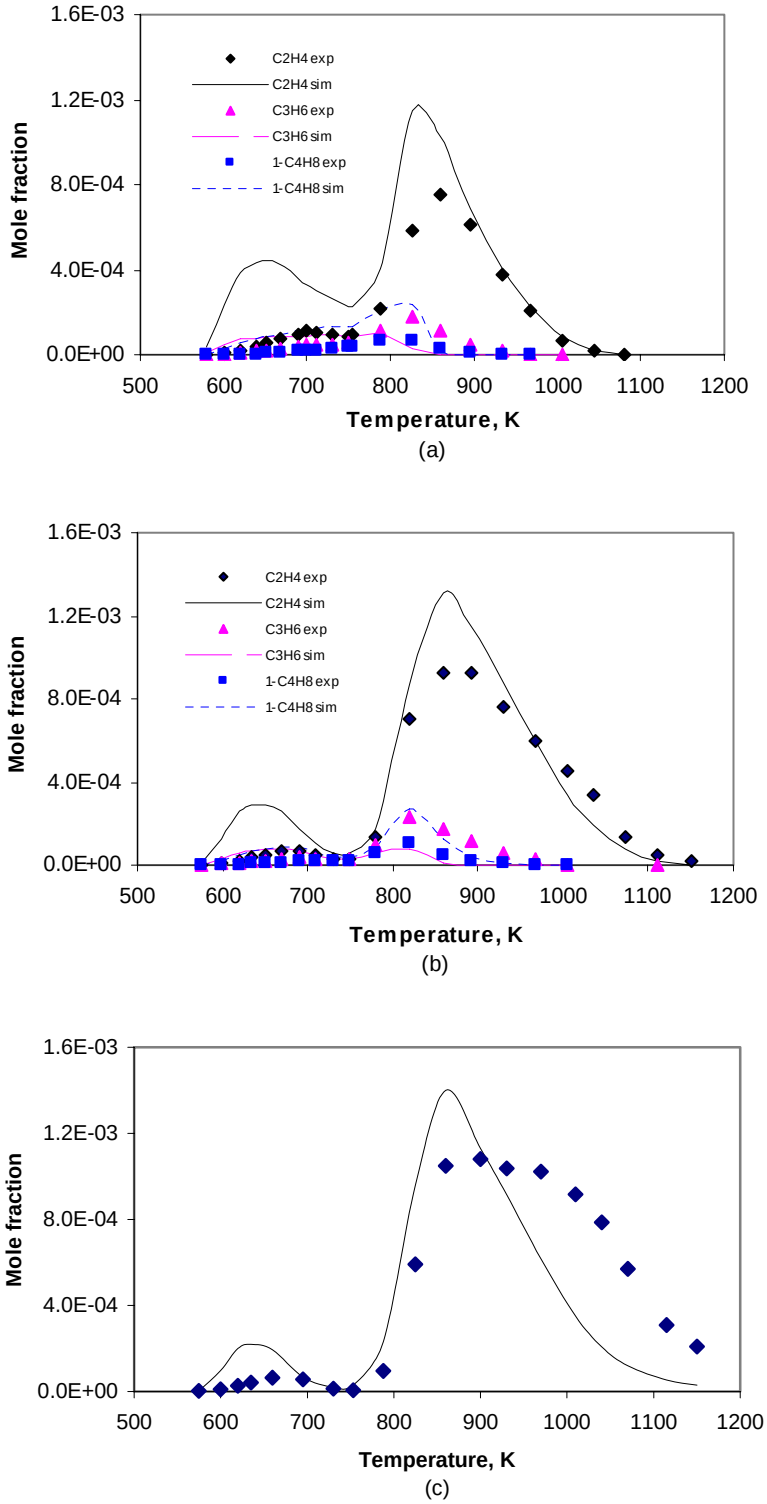

Fig. 5.9: Oxidation of 0.1 % n-heptane in a jet-stirred reactor at 10 bar and a contact time of 1 s. Comparison between experimental and calculated concentrations of C_2H_4, C_3H_6 and 1-C_4H_8. Equivalence ratio = 0.5 (a); 1.0 (b); 1.5 (c).

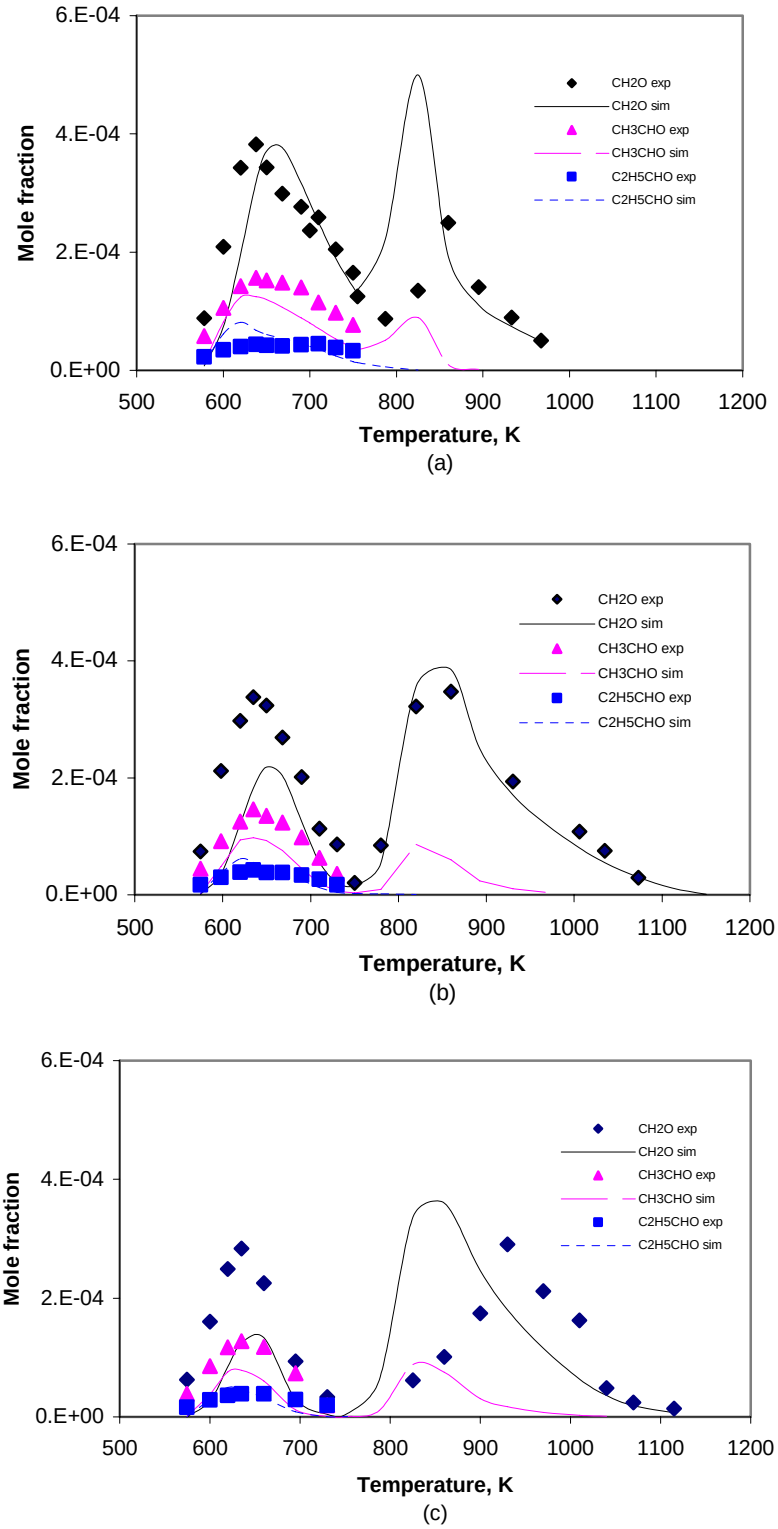

Fig. 5.10: *Oxidation of 0.1 % n-heptane in a jet-stirred reactor at 10 bar and a contact time of 1 s. Comparison between experimental and calculated concentrations of CH_2O, CH_3CHO and C_2H_5CHO. Equivalence ratio = 0.5 (a); 1.0 (b); 1.5 (c).*

5.3 Iso-octane

The coupling of the sub-mechanism from MOLEC and the handwritten C_0-C_4 sub-mechanism for a branched paraffin fuel, i.e. iso-octane, composes a kinetic model of this fuel comprising 3361 elementary reactions among 950 species. The model was simulated to reproduce experimental measurements investigated by Dagaut et al. [23] in an isothermal jet-stirred reactor at 10 bar in a temperature range of 550 K - 1150 K for four equivalence ratios (0.3, 0.5, 1.0 and 1.5) and 99 vol.-% dilution by nitrogen with a residence time of 1 s. The comparisons between the experimental and predicted concentrations of products and major intermediates are depicted in Fig. 5.11 to Fig. 5.19.

Fig. 5.11 shows the profiles of the iso-octane concentration for equivalence ratios of 0.5, 1.0 and 1.5. The kinetic model gives a good prediction, especially for the fuel-lean and stoichiometric mixtures. From this figure it can be seen that in the low-temperature regime only a very small fraction of iso-octane is converted to products, showing the non-knocking tendency of this fuel under these conditions. A weak NTC is experimentally observed and numerically calculated, which is obvious for the equivalence ratio 0.5. Above 780 K, a high temperature oxidation of iso-octane takes place.

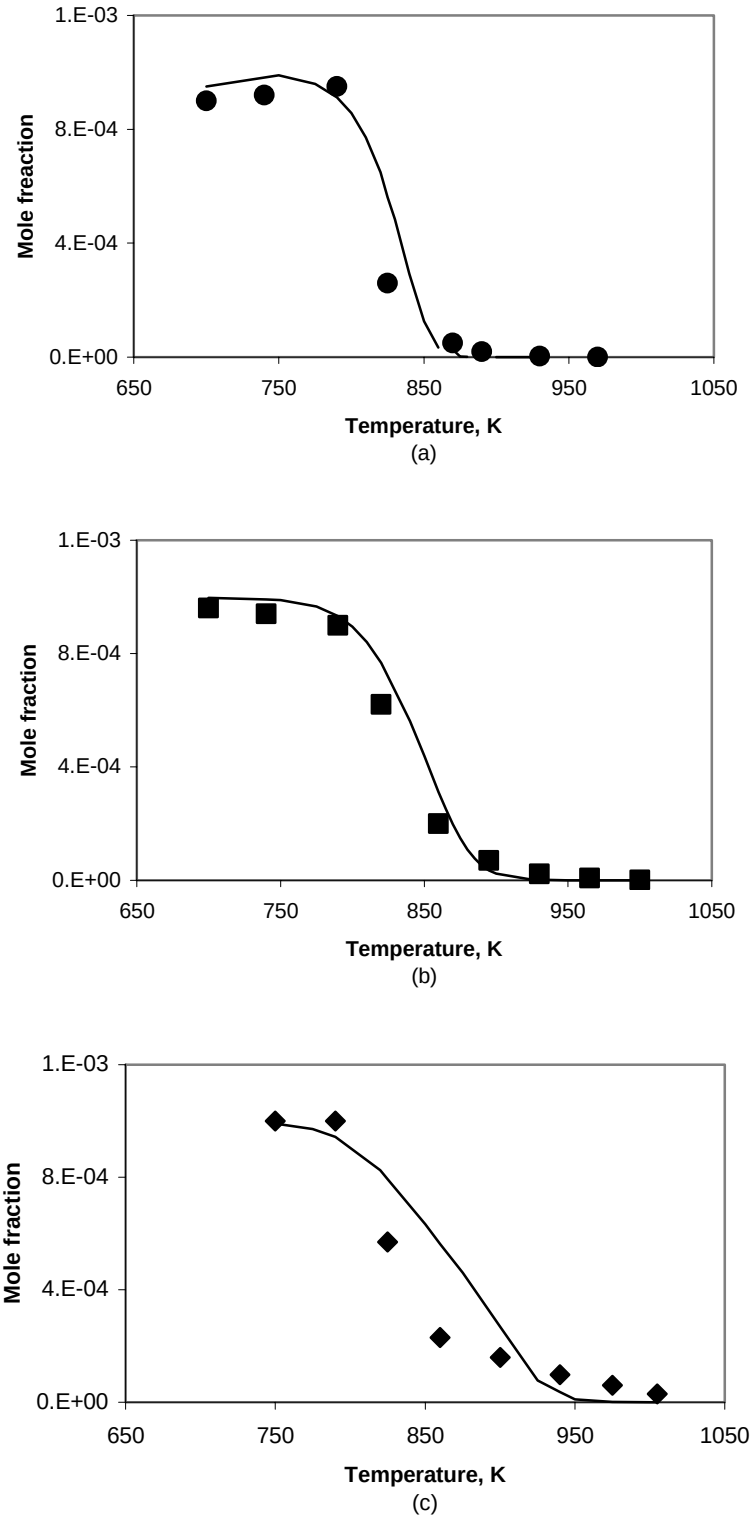

Fig. 5.11: Oxidation of 0.1 % iso-octane in a jet-stirred reactor at 10 bar and a contact time of 1 s. Comparison between experimental and calculated concentrations of iso-octane. Equivalence ratio = 0.5 (a); 1.0 (b); 1.5 (c).

Figures 5.12 and 5.13 exhibit the profiles of the experimental and calculated concentrations of carbon monoxide and carbon dioxide for the equivalence ratios 0.5 and 1.0. The calculations generally agree with the experiments for both species. The experiments show that carbon monoxide is the intermediate of highest concentration in the low- and high-temperature oxidation regimes. This species is produced rapidly above 780 K and reaches a maximum value. The peak of its concentration is shifted towards higher temperatures with decreasing the oxygen concentration in the initial mixture. As seen in Fig. 5.13, it is clear that by decreasing the amount of oxygen in the initial mixture, the rate of carbon dioxide formation will slow down.

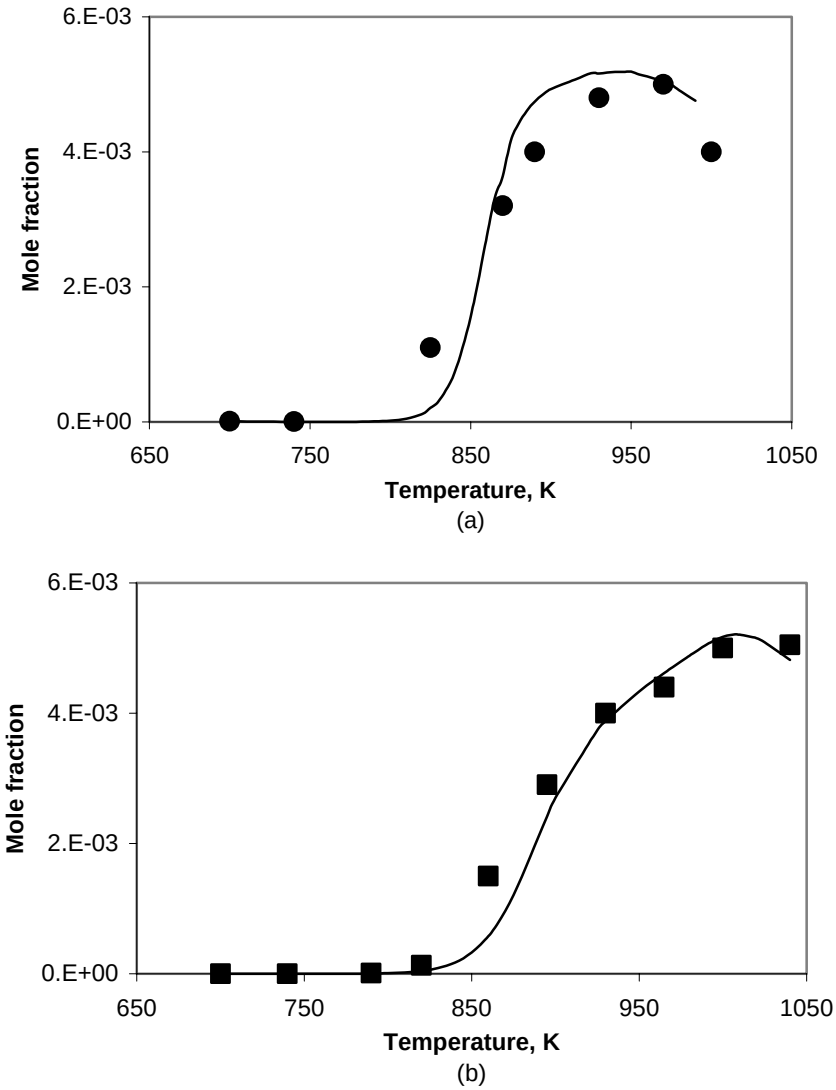

Fig. 5.12: Oxidation of 0.1 % iso-octane in a jet-stirred reactor at 10 bar and a contact time of 1 s. Comparison between experimental and calculated concentrations of carbon monoxide. Equivalence ratio = 0.5 (a); 1.0 (b).

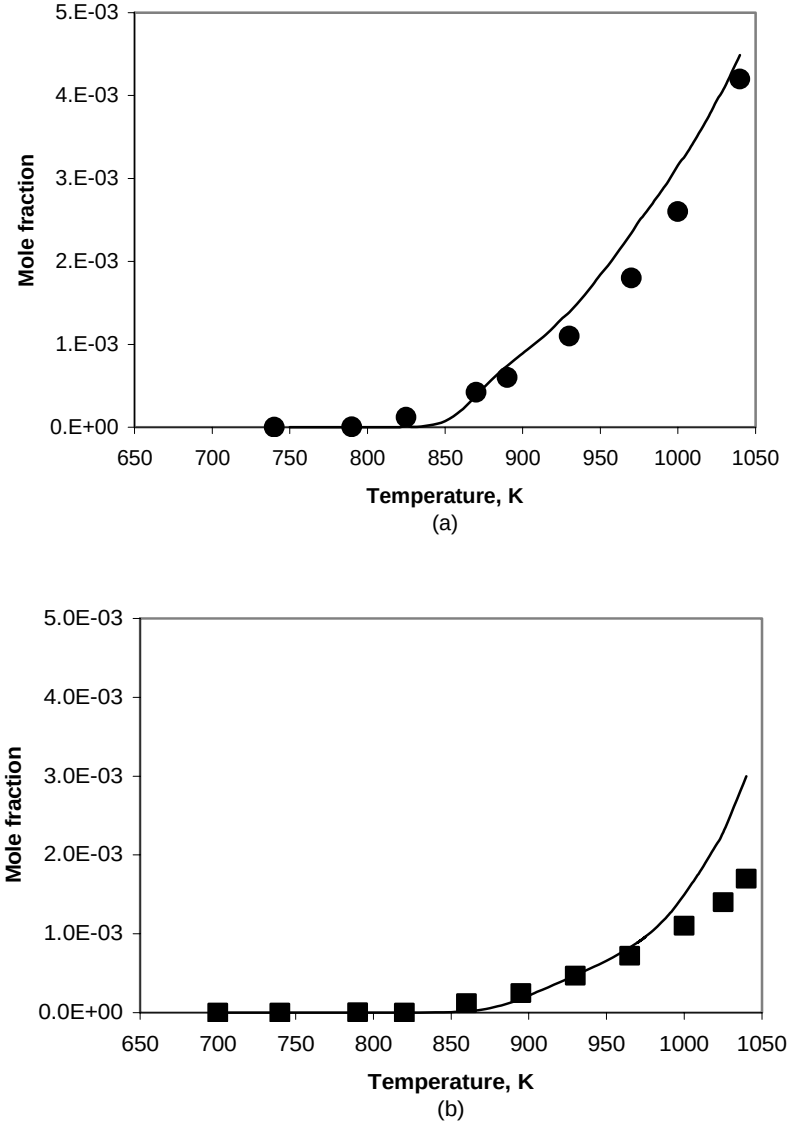

Fig. 5.13: Oxidation of 0.1 % iso-octane in a jet-stirred reactor at 10 bar and a contact time of 1 s. Comparison between experimental and calculated concentrations of carbon dioxide. Equivalence ratio = 0.5 (a); 1. 0 (b).

Methane is a major paraffinic intermediate in the high temperature oxidation of iso-octane, followed by ethane. The profiles of the experimental and calculated concentrations of methane and ethane are shown in Figs. 5.14 and 5.15, respectively. The calculations overpredict the concentrations of these intermediates by the order of 1.5 for all mixture conditions. Calculations and experiments show that the decrease of the oxygen concentration in the initial mixture will increase the concentrations of methane and ethane and shift the peaks of these concentrations towards higher temperatures.

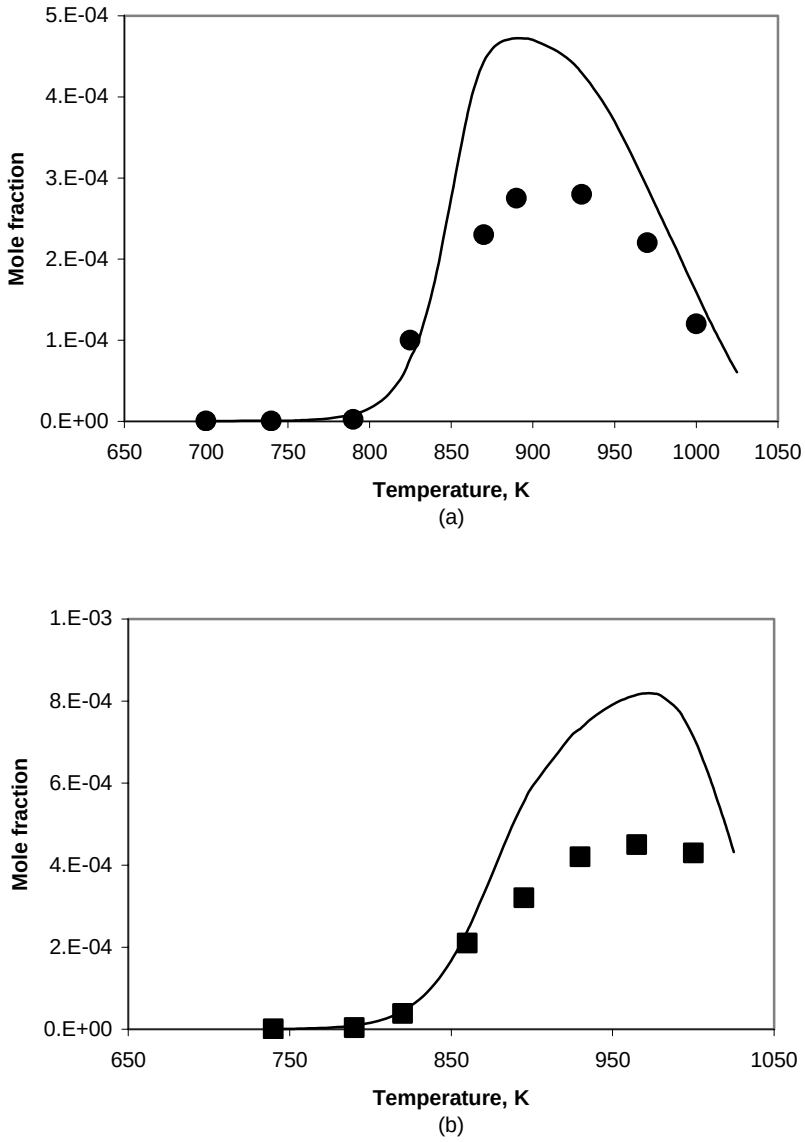

Fig. 5.14: Oxidation of 0.1 % iso-octane in a jet-stirred reactor at 10 bar and a contact time of 1 s. Comparison between experimental and calculated concentrations of methane. Equivalence ratio = 0.5 (a); 1.0 (b).

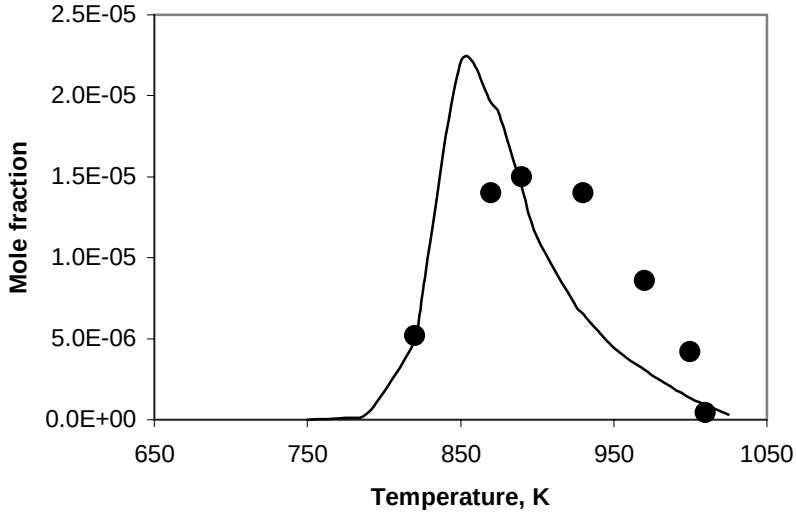

(a)

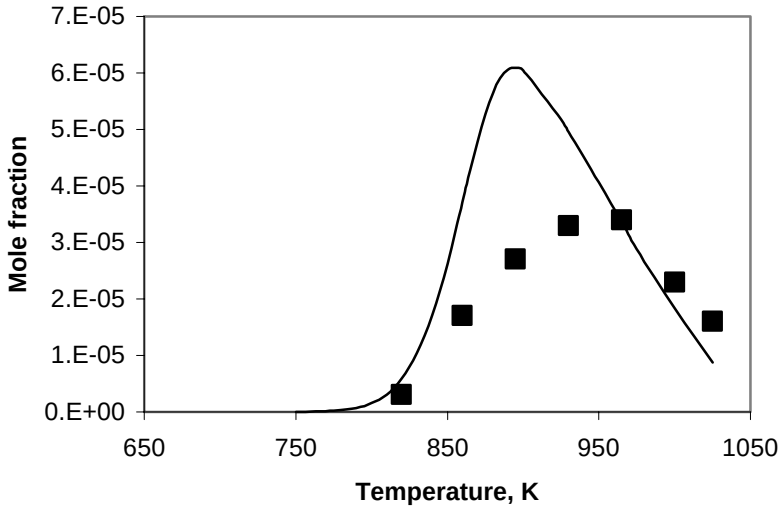

(b)

Fig. 5.15: Oxidation of 0.1 % iso-octane in a jet-stirred reactor at 10 bar and a contact time of 1 s. Comparison between experimental and calculated concentrations of ethane. Equivalence ratio = 0.5 (a); 1.0 (b).

Good agreement for the experimental and predicted concentrations of 1-butene and ethylene, which are major olefinic intermediates, is achieved as shown in Fig. 5.16 and Fig. 5.17, respectively, while the propene concentration is overestimated by the model by the order of 2 as presented in Fig. 5.18. The increases of the 1-butene and ethylene concentration with decreasing the amount of oxygen are evident. The shifts of the peaks of

the 1-butene and ethylene concentration towards higher temperatures with decreasing the amount of oxygen are also obvious.

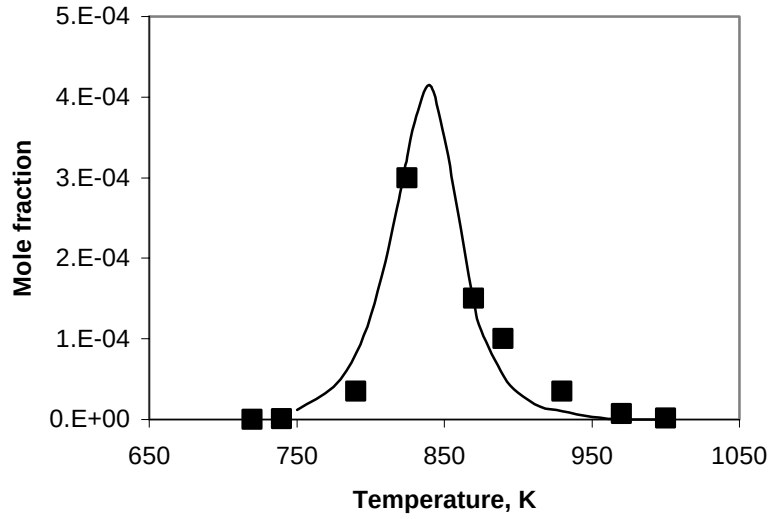

(a)

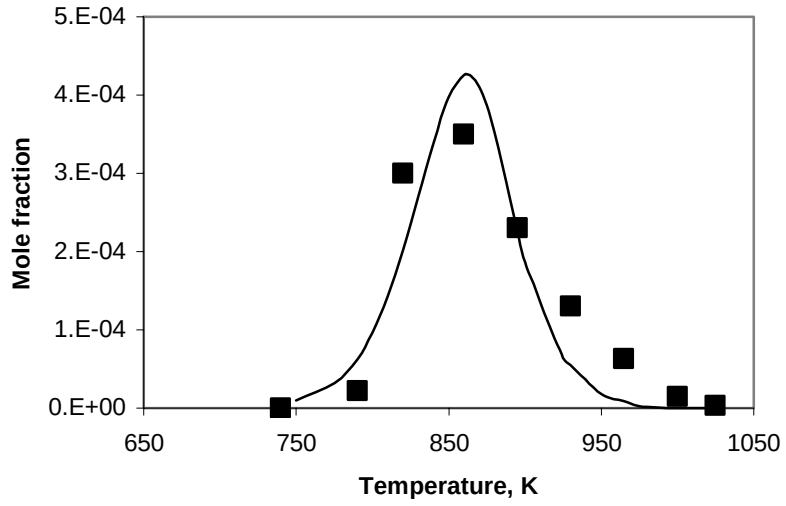

(b)

Fig. 5.16: Oxidation of 0.1 % iso-octane in a jet-stirred reactor at 10 bar and a contact time of 1 s. Comparison between experimental and calculated concentrations of 1-butene. Equivalence ratio = 0.5 (a); 1.0 (b).

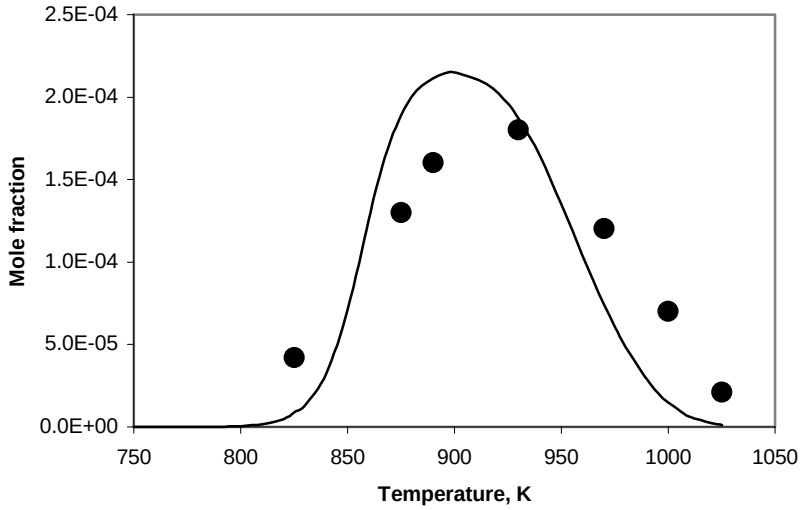

(a)

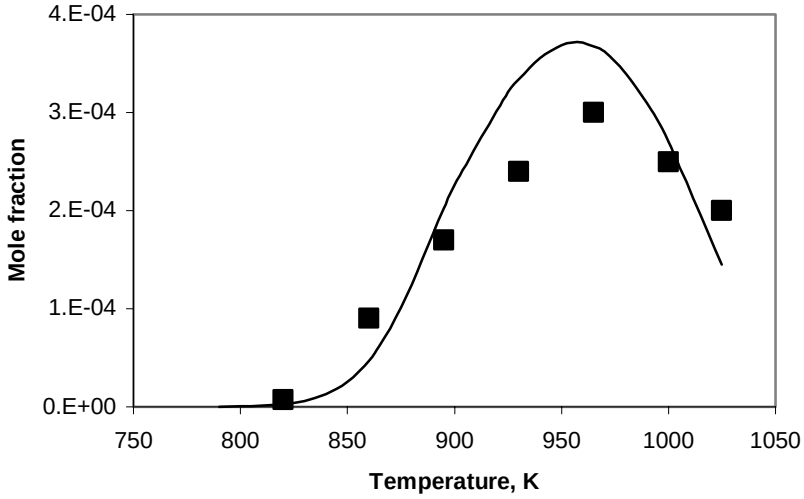

(b)

Fig. 5.17: Oxidation of 0.1 % iso-octane in a jet-stirred reactor at 10 bar and a contact time of 1 s. Comparison between experimental and calculated concentrations of ethylene. Equivalence ratio = 0.5 (a); 1.0 (b).

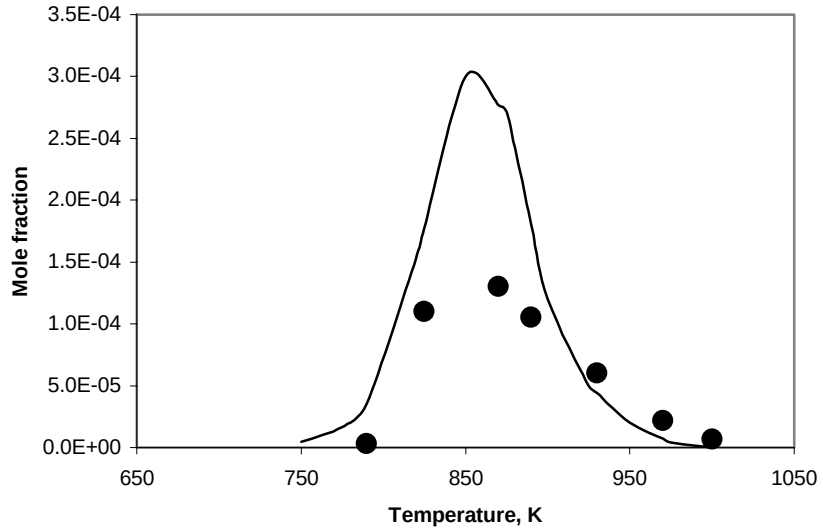

(a)

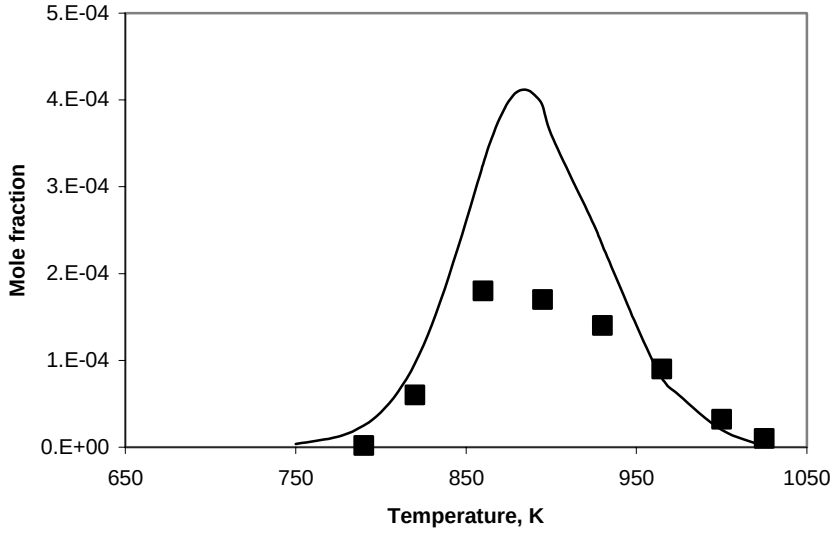

(b)

Fig. 5.18: Oxidation of 0.1 % iso-octane in a jet-stirred reactor at 10 bar and a contact time of 1 s. Comparison between experimental and calculated concentrations of propene. Equivalence ratio = 0.5 (a); 1.0 (b).

The highest concentration level of any oxygenated intermediate produced during the iso-octane oxidation is achieved by formaldehyde. Even though the model slightly overestimates the experimental concentration, the tendency that the fuel-rich mixtures produce a higher concentration of formaldehyde than the fuel-lean mixtures is evident, as shown in Fig. 5.19. The tendency that the fuel-rich mixtures shift the peak of the formaldehyde concentration towards higher temperatures is also obvious.

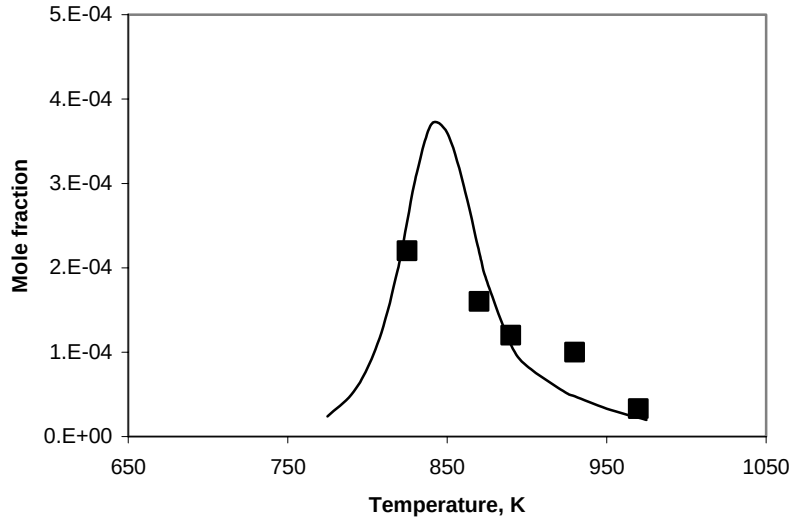

(a)

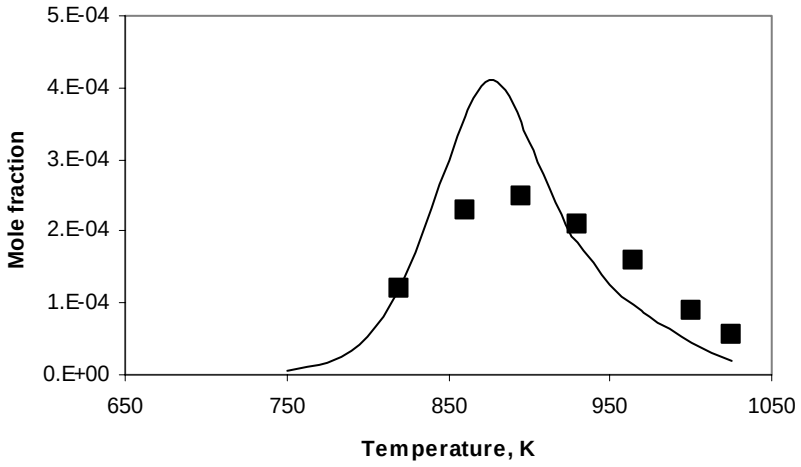

(b)

Fig. 5.19: Oxidation of 0.1 % iso-octane in a jet-stirred reactor at 10 bar and a contact time of 1 s. Comparison between experimental and calculated concentrations of formaldehyde. Equivalence ratio = 0.5 (a); 1.0 (b).

5.4 N-decane

The mechanism for n-decane oxidation involves 1253 species taking part in 4177 reactions. Two different experimental environments are used to verify the mechanism. They are experiments in a shock tube and in a jet-stirred reactor.

5.4.1 Shock tube

Pfahl et al. [20] have investigated ignition delay times of n-decane in the temperature range 700 K - 1300 K and at two pressure levels, 13 bar and 50 bar. Figure 5.20 shows the ignition delay time at 13.5 bar versus the inverse of initial temperatures for the equivalence ratios 0.5, 1.0 and 2.0.

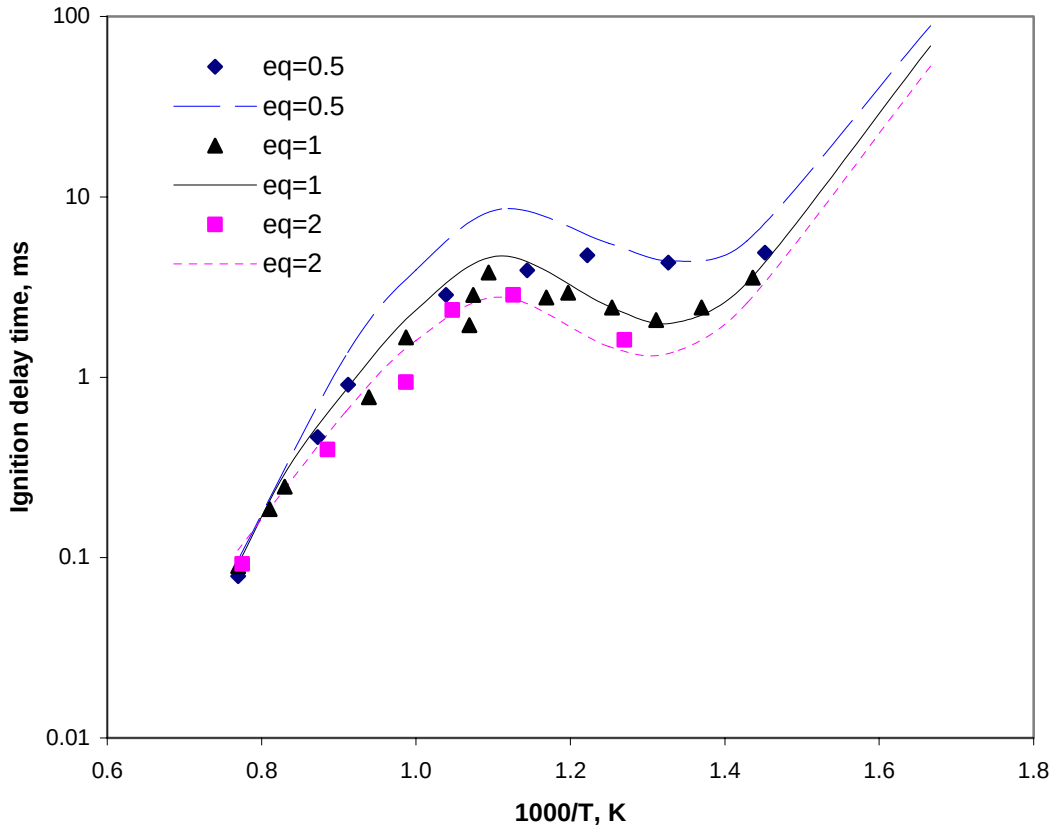

Fig. 5.20: Ignition delay times of stoichiometric n-decane/air versus the inverse of the initial temperature behind the reflected shock wave at 13.5 bar. Symbols indicate the experimental results; lines, calculations.

In general, the numerically predicted ignition delay times agree well with the experimentally derived ones. A linear temperature dependency of the ignition delay times in the low-temperature region is shown experimentally and numerically. The S-shaped dependence (NTC) of the ignition-delay times on the temperature marks the transition from high- to low- temperature kinetics, which is typical for n-alkanes and was also obtained for n-heptane. The dependence of the ignition delay times on the equivalence ratio is not distinct for temperatures below 700 K and above 900 K, but in the intermediate-temperature regime a strong dependence can be observed. At the constant initial pressure 13.5 bar and temperatures up to 1250 K the model exhibits that the fuel-rich mixtures autoignite more easily than the fuel-lean mixtures. At higher temperatures the contrary trend occurs where the fuel-lean mixtures burn faster than the fuel-rich mixtures. Recalling the discussion on n-heptane above, the temperature point at which the contrary trend occurs is practically constant with increasing the number of C atoms in normal alkanes.

Figure 5.21 depicts the ignition delay times at a pressure of 50 bar for the equivalence ratios 0.67, 1.0 and 2.0. As can be seen, the model reproduces well the ignition delay times of the stoichiometric mixtures, but overpredicts those of the fuel-lean and fuel-rich ones. The behavior of the ignition delay times at 50 bar is experimentally and numerically similar to that at 13.5 bar.

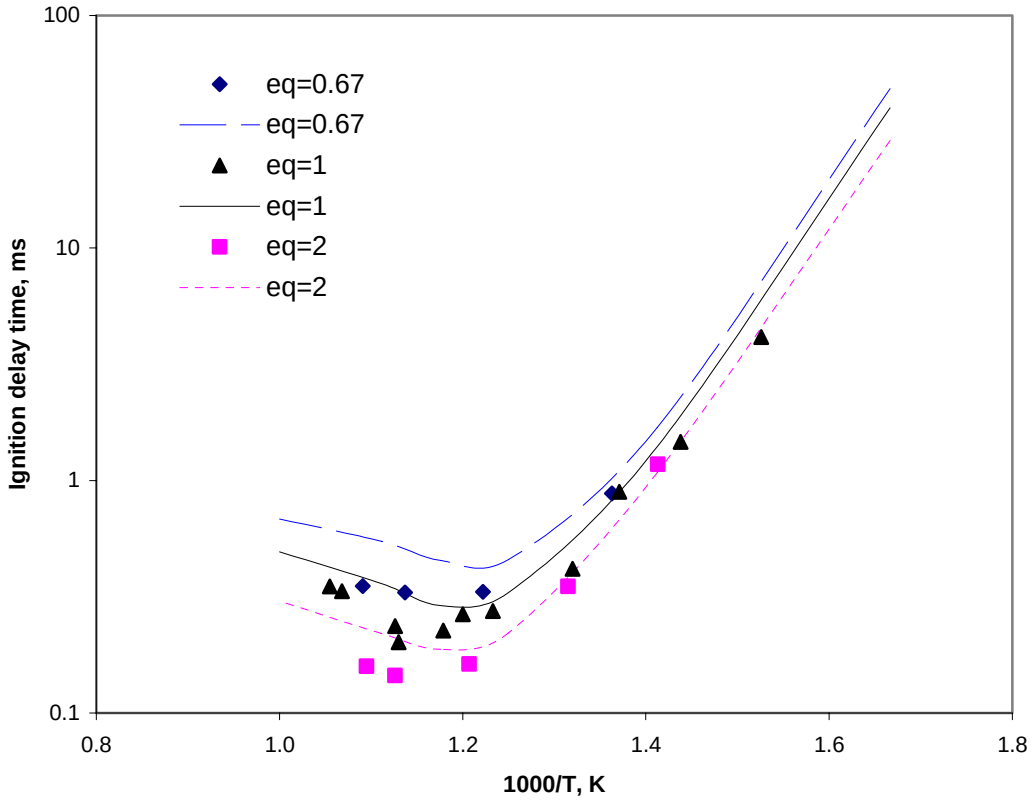

Fig. 5.21: Ignition delay times of stoichiometric n-decane/air versus the inverse of the initial temperature behind the reflected shock wave at 50 bar. Symbols indicate the experimental results; lines, calculations.

5.4.2 Jet-stirred reactor

The oxidation of n-decane in a high-pressure jet-stirred reactor has been investigated experimentally by Dagaut et al. [45]. The experiments were performed for a wide range of temperatures (550 K - 1150 K) at a pressure of 10 bar, an equivalence ratio of 1 and 99 vol.-% dilution by nitrogen. Reactants, intermediates and final products have been measured. Thus, this data set provides a detailed picture of n-decane oxidation. Numerical calculations were performed under isothermal and constant pressure conditions. Figure 5.22 presents a comparison between experimentally derived and numerically predicted concentrations of n-decane at a contact time of 1 s. Good agreement is achieved by the model within the investigated temperature range.

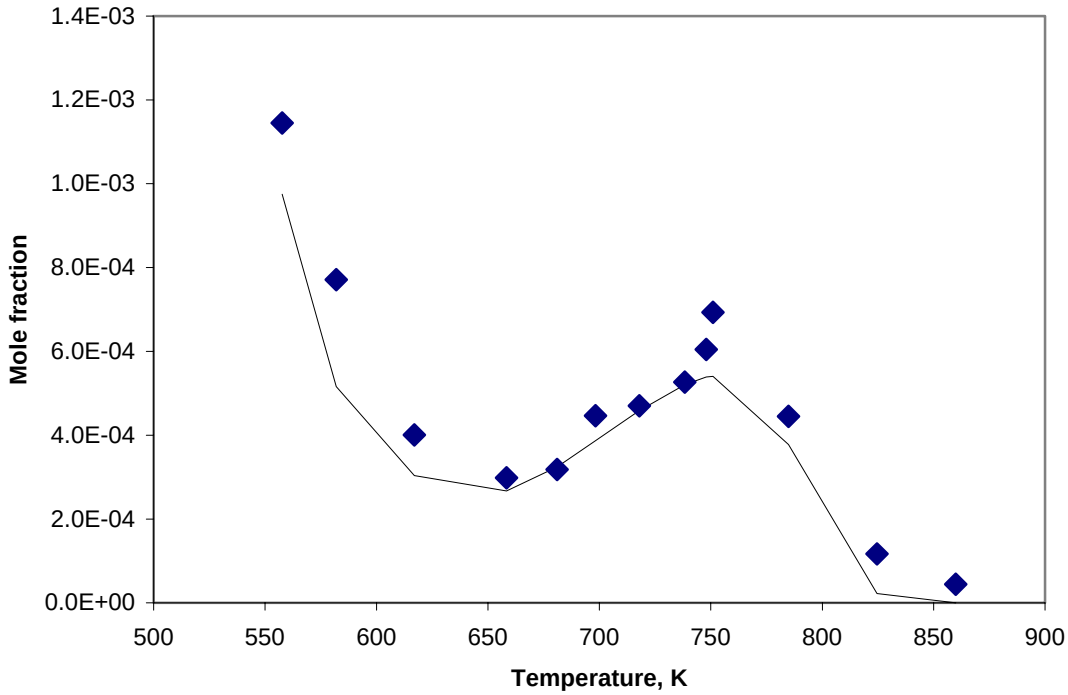

Fig. 5.22: Oxidation of 0.1 % n-decane in a jet-stirred reactor at 10 bar, an equivalence ratio of 1.0 and a contact time of 1 s. Comparison between experimental and calculated conversion of n-decane.

As seen in Fig. 5.22, below 750 K the oxidation of n-decane takes place through the low temperature mechanism. Below 660 K, a large fraction of n-decane is converted to products, corresponding to a slow oxidation and a cool flame region. Between 660 K and 750 K, a negative temperature coefficient is observed experimentally and this region is also reproduced well by the kinetic model. Above 750 K, a fast oxidation takes place though the high temperature mechanism.

The experimental and calculated profiles of carbon monoxide and carbon dioxide are shown in Figs. 5.23. The model predicts the concentration of carbon monoxide within the investigated temperature range very well. For carbon dioxide, the concentration is also very well reproduced in the high-temperature regime, but underestimated in the low-temperature region. The high concentration of carbon monoxide shows that this species is a major oxygenated intermediate in both low- and high- temperature regimes. The behavior of carbon monoxide and carbon dioxide in n-decane oxidation is similar to that in n-heptane oxidation. In the low-temperature region the concentration of carbon monoxide peaks at 660 K, corresponding to the highest level of conversion of n-decane (Fig. 5.22).

Above 780 K, the CO concentration sharply increases until a maximum value at about 980 K is achieved. Meanwhile, the CO_2 concentration exponentially increases above 780 K.

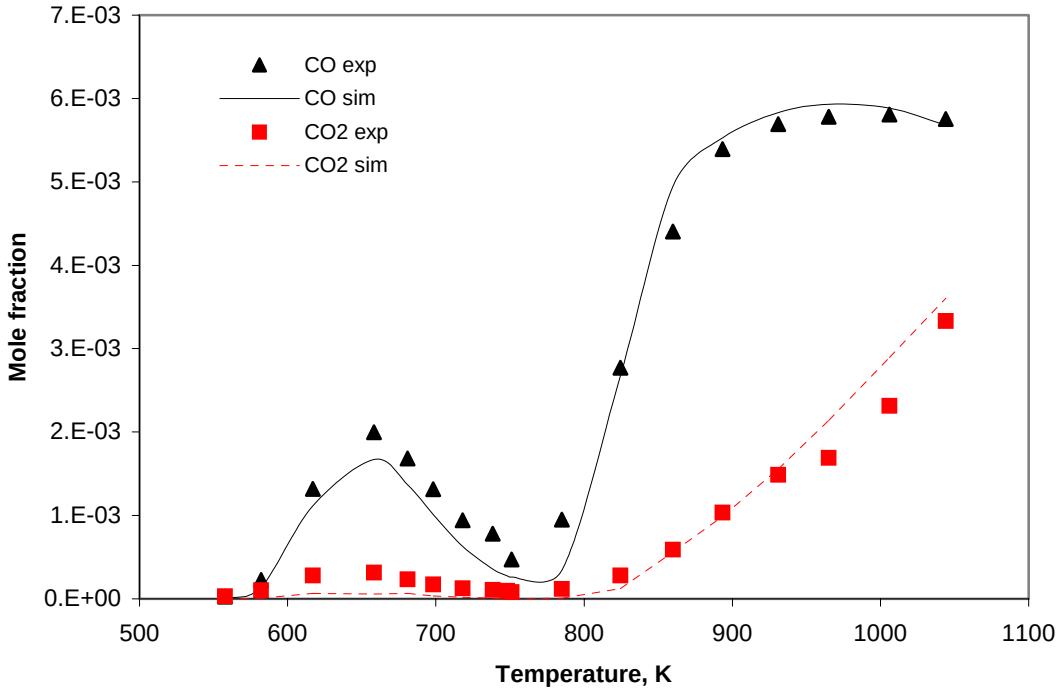

Fig. 5.23: Oxidation of 0.1 % n-decane in a jet-stirred reactor at 10 bar, an equivalence ratio of 1.0 and a contact time of 1 s. Comparison between experimental and calculated conversion of carbon monoxide and carbon dioxide.

Methane is a major paraffinic intermediate of n-decane oxidation in the high-temperature regime. The concentration of this intermediate is also very well reproduced by the mechanism, as presented in Fig. 5.24. Similar to its behavior in n-heptane oxidation, under the same conditions the methane concentration increases above 750 K and peaks at 950 K. Experiments and the model show this behavior.

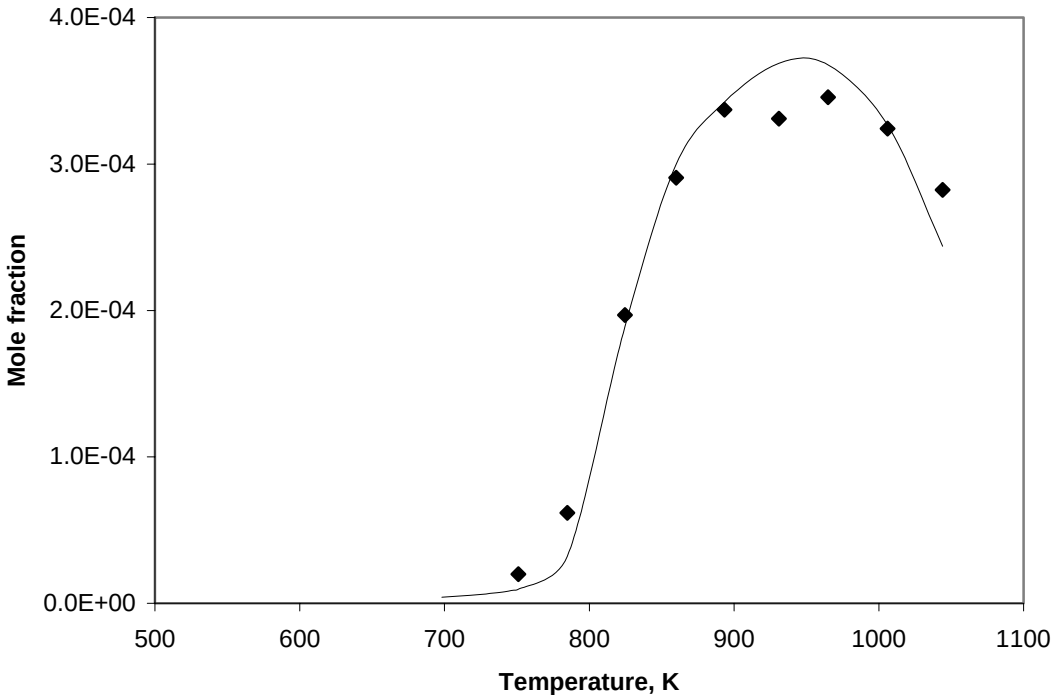

Fig. 5.24: Oxidation of 0.1 % n-decane in a jet-stirred reactor at 10 bar, an equivalence ratio of 1.0 and a contact time of 1 s. Comparison between experimental and calculated conversion of methane.

Among the olefins, ethylene is a major intermediate, followed by propene and 1-butene. Their experimental and predicted concentrations are exhibited in Fig. 5.25. The model clearly overestimates these olefin concentrations in the low-temperature region. In the high-temperature regime the model overpredicts the 1-butene concentration and underpredicts the propene concentration.

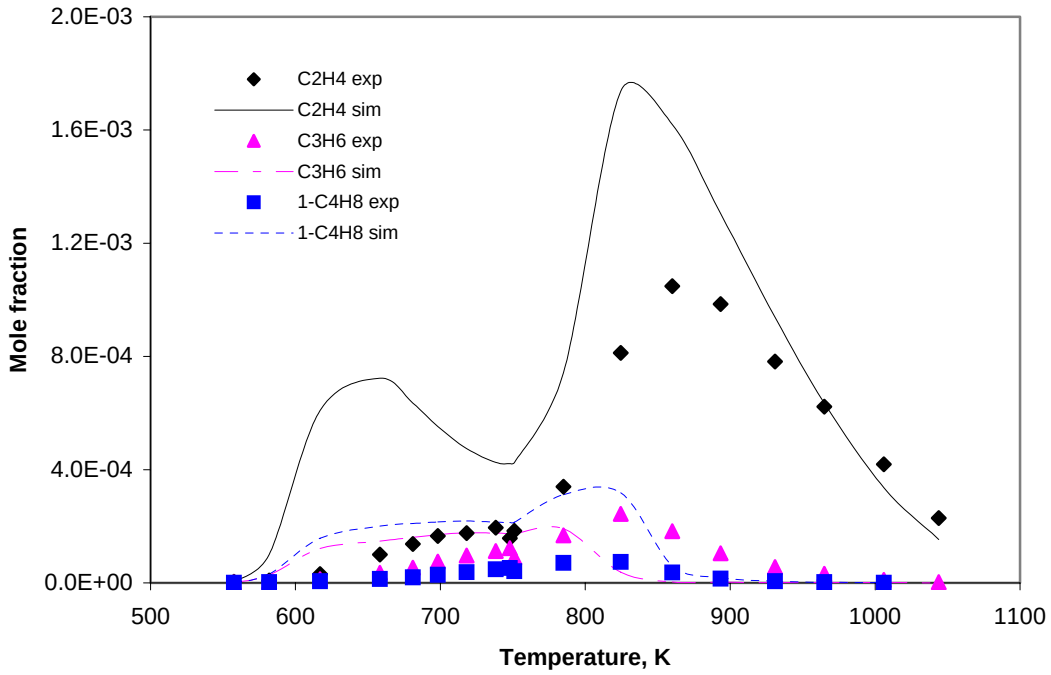

Fig. 5.25: Oxidation of 0.1 % n-decane in a jet-stirred reactor at 10 bar, an equivalence ratio of 1.0 and a contact time of 1 s. Comparison between experimental and calculated conversion of ethylene, propene and 1-butene.

The importance of formaldehyde in the cool-flame chemistry besides carbon monoxide is correctly predicted by the model in the low-temperature region, but rather overestimated in the high-temperature regime, as can be seen in Fig. 5.26. Nevertheless, in the high-temperature region the formaldehyde concentration peaks at the same temperature as experimental observation. For acetaldehyde and propylaldehyde, the same behaviors as for formaldehyde in the low-temperature regime are seen numerically. Their maximum concentration values are slightly shifted towards higher temperatures in the order propylaldehyde to formaldehyde. In the high-temperature regime acetaldehyde is still produced in significant concentrations, which peak at approximately the same temperature as formaldehyde.

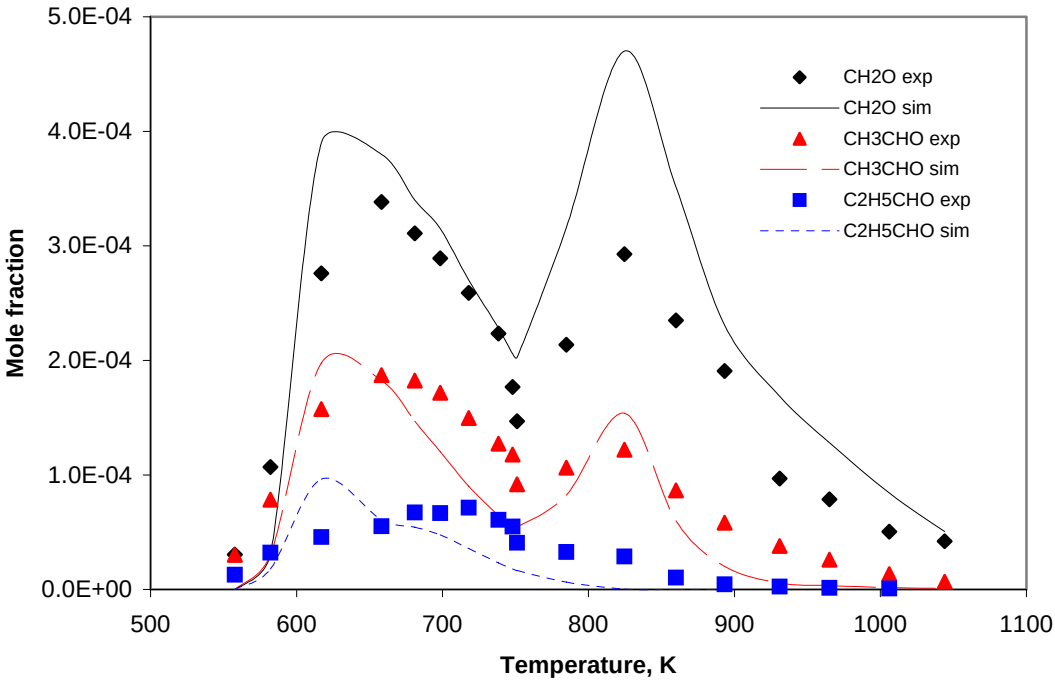

Fig. 5.26: Oxidation of 0.1 % n-decane in a jet-stirred reactor at 10 bar, an equivalence ratio of 1.0 and a contact time of 1 s. Comparison between experimental and calculated conversion of formaldehyde, acetaldehyde and propylaldehyde.

Chapter 6

MECHANISM ANALYSES

Complete reaction mechanisms for the oxidation and combustion of large hydrocarbons may consist of several thousand elementary reactions. Many of them may be unimportant, so that they can be neglected. Therefore, analysis methods eliminating negligible reactions are of interests. Two of these methods, sensitivity and reaction flow analysis, were applied on the mechanisms that have been validated and discussed in Chapter 5.

6.1 Sensitivity Analysis

A sensitivity analysis is used to identify rate-limiting reaction steps. This analysis will be performed in detail on each reaction in the mechanisms. In view of its greater impact on engine knock chemistry, only sensitivity analysis for shock-tube experimental results of Ciezki and Adomeit [19] and Pfahl et al. [20] covering low-temperature kinetics will be discussed in this chapter.

Numerical calculations for sensitivity analysis were carried out by changing the rate coefficient of a particular reaction and calculating the OH concentration. The difference between the OH concentration before and after changing the rate coefficient was then calculated. This result was compared to the largest difference obtained in the system. This is called sensitivity coefficient. A sensitivity coefficient might be positive or negative. A positive sensitivity coefficient indicates a higher OH concentration and an increased overall reaction rate, and a negative sensitivity coefficient indicates a lower OH concentration and a decreased overall reaction rate of the system. Sensitivity coefficients in a system are drawn in the form of a bar diagram. Only major oxidation pathways responsible for the fuel oxidation are shown. Figures 6.1 to 6.5 show this type of diagram. Emphasis was placed on determining the differences between reaction pathways at low, intermediate and high temperatures.

6.1.1 Low temperature

Figure 6.1 shows sensitivity coefficients of a stoichiometric n-heptane/air mixture in a shock tube at a pressure of 13.5 bar and an initial temperature of 600 K. From this figure,

we observe that at low temperatures the ignition of normal alkane is governed by fuel-specific processes leading to very complex reaction systems, if the numerous isomeric structures are taken into account. It is clear that the overall rate of fuel oxidation is directly controlled by the fuel so that the ignition process of fuel-rich mixtures is faster than that of fuel-lean mixtures.

The type of reaction possessing the most effective (highest positive sensitivity) in promoting the overall rate of the fuel oxidation is homolytic O-O scission of hydroperoxydes to form alkoxy radicals and OH radicals (Rule 3.2.6),

$4C_7OOH \rightarrow OH + 4C_7H_{15}O$
$5C_7OOH \rightarrow OH + 5C_7H_{15}O$
$6C_7OOH \rightarrow OH + 6C_7H_{15}O.$

This type of reaction is chain branching because it produces two radicals from a stable molecule. Because of the high activation energy (170 kJ/mol), this reaction occurs quite slowly at 600 K. As the fuel oxidation proceeds, heat released is used to raise the temperature of the reacting system so that these stable hydroperoxyde molecules decompose more easily. This dynamic behaviour ensures a greater reactivity of the system and is responsible for cool-flame ignitions at low temperatures.

Alkyl radicals produced through initiation steps in the fuel oxidation undergo addition to molecular oxygen, leading to the formation of alkylperoxy radicals at low temperatures. We observe a low sensitivity to this reaction. However, the subsequent reaction involving alkylperoxy radicals, i.e. external H-atom abstraction from fuel to yield hydroperoxydes (Rule 3.2.3), possesses a positive high sensitivity coefficient. Thus, it promotes the overall rate of the fuel oxidation,

$C_7H_{16} + 4\text{-}C_7O_2 \rightarrow 2\text{-}C_7H_{15} + 4C_7OOH$
$C_7H_{16} + 5\text{-}C_7O_2 \rightarrow 1\text{-}C_7H_{15} + 5C_7OOH$
$C_7H_{16} + 5\text{-}C_7O_2 \rightarrow 3\text{-}C_7H_{15} + 5C_7OOH$
$C_7H_{16} + 6\text{-}C_7O_2 \rightarrow 2\text{-}C_7H_{15} + 6C_7OOH$
$C_7H_{16} + 6\text{-}C_7O_2 \rightarrow 3\text{-}C_7H_{15} + 6C_7OOH.$

This high positive sensitivity coefficient is easily understood as the subsequent reaction, i.e. decomposition of hydroperoxyde molecules, is a chain branching process as explained above.

H-atom abstraction from fuel by hydroxyl radicals has also a high positive sensitivity coefficient because the hydroxyl radical is the most reactive radical and possesses a high concentration during ignition delays.

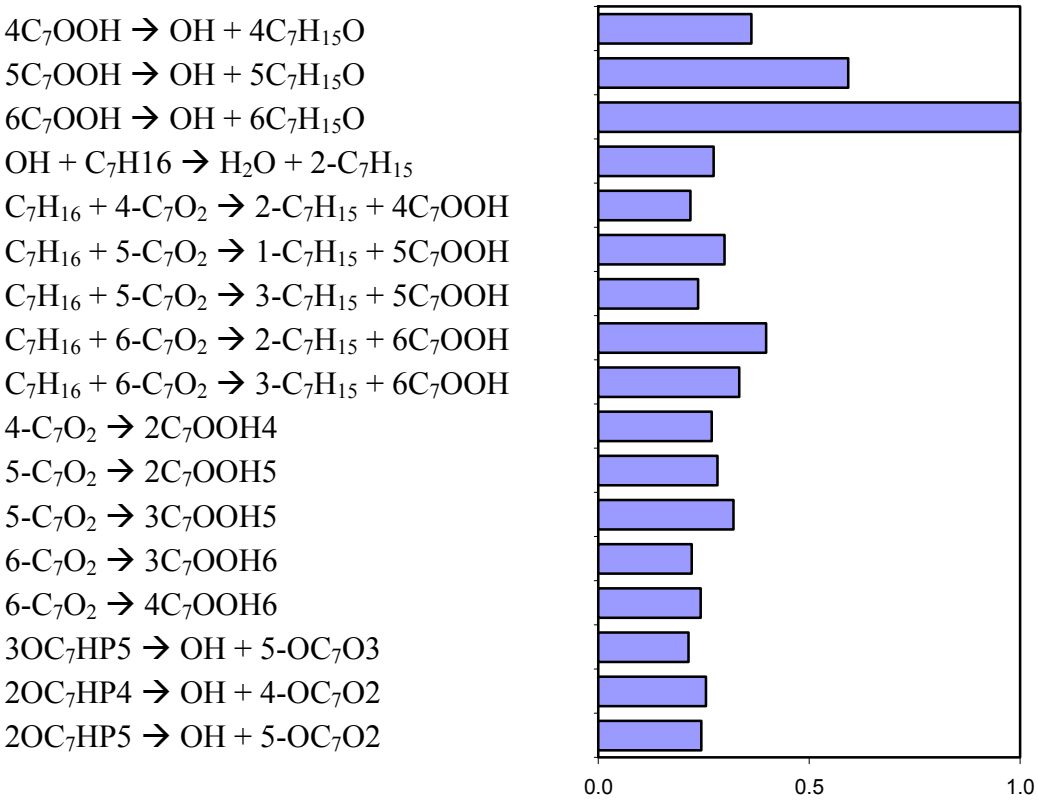

Fig. 6.1: Sensitivity coefficients of a stoichiometric n-heptane/air mixture in a shock tube at a pressure of 13.5 bar and an initial temperature of 600 K. Only sensitivity coefficient larger than 0.2 are listed.

Another chain branching, i.e. decomposition of a ketohydroperoxyde molecule leading to the formation of two radicals, a carbonyl radical and a hydroxyl radical (Rule 3.1.18), is the next greatest in promoting the overall rate of the fuel oxidation at low temperatures,

$3OC_7HP5 \rightarrow OH + 5\text{-}OC_7O3$
$2OC_7HP4 \rightarrow OH + 4\text{-}OC_7O2$
$2OC_7HP5 \rightarrow OH + 5\text{-}OC_7O2.$

In the symbol of ketohydroperoxyde molecules above, $3OC_7HP5$ for instance, 3 refers to the site at which the keto group is attached and 5 refers to the site at which the

hydroperoxy group is attached. In the symbol of carbonyl radicals, 5-OC_7O3 for example, 3 refers to the site at which the keto group is attached and 5 refers to the site at which the oxo group is attached. Similar to decomposition of hydroperoxyde molecules, this type of reaction has a high activation energy that is difficult to overcome. However, as the fuel oxidation proceeds, heat released is used to raise the temperature of the reacting system so that these ketohydroperoxyde molecules decompose more easily.

Internal H-atom abstraction of alkylperoxy radicals (Rule 3.2.2) also shows a positive sensitivity coefficient. Thus, its influence on the reactivity of the system is positively large,

4-C_7O_2 → $2C_7OOH4$
5-C_7O_2 → $2C_7OOH5$
5-C_7O_2 → $3C_7OOH5$
6-C_7O_2 → $3C_7OOH6$
6-C_7O_2 → $4C_7OOH6$.

This type of reaction competes with external H-atom abstraction from fuel via alkylperoxy radical attack described above, produces hydroperoxy alkyl radicals, which in turn undergo second addition to molecular oxygen (Rule 3.2.8) to yield peroxy hydroperoxy alkyl radicals. After isomerization of peroxy hydroperoxy alkyl radicals (Rule 3.2.15), the successive reactions, i.e. decomposition of a dihydroperoxy alkyl radical (Rule 3.2.16) and decomposition of a ketohydroperoxyde molecule (Rule 3.2.18), occur and lead to the production of two reactive hydroxyl radicals. These types of reactions lead to an increased reactivity of the fuel oxidation.

6.1.2 Intermediate temperatures

Sensitivity analysis at the onset (750 K), within (800 K) and at the end (900 K) of the NTC region of a stoichiometric n-heptane/air mixture in a shock tube at a pressure of 13.5 bar is exhibited in Fig. 6.2. From this figure it is clear that the most positive sensitivity coefficient in the NTC region is shown by the chain branching reaction, H_2O_2 +M(1) → OH +OH +M(1). Thus, it has the greatest effect in controlling the reactivity of the fuel combustion. The fuel-specific reactions still dominate during the ignition process. H-atom abstraction from fuel via alkylperoxy radical attack, which is a rate-limiting reaction step at 600 K, is not preferred any more in the NTC region. Therefore, the subsequent reaction, i.e. decomposition of hydroperoxy molecules, is not a main chain branching process. H atoms in the fuel are mainly abstracted by the OH radicals at the onset of the NTC region and by the HO_2 radicals at the end of the NTC region,

$OH + C_7H_{16} \rightarrow H_2O + 2\text{-}C_7H_{15}$
$OH + C_7H_{16} \rightarrow H_2O + 3\text{-}C_7H_{15}$
$C_7H_{16} + HO_2 \rightarrow H_2O_2 + 2\text{-}C_7H_{15}$
$C_7H_{16} + HO_2 \rightarrow H_2O_2 + 3\text{-}C_7H_{15}$
$C_7H_{16} + HO_2 \rightarrow H_2O_2 + 1\text{-}C_7H_{15}$

This phenomenon can be described as follows: Although it is not a main pathway, H-atom abstraction from fuel via alkylperoxy radical attack still has a significant effect on the overall rate at 750 K. Therefore, in addition to the decomposition of H_2O_2, decomposition of hydroperoxyde and ketohydroperoxy molecules still has a significant contribution to the OH radical concentration. If temperature increases, alkylperoxy radicals decompose back to alkyl radicals. This leads to an inverse temperature dependency of the reaction or a degenerate chain branching where the OH radical concentration decreases. Due to its high concentration at 900 K, the rather unreactive HO_2 radical, produced directly from the bimolecular initiation step, takes over the role in abstracting H atoms from the fuel so that the fuel oxidation proceeds more slowly than that at 750 K.

Alkyl radicals can undergo addition to molecular oxygen to produce alkylperoxy radicals (Rule 3.2.1) in the NTC region. This type of reaction has a high positive sensitivity coefficient,

$O_2 + 4\text{-}C_7H_{15} \rightarrow 4\text{-}C_7O_2$
$O_2 + 3\text{-}C_7H_{15} \rightarrow 5\text{-}C_7O_2$
$O_2 + 2\text{-}C_7H_{15} \rightarrow 6\text{-}C_7O_2$.

However, since the inverse reaction, i.e. decomposition of hydroperoxy alkyl radicals to alkyl radicals,

$4\text{-}C_7O_2 \rightarrow O_2 + 4\text{-}C_7H_{15}$
$5\text{-}C_7O_2 \rightarrow O_2 + 3\text{-}C_7H_{15}$
$6\text{-}C_7O_2 \rightarrow O_2 + 2\text{-}C_7H_{15}$

possesses a negative sensitivity coefficient with the nearly same order of magnitude to the forward reaction, this type of reaction gives little effect on the reactivity of the fuel oxidation.

The next high positive sensitivity coefficient is exhibited by internal H-atom abstraction of alkylperoxy radicals to yield hydroperoxy alkyl radicals. The fate of these hydroperoxy alkyl radicals has been described above.

$O_2 + N\text{-}C_3H_7 \rightarrow HO_2 + C_3H_6$
$N\text{-}C_3H_7 \rightarrow C_2H_4 + CH_3$
$OH + C_3H_6 \rightarrow H_2O + C_3H_5$
$HO_2 + CH_3O_2 \rightarrow O_2 + CH_3OOH$
$O_2 + CH_3 + M(1) \rightarrow CH_3O_2 + M(1)$
$H_2O_2 + M(1) \rightarrow OH + OH + M(1)$
$HO_2 + HO_2 \rightarrow O_2 + H_2O_2$
$OH + HO_2 \rightarrow O_2 + H_2O$
$OH + C_7H_{16} \rightarrow H_2O + 2\text{-}C_7H_{15}$
$OH + C_7H_{16} \rightarrow H_2O + 3\text{-}C_7H_{15}$
$C_7H_{16} + HO_2 \rightarrow H_2O_2 + 2\text{-}C_7H_{15}$
$C_7H_{16} + HO_2 \rightarrow H_2O_2 + 3\text{-}C_7H_{15}$
$C_7H_{16} + HO_2 \rightarrow H_2O_2 + 1\text{-}C_7H_{15}$
$4\text{-}C_7O_2 \rightarrow O_2 + 4\text{-}C_7H_{15}$
$5\text{-}C_7O_2 \rightarrow O_2 + 3\text{-}C_7H_{15}$
$6\text{-}C_7O_2 \rightarrow O_2 + 2\text{-}C_7H_{15}$
$4\text{-}C_7O_2 \rightarrow 2C_7OOH4$
$6\text{-}C_7O_2 \rightarrow 4C_7OOH6$
$6\text{-}C_7O_2 \rightarrow 5C_7OOH6$
$1\text{-}C_7H_{15} \rightarrow 3\text{-}C_7H_{15}$
$1\text{-}C_7H_{15} \rightarrow 4\text{-}C_7H_{15}$
$3\text{-}C_7H_{15} \rightarrow 1\text{-}C_7H_{15}$
$4\text{-}C_7H_{15} \rightarrow C_2H_5 + 1\text{-}C_5H_{10}$
$3\text{-}C_7H_{15} \rightarrow N\text{-}C_3H_7 + 1\text{-}C_4H_8$
$2\text{-}C_7H_{15} \rightarrow C_3H_6 + P\text{-}C_4H_9$
$O_2 + 4\text{-}C_7H_{15} \rightarrow 4\text{-}C_7O_2$
$O_2 + 3\text{-}C_7H_{15} \rightarrow 5\text{-}C_7O_2$
$O_2 + 2\text{-}C_7H_{15} \rightarrow 6\text{-}C_7O_2$

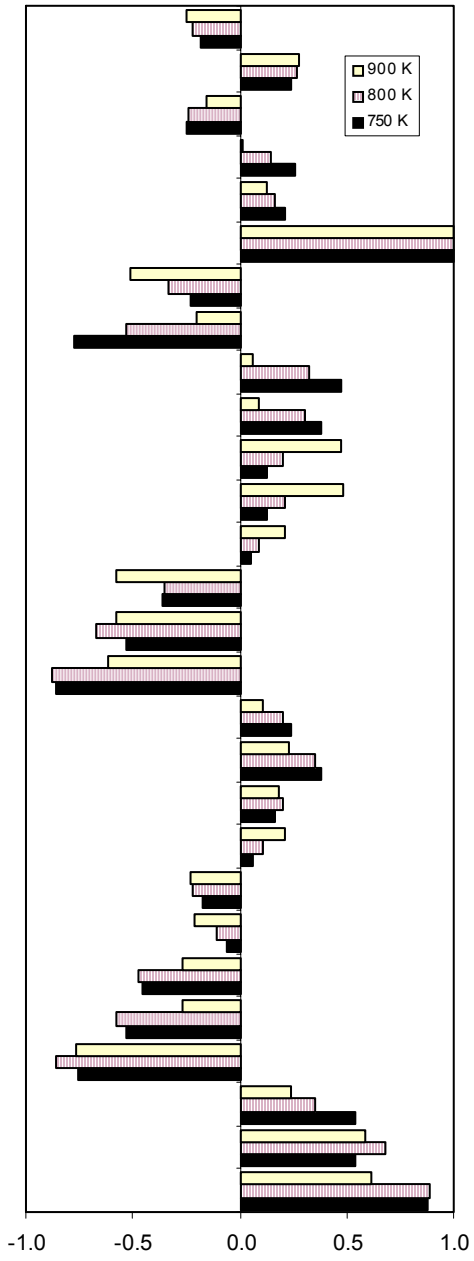

Fig. 6.2: Sensitivity coefficients of a stoichiometric n-heptane/air mixture in a shock tube at a pressure of 13.5 bar and initial temperatures of 750, 800 and 900 K. Only sensitivity coefficients larger than 0.2 are listed.

Decomposition of alkyl radicals through β scission to produce small alkyl radicals and olefins (Rule 3.1.3) shows a high negative sensitivity coefficient and is a competitor to Rule 3.2.1 in consuming alkyl radicals,

$4\text{-}C_7H_{15} \rightarrow C_2H_5 + 1\text{-}C_5H_{10}$
$3\text{-}C_7H_{15} \rightarrow N\text{-}C_3H_7 + 1\text{-}C_4H_8$
$2\text{-}C_7H_{15} \rightarrow C_3H_6 + P\text{-}C_4H_9$.

This type of reaction has a large inhibiting effect on the overall rate of the fuel oxidation and plays an important role in producing NTC behavior as its inhibiting effect increases with increasing temperature, while the promoting effect of Rule 3.2.1 decreases with increasing temperature.

The next-highest negative sensitivity coefficients are shown by the reactions consuming two alkyl radicals,

$HO_2 + HO_2 \rightarrow O_2 + H_2O_2$
$OH + HO_2 \rightarrow O_2 + H_2O$.

These reactions have inhibiting effects on the overall rate of the reaction. The inhibiting effect of the self-reaction of hydroperoxyl radicals is pronounced at 900 K, while that of the reaction between hydroxyl and hydroperoxyl radicals is pronounced at 750 K. This behavior happens because the HO_2 concentration becomes dominant and the OH concentration decreases with increasing temperature.

6.1.3 High temperature

Figure 6.3 depicts sensitivity coefficients of a stoichiometric n-heptane/air mixture in a shock tube at a pressure of 13.5 bar and an initial temperature of 1200 K. This figure is totally different to that at 600 K (Figure 6.1). The ignition is mainly governed by chain branching processes, which are rather fuel-unspecific. The most positive sensitivity coefficient is shown by the chain branching reaction

$O_2 + H \rightarrow OH + O$.

Thus, this reaction controls the overall rate of fuel oxidation. The next highest positive sensitivity coefficients are

$HO_2 + CH_3 \rightarrow OH + CH_3O$ and
$OH + C_2H_4 \rightarrow H_2O + C_2H_3$.

These reactions are not fuel-consuming reactions. The relative high importance of reactions involving HO_2, CH_3 and C_2H_5 radical in controlling the overall rate of the

reaction is due to the fact that the concentrations of these rather unreactive radicals are relatively high at higher temperatures.

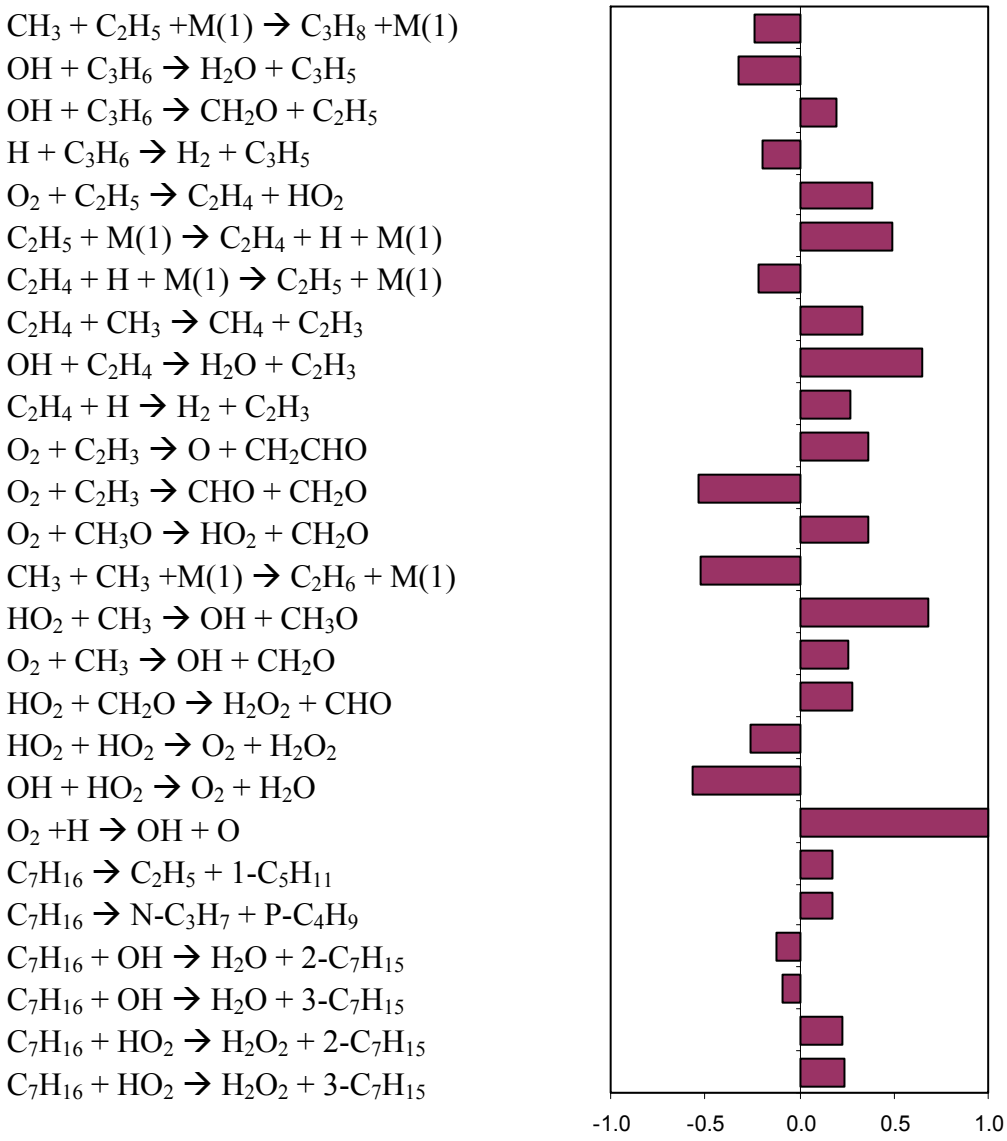

Fig. 6.3: Sensitivity coefficients of a stoichiometric n-heptane/air mixture in a shock tube at a pressure of 13.5 bar and an initial temperature of 1200 K. Only sensitivity coefficients larger than 0.2 are listed, except for H-atom abstraction from fuel by OH.

6.1.4 Different pressures

Figure 6.4 shows sensitivity coefficients of a stoichiometric n-heptane/air mixture at two different pressure levels, 13.5 bar and 41 bar and an initial temperature of 800 K. It can be seen that at different pressures the ignition process is governed by the same reactions. Recalling our discussion in Chapter 5 we have known that the reactivity of the fuel oxidation at higher pressures is larger than that at lower pressures. Unfortunately, we can not observe this trend from sensitivity analysis, because sensitivity coefficients of a particular type of reaction under different conditions can not be compared. Only relative importance of a particular type of reaction under a certain condition can be considered.

From Fig. 6.4 we can see that the hydrogen peroxide decomposition possesses the greatest effect in promoting the overall rate of the reaction at both pressure levels. At 41 bar reactions involving the hydroxyl radicals have larger sensitivity coefficients than at 10 bar. These reactions are

$OH + C_2H_4 \rightarrow H_2O + C_2H_3$
$OH + C_7H16 \rightarrow H_2O + 2\text{-}C_7H_{15}$
$OH + C_7H16 \rightarrow H_2O + 3\text{-}C_7H_{15}$
$OH + HO_2 \rightarrow O_2 + H_2O.$

The first three reactions have a positive sensitivity coefficient. Thus, at 41 bar their influence in promoting the overall rate of the reaction are larger than at 10 bar. The reaction between OH and HO_2 radical has a larger inhibiting effect on the reactivity if pressure increases.

6.1.5 Different mixtures

The sensitivity analyses of stoichiometric and fuel-lean n-heptane/air mixtures at a pressure of 13.5 bar and an initial temperature of 800 K are exhibited in Fig. 6.5. As discussed above, the largest sensitivity of the stoichiometric mixture is connected with the hydrogen peroxide decomposition reaction. This reaction has a positive effect on the reactivity. However, under the fuel-lean condition the largest sensitivity is depicted by

$OH + HO_2 \rightarrow O_2 + H_2O.$

This reaction possesses an inhibiting effect as it consumes two radicals. This is the reason why at low and intermediate temperatures fuel-lean mixtures burn more slowly than stoichiometric and fuel-rich mixtures.

O_2 + N-C_3H_7 → HO_2 + C_3H_6
N-C_3H_7 → C_2H_4 + CH_3
OH + C_3H_6 → H_2O + C_3H_5
OH + C_2H_4 → H_2O + C_2H_3
HO_2 + CH_3O_2 → O_2 + CH_3OOH
H_2O_2 +M(1) → OH +OH +M(1)
HO_2 + HO_2 → O_2 + H_2O_2
OH + HO_2 → O_2 + H_2O
OH + C_7H16 → H_2O + 2-C_7H_{15}
OH + C_7H16 → H_2O + 3-C_7H_{15}
C_7H_{16} + HO_2 → H_2O_2 + 2-C_7H_{15}
C_7H_{16} + HO_2 → H_2O_2 + 3-C_7H_{15}
4-C_7O_2 → O_2 + 4-C_7H_{15}
5-C_7O_2 → O_2 + 3-C_7H_{15}
6-C_7O_2 → O_2 + 2-C_7H_{15}
4-C_7O_2 → 2C_7OOH_4
6-C_7O_2 → 4C_7OOH_6
6-C_7O_2 → 5C_7OOH_6
1-C_7H_{15} → 4-C_7H_{15}
4-C_7H_{15} → C_2H_5 + 1-C_5H_{10}
3-C_7H_{15} → N-C_3H_7 + 1-C_4H_8
2-C_7H_{15} → C_3H_6 + P-C_4H_9
O_2 + 4-C_7H_{15} → 4-C_7O_2
O_2 + 3-C_7H_{15} → 5-C_7O_2
O_2 + 2-C_7H_{15} → 6-C_7O_2

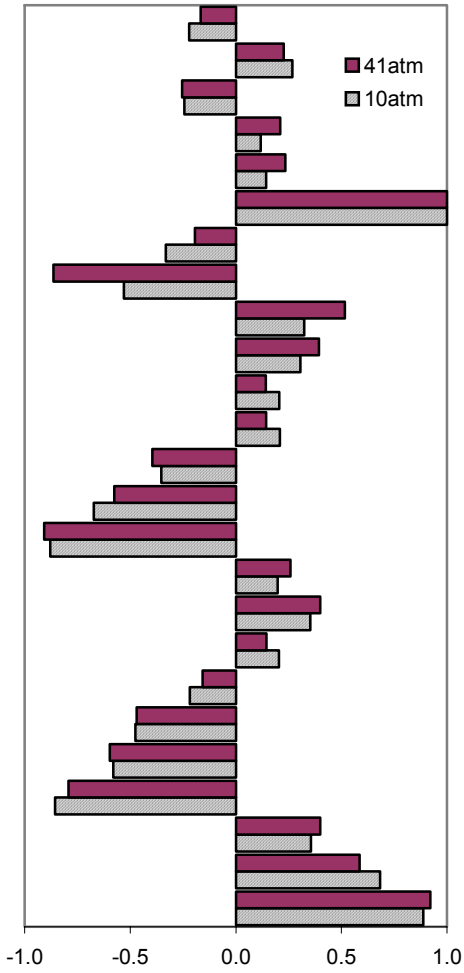

Fig. 6.4: Sensitivity coefficients of a stoichiometric n-heptane/air mixture in a shock tube at pressures of 13.5 bar and 41 bar and an initial temperature of 800 K. Only sensitivity coefficients larger than 0.2 are listed.

$O_2 + N\text{-}C_3H_7 \rightarrow HO_2 + C_3H_6$
$N\text{-}C_3H_7 \rightarrow C_2H_4 + CH_3$
$OH + C_3H_6 \rightarrow H_2O + C_3H_5$
$OH + C_3H_6 \rightarrow CH_3 + CH_3CHO$
$OH + C_2H_4 \rightarrow H_2O + C_2H_3$
$HO_2 + CH_3O_2 \rightarrow O_2 + CH_3OOH$
$H_2O_2 + M(1) \rightarrow OH + OH + M(1)$
$HO_2 + HO_2 \rightarrow O_2 + H_2O_2$
$OH + HO_2 \rightarrow O_2 + H_2O$
$OH + C_7H16 \rightarrow H_2O + 2\text{-}C_7H_{15}$
$OH + C_7H16 \rightarrow H_2O + 3\text{-}C_7H_{15}$
$C_7H_{16} + HO_2 \rightarrow H_2O_2 + 2\text{-}C_7H_{15}$
$C_7H_{16} + HO_2 \rightarrow H_2O_2 + 3\text{-}C_7H_{15}$
$4\text{-}C_7O_2 \rightarrow O_2 + 4\text{-}C_7H_{15}$
$5\text{-}C_7O_2 \rightarrow O_2 + 3\text{-}C_7H_{15}$
$6\text{-}C_7O_2 \rightarrow O_2 + 2\text{-}C_7H_{15}$
$4\text{-}C_7O_2 \rightarrow 2C_7OOH_4$
$6\text{-}C_7O_2 \rightarrow 4C_7OOH_6$
$6\text{-}C_7O_2 \rightarrow 5C_7OOH_6$
$1\text{-}C_7H_{15} \rightarrow 4\text{-}C_7H_{15}$
$4\text{-}C_7H_{15} \rightarrow C_2H_5 + 1\text{-}C_5H_{10}$
$3\text{-}C_7H_{15} \rightarrow N\text{-}C_3H_7 + 1\text{-}C_4H_8$
$2\text{-}C_7H_{15} \rightarrow C_3H_6 + P\text{-}C_4H_9$
$O_2 + 4\text{-}C_7H_{15} \rightarrow 4\text{-}C_7O_2$
$O_2 + 3\text{-}C_7H_{15} \rightarrow 5\text{-}C_7O_2$
$O_2 + 2\text{-}C_7H_{15} \rightarrow 6\text{-}C_7O_2$

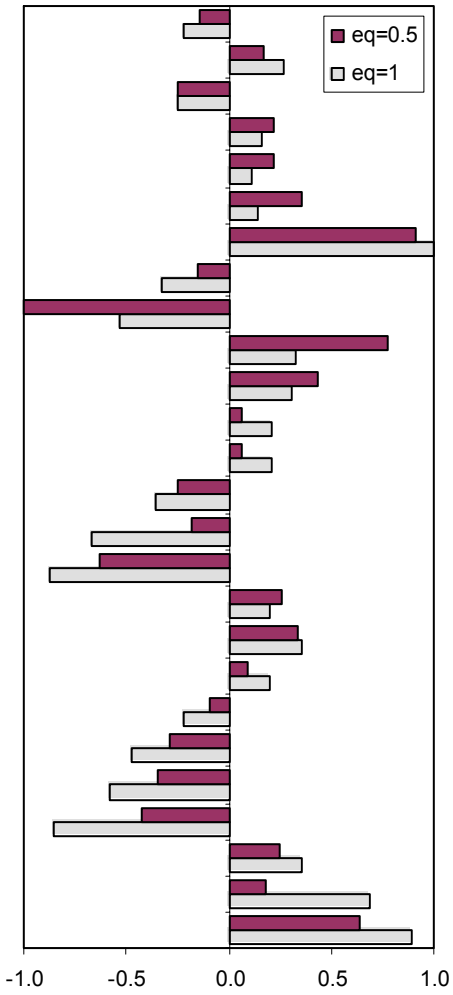

Fig. 6.5: Sensitivity coefficients of n-heptane/air mixture in a shock tube at a pressure of 13.5 bar and an initial temperature of 800 K. The difference between stoichiometric (equivalence ratio =1) and lean (equivalence ratio =0.5) mixtures. Only sensitivity coefficients larger than 0.2 are listed.

6.1.6 Ignition delay times of normal alkanes

We also carried out calculations of ignition delays of other normal alkanes, i.e. n-pentane, n-hexane, n-octane and n-nonane under the same condition as those of n-heptane experimentally carried out by Ciezki and Adomeit [19] and n-decane by Pfahl et al. [20] in high-pressure shock tubes. The aim of this work is to study the ignition behaviour among different normal alkanes. Figure 6.6 shows the ignition delays of n-pentane, n-hexane, n-heptane, n-octane, n-nonane and n-decane in stoichiometric mixtures with air at 13.5 bar.

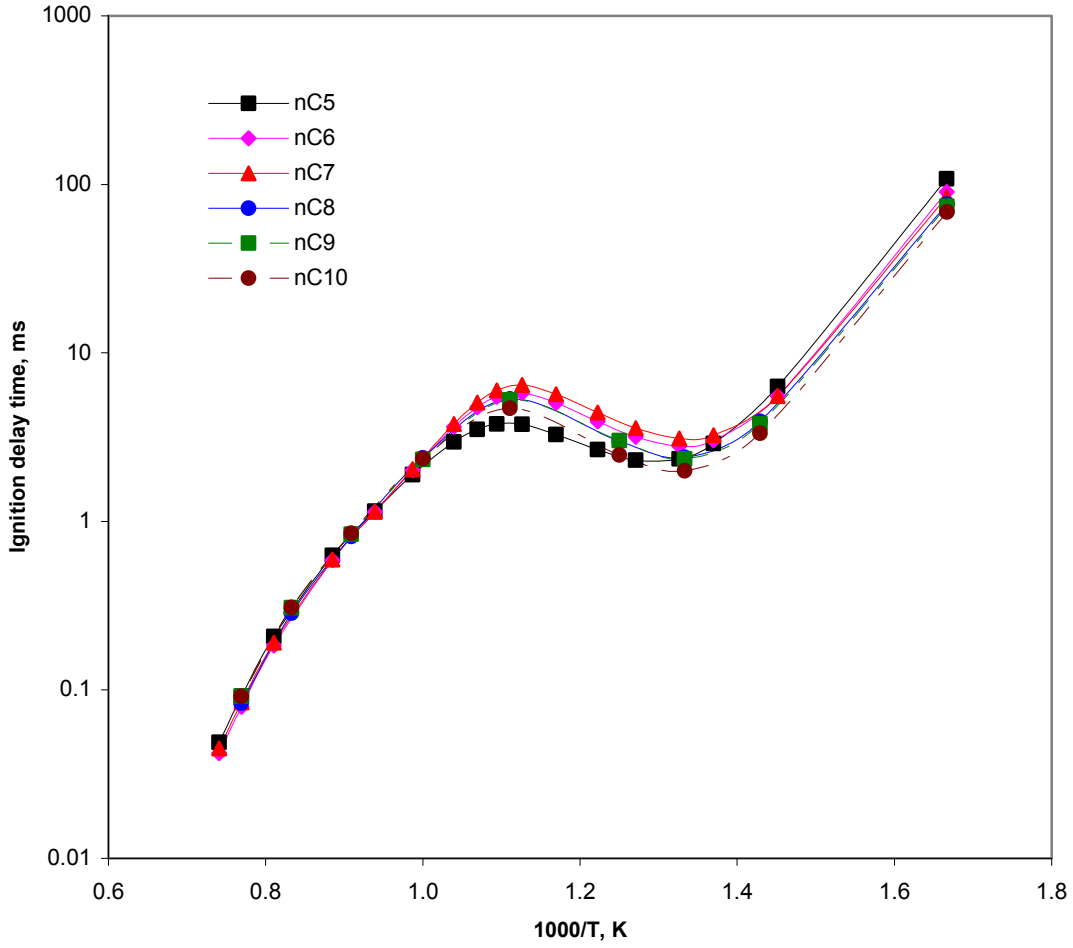

Fig. 6.6: Ignition delays of n-pentane, n-hexane, n-heptane, n-octane, n-nonane and n-decane in stoichiometric mixtures with air at 13.5 bar.

From this figure, it can be seen that there are slightly different reactivities among different normal alkanes at low, intermediate and high temperatures. N-decane has the highest

reactivity, while n-pentane possesses the lowest reactivity at low temperatures. We can observe that at low temperatures the reactivity of normal alkanes increases as the carbon length increases. This trend occurs because at low temperatures the overall rate of the reaction is governed by processes directly related to fuel. As the number of isomeric structures in n-decane is largest, this paraffin produces hydroxyl radicals at highest concentration so that it reacts faster than others. We can observe that the differences between n-pentane and n-hexane reactivity as well as between n-nonane and n-decane reactivity are pronounced. However, the differences between n-hexane and n-heptane reactivity as well as between n-octane and n-nonane reactivity are indistinct.

At intermediate temperatures the same trend generally occurs where the reactivity increases as the chain length increases. However, a very interesting and unexpected result is that the reactivity of n-pentane precedes that of other alkanes, with the reactivity of n-heptane being the lowest. The difference between n-octane and n-nonane reactivity is still indistinct, but the difference between n-hexane and n-heptane reactivity is pronounced. At higher temperatures the reactivity of all normal alkenes is practically the same.

6.2 Reaction Flow Analysis

A reaction flow analysis calculates the percentage of reaction contribution to the formation or consumption of chemical species. We will discuss as a typical case the reaction flow analysis for n-heptane/O_2 mixture in a jet-stirred reactor at 10 bar for an equivalence ratio equals to 1 and at a resident time of 1 s. The temperatures chosen are 600 K (slow oxidation), 700 K (the NTC region) and 1250 K (fast oxidation).

6.2.1 Reaction pathways

At 600 K (33 % conversion) the flow reaction analysis shows that the consumption of n-heptane mainly occurs through H-atom abstraction via OH-radical attack to form four n-heptyl isomers,

$$C_7H_{16} + OH \rightarrow 1\text{-}C_7H_{15} + H_2O \qquad 11\ \%$$
$$C_7H_{16} + OH \rightarrow 2\text{-}C_7H_{15} + H_2O \qquad 32\ \%$$
$$C_7H_{16} + OH \rightarrow 3\text{-}C_7H_{15} + H_2O \qquad 32\ \%$$
$$C_7H_{16} + OH \rightarrow 4\text{-}C_7H_{15} + H_2O \qquad 16\ \%$$

The initiation step, i.e. H-atom abstraction via O_2 attack to produce heptyl radicals and hydroperoxy radicals (HO_2), is characterized by a high activation energy so that at this

temperature the rate is quite slow. Hydroperoxyl radicals can abstract H atoms from the fuel to form dihydroperoxydes (H_2O_2). Dihydroperoxydes then undergo homolytic O-O scission yielding OH radicals,

$$RH + O_2 \rightarrow R' + HO_2$$
$$RH + HO_2 \rightarrow R' + H_2O_2$$
$$H_2O_2 + M \rightarrow OH + OH + M$$

The decomposition of H_2O_2 is a branching process since it generates two very active radicals. However, this reaction is slow in the cool flame range. This is consistent with the sensitivity results described above.

At 700 K (22 % fuel consumption) the consumption of n-heptane was found to primarily proceeds through H-atom abstraction via OH-radical attack. However, H-atom abstraction via HO_2 attack is also significant, with the remainder of n-heptane undergoing H-atom abstraction via methoxy attack,

$C_7H_{16} + CH_3O \rightarrow CH_3OH + 4\text{-}C_7H_{15}$	1 %
$C_7H_{16} + CH_3O \rightarrow CH_3OH + 3\text{-}C_7H_{15}$	2 %
$C_7H_{16} + CH_3O \rightarrow CH_3OH + 2\text{-}C_7H_{15}$	2 %
$C_7H_{16} + HO_2 \rightarrow H_2O_2 + 1\text{-}C_7H_{15}$	2 %
$C_7H_{16} + HO_2 \rightarrow H_2O_2 + 4\text{-}C_7H_{15}$	3 %
$C_7H_{16} + HO_2 \rightarrow H_2O_2 + 3\text{-}C_7H_{15}$	6 %
$C_7H_{16} + HO_2 \rightarrow H_2O_2 + 2\text{-}C_7H_{15}$	6 %
$C_7H_{16} + OH \rightarrow H_2O + 1\text{-}C_7H_{15}$	9 %
$C_7H_{16} + OH \rightarrow H_2O + 4\text{-}C_7H_{15}$	12 %
$C_7H_{16} + OH \rightarrow H_2O + 3\text{-}C_7H_{15}$	24 %
$C_7H_{16} + OH \rightarrow H_2O + 2\text{-}C_7H_{15}$.	24 %

The rate of H-atom abstraction from the fuel via O_2 attack to produce HO_2 radicals at 700 K is higher than that at 600 K, so that the HO_2 concentration at 700 K is higher. The HO_2 radicals can then abstract H atoms from the fuel, leading to the formation of H_2O_2. Because the H_2O_2 concentration is higher, the influence of the H_2O_2 decomposition on the overall reactivity is more positive.

At 1250 K the high activation energy associated with thermal decomposition of fuel is easy to overcome so that this unimolecular initiation step has a major contribution to the fuel consumption,

$C_7H_{16} \rightarrow N\text{-}C_3H_7 + P\text{-}C_4H_9$	12 %
$C_7H_{16} \rightarrow C_2H_5 + 1\text{-}C_5H_{11}$	12 %
$C_7H_{16} \rightarrow CH_3 + 1\text{-}C_6H_{13}$.	1 %

Among the H-abstraction reactions, the attack by H atom is the preferred pathway, and that by OH radical is also important,

$C_7H_{16} + H \rightarrow H_2 + 1\text{-}C_7H_{15}$	12 %
$C_7H_{16} + H \rightarrow H_2 + 4\text{-}C_7H_{15}$	5 %
$C_7H_{16} + H \rightarrow H_2 + 3\text{-}C_7H_{15}$	11 %
$C_7H_{16} + H \rightarrow H_2 + 2\text{-}C_7H_{15}$	11 %
$C_7H_{16} + OH \rightarrow H_2O + 1\text{-}C_7H_{15}$	2 %
$C_7H_{16} + OH \rightarrow H_2O + 4\text{-}C_7H_{15}$	3 %
$C_7H_{16} + OH \rightarrow H_2O + 3\text{-}C_7H_{15}$	5 %
$C_7H_{16} + OH \rightarrow H_2O + 2\text{-}C_7H_{15}$.	5 %

The major reaction pathway of heptyl radicals at 600 K is addition to molecular oxygen, leading to the formation of heptyl peroxy radicals,

$1\text{-}C_7H_{15} + O_2 \rightarrow 7\text{-}C_7O_2$	19 %
$2\text{-}C_7H_{15} + O_2 \rightarrow 6\text{-}C_7O_2$	98 %
$3\text{-}C_7H_{15} + O_2 \rightarrow 5\text{-}C_7O_2$	65 %
$4\text{-}C_7H_{15} + O_2 \rightarrow 4\text{-}C_7O_2$.	99 %

Because these reactions are reversible, most of heptyl peroxy radicals transform back to heptyl radicals,

$7\text{-}C_7O_2 \rightarrow 1\text{-}C_7H_{15} + O_2$	93 %
$6\text{-}C_7O_2 \rightarrow 2\text{-}C_7H_{15} + O_2$	93 %
$5\text{-}C_7O_2 \rightarrow 3\text{-}C_7H_{15} + O_2$	92 %
$4\text{-}C_7O_2 \rightarrow 4\text{-}C_7H_{15} + O_2$	95 %

and only a small part of these radicals undergo internal H-atom abstraction to yield hydroperoxy alkyl radicals,

$7\text{-}C_7O_2 \rightarrow 5C_7OOH7$	3 %
$7\text{-}C_7O_2 \rightarrow 4C_7OOH7$	2 %
$6\text{-}C_7O_2 \rightarrow 4C_7OOH6$	3 %
$6\text{-}C_7O_2 \rightarrow 3C_7OOH6$	2 %
$5\text{-}C_7O_2 \rightarrow 3C_7OOH5$	3 %
$5\text{-}C_7O_2 \rightarrow 2C_7OOH5$	2 %
$5\text{-}C_7O_2 \rightarrow 1C_7OOH3$	1 %
$4\text{-}C_7O_2 \rightarrow 2C_7OOH4.$	3 %

At 700 K the contribution of alkyl radical addition to molecular oxygen to the consumption of alkyl radicals decreases, with the 1-heptyl radical preferring to undergo isomerization reaction,

$1\text{-}C_7H_{15} + O_2 \rightarrow 7\text{-}C_7O_2$	5 %
$2\text{-}C_7H_{15} + O_2 \rightarrow 6\text{-}C_7O_2$	87 %
$3\text{-}C_7H_{15} + O_2 \rightarrow 5\text{-}C_7O_2$	23 %
$4\text{-}C_7H_{15} + O_2 \rightarrow 4\text{-}C_7O_2.$	98 %

At 1200 K the addition of alkyl radicals to molecular oxygen has no more kinetic effect, and thermal decomposition of alkyl radicals through β scission to produce small olefins and smaller alkyl radicals is a preferred pathway,

$1\text{-}C_7H_{15} \rightarrow C_2H_4 + 1\text{-}C_5H_{11}$	7 %
$2\text{-}C_7H_{15} \rightarrow C_3H_6 + P\text{-}C_4H_9$	49 %
$3\text{-}C_7H_{15} \rightarrow 1\text{-}C_4H_8 + N\text{-}C_3H_7$	14 %
$4\text{-}C_7H_{15} \rightarrow 1\text{-}C_5H_{10} + C_2H_5.$	99 %

All reactions consuming alkyl radicals at the three kinetic regimes compete with isomerization reactions.

The second addition to molecular oxygen is a major pathway of hydroperoxy alkyl radicals at 600 K. These reactions compete with isomerization reactions transforming back hydroperoxy alkyl radicals to alkyl peroxy radicals and OH elimination reactions producing cyclic ethers,

$5C_7OOH7 + O_2 \rightarrow 5OO7HP7$	21 %
$5C_7OOH7 \rightarrow 7 - C_7O_2$	78 %
$4C_7OOH7 + O_2 \rightarrow 4OO7HP7$	26 %
$4C_7OOH7 \rightarrow 7 - C_7O_2$	67 %
$4C_7OOH7 \rightarrow 2PTHF + OH$	6 %
$4C_7OOH6 + O_2 \rightarrow 4OO7HP6$	21 %
$4C_7OOH6 \rightarrow 6 - C_7O_2$	78 %
$3C_7OOH6 + O_2 \rightarrow 3OO7HP6$	26 %
$3C_7OOH6 \rightarrow 6 - C_7O_2$	67 %
$3C_7OOH6 \rightarrow 2E5MTHF + OH$	6 %
$3C_7OOH5 + O_2 \rightarrow 3OO7HP5$	21 %
$3C_7OOH5 \rightarrow 5 - C_7O_2$	78 %
$1C_7OOH3 + O_2 \rightarrow 7OO7HP5$	21 %
$1C_7OOH3 \rightarrow 5 - C_7O_2$	78 %
$2C_7OOH5 + O_2 \rightarrow 6OO7HP3$	26 %
$2C_7OOH5 \rightarrow 5 - C_7O_2$	67 %
$2C_7OOH5 \rightarrow 2E5MTHF + OH$	6 %
$2C_7OOH4 + O_2 \rightarrow 6OO7HP4$	21 %
$2C_7OOH4 \rightarrow 4 - C_7O_2$	78 %

In the symbol of peroxy hydroperoxy alkyl radicals above, 4OO7HP6 for instance, 4 refers to the site at which the peroxy group is attached, 6 refers to the site at which the hydroperoxy group is attached and 7 refers to the number of C atom.

At 700 K a major part of alkyl peroxy radicals is transformed back to alkyl radicals, and only less than 5 % of each alkyl peroxy radical isomer is converted to other species via many pathways, whose contribution to the consumption of alkyl peroxy radicals is very small.

At 600 K peroxy hydroperoxy alkyl radicals exclusively undergo internal H-atom abstraction to yield dihydroperoxy alkyl radicals,

*x*OO7HP*y* → *y*-*x*C7HP,

where in *y*-*x*C7HP, *x* refers to the site at which the hydroperoxy group is attached and *y* denotes the site at which the hydroperoxy group is attached to C atom containing radical.

The primary pathways of the dihydroperoxy alkyl radical consumption are through isomerization reactions transforming back dihydroperoxy alkyl radicals to peroxy hydroperoxy alkyl radicals and decomposition leading to the formation of ketohydroperoxyde molecules and hydroxyl radicals,

7-5C_7HP → 1OC_7HP3 + OH	24 %
7-5C_7HP → 5OO7HP7	75 %
7-4C_7HP → 1OC_7HP4 + OH	24 %
7-4C_7HP → 4OO7HP7	75 %
6-4C_7HP → 2OC_7HP4 + OH	39 %
6-4C_7HP → 4OO7HP6	60 %
6-3C_7HP → 2OC_7HP5 + OH	39 %
6-3C_7HP → 3OO7HP6	60 %
3-5C_7HP → 3OC_7HP5 + OH	39 %
3-5C_7HP → 3OO7HP5	60 %
5-7C_7HP → 5OC7HP7 + OH	39 %
5-7C_7HP → 7OO7HP5	60 %
3-6C_7HP → 3OC_7HP6 + OH	39 %
3-6C_7HP → 6OO7HP3	60 %
4-6C_7HP → 4OC_7HP6 + OH	39 %
4-6C_7HP → 6OO7HP4.	60 %

6.2.2 Carbon monoxide

Carbon monoxide, whose concentration profile at low temperatures is underestimated by our kinetic model, is mainly produced through the decomposition and oxidation of small ketyl radicals (CHO, CH_3CO, C_2H_5CO and C_3H_7CO) at 600 K,

$CH_3CO + M(1) \rightarrow CH_3 + CO + M(1)$	31 %
$C_2H_5CO \rightarrow C_2H_5 + CO$	27 %
$CHO + O_2 \rightarrow CO + HO_2$	19 %
$C_3H_7CO \rightarrow CO + N\text{-}C_3H_7$.	10 %

These small ketyl radicals are mainly produced through the decomposition of larger ketyl radicals. The main pathway of the acetyl radical (CH_3CO) production is the decomposition of an isomer of ethyl methyl ketone radical (1-3C_4O), with about 53 % of the acetyl

radicals being produced through H-atom abstraction from acetaldehydes (CH_3CHO) via OH-radical attack, the decomposition of an isomer of carbonly radical (3-OC7O2) and the isomerization reaction 1-2C_2H_3O → CH_3CO,

1-3C_4O → C_2H_4 + CH_3CO	43 %
CH_3CHO + OH → H_2O + CH_3CO	22 %
3-OC7O2 → CH_3CO + 1C5H10O	17 %
1-2C_2H_3O → CH_3CO.	14 %

The 1-3C_4O radical almost exclusively stems from the decomposition of an isomer of carbonyl radical (5-OC_7O2),

5-OC_7O2 → C_2H_5CHO + 1-3C_4O.	97 %

Acetaldehyde (CH_3CHO) is mostly produced through decomposition of three C7-carbonyl radical isomers (6-OC7O3, 6-OC7O4 and 6-OC7O5) and the reaction of OH radicals with propenes,

6-OC7O3 → CH_3CHO + 1-3C5O	33 %
6-OC7O4 → CH_3CHO + 1-2C5O	23 %
6-OC7O5 → CH_3CHO + 1-1C5O	13 %
C_3H_6 + OH → CH_3CHO + CH_3.	19 %

The production of the propionyl radical (C_2H_5CO) was found to primarily occur via the decomposition of an isomer of diethyl ketone radical (1-3C5O), H-atom abstraction from propionaldehydes (C_2H_5CHO) via OH-radical attack and the decomposition of 4-OC7O3 radicals,

1-3C5O → C_2H_4 + C_2H_5CO	48 %
C_2H_5CHO + OH → H_2O + C_2H_5CO	29 %
4-OC7O3 → C_2H_5CO + C_3H_7CHO.	19 %

The 1-3C5O radical is exclusively formed through the decomposition of 6-OC7O3 radicals,

6-OC7O3 → CH_3CHO + 1-3C5O,	99 %

and most of the propionaldehydes (C_2H_5CHO) are directly produced through decomposition of 5-OC7O2, 5-OC7O3 and 5-OC7O4 radicals,

5-OC7O2 → C_2H_5CHO + 1-3C4O	40 %
5-OC7O3 → C_2H_5CHO + 1-2C4O	37 %
5-OC7O4 → C_2H_5CHO + C_3H_7CO.	12 %

The formyl radical (CHO) is primarily produced through the reaction of ketenes (CH_2CO) with OH radicals, with H-atom abstraction from formaldehydes via OH-radical attack and the decomposition of an isomer of propanal radical ($1C_2H_4CHO$) being found to be also important,

OH + CH_2CO → CH_2O + CHO	49 %
CH_2O + OH → H_2O + CHO	17 %
$1C_2H_4CHO$ → C_2H_4 + CHO.	12 %

The butyryl radical (C_3H_7CO) is mainly produced via OH attack on butyraldehydes and the decomposition of 5-OC7O4 radicals, with the decomposition of an isomer of ethyl propyl ketone radical (1-3C6O) being also important,

OH + C_3H_7CHO → H_2O + C_3H_7CO	46 %
5-OC7O4 → C_2H_5CHO + C_3H_7CO	37 %
1-3C6O → C_2H_4 + C_3H_7CO.	12 %

The pathways of the carbon monoxide formation at 600 K are shown schematically in Fig. 6.7.

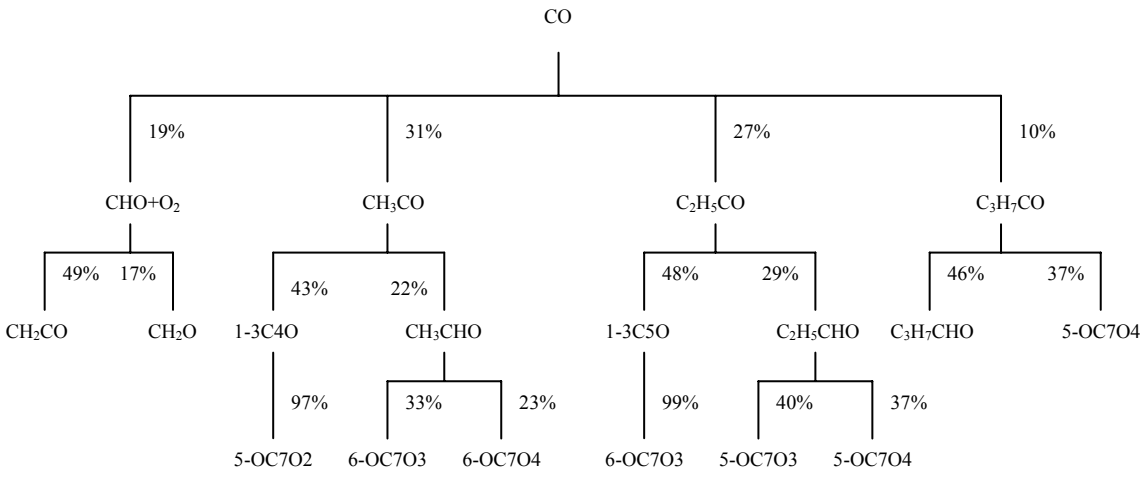

Fig. 6.7: The pathways of the carbon monoxide formation at 600 K.

At 700 K the same pathways of the carbon monoxide formation described above are still preferred. The contribution of the formyl and butyryl radical decomposition was found to be larger at this temperature, while that of the acetyl and propionyl radical decomposition was found to be lower,

$CH_3CO + M \rightarrow CH_3 + CO + M$	27 %
$CHO + O_2 \rightarrow CO + HO_2$	21 %
$C_2H_5CO \rightarrow C_2H_5 + CO$	19 %
$C_3H_7CO \rightarrow CO + N\text{-}C_3H_7$.	13 %

The decomposition of the $1\text{-}3C_4O$ radical is not the main pathway of the acetyl radical (CH_3CO) formation anymore. The acetyl radical is primarily produced through the decomposition of 3-OC7O2 radicals. In addition to H-atom abstraction via OH-radical attack, the abstraction via HO_2 attack has also a great influence in producing acetyl radicals,

$3\text{-}OC7O2 \rightarrow CH_3CO + 1C5H10O$	35 %
$1\text{-}3C_4O \rightarrow C_2H_4 + CH_3CO$	18 %
$CH_3CHO + HO_2 \rightarrow H_2O_2 + CH_3CO$	15 %
$1\text{-}2C_2H_3O \rightarrow CH_3CO$	14 %
$CH_3CHO + OH \rightarrow H_2O + CH_3CO$.	10 %

The formly radical (CHO) is formed through the route $CH_3 \rightarrow CH_3O_2 \rightarrow CH_3OOH \rightarrow CH_3O \rightarrow CH_2O \rightarrow CHO$. In this route, H-atom abstraction from formaldehydes occurs via OH and H_2O attack.

The formation of the propionyl radical (C_2H_5CO) was found to primarily occur through the decomposition of 4-OC7O3 radicals, with the decomposition of an isomer of diethyl ketone radical (1-3C5O) and H-atom abstraction from propionaldehydes (C_2H_5CHO) via OH-radical attack being also important,

$4\text{-}OC7O3 \rightarrow C_2H_5CO + C_3H_7CHO$	49 %
$1\text{-}3C5O \rightarrow C_2H_4 + C_2H_5CO$	23 %
$C_2H_5CHO + OH \rightarrow H_2O + C_2H_5CO$.	16 %

The butyraldehyde radical (C_3H_7CO) formation is primary contributed by the decomposition of 5-OC7O4 radicals, with a significant contribution being from OH-radical attack on butyraldehydes and the decomposition of 1-3C6O radicals,

5-OC7O4 → C2H5CHO + C3H7CO	53 %
OH + C_3H_7CHO → H_2O + C_3H_7CO	19 %
1-3C6O → C_2H_4 + C_3H_7CO.	10 %

The pathways of the carbon monoxide formation at 700 K are shown schematically in Fig. 6.8.

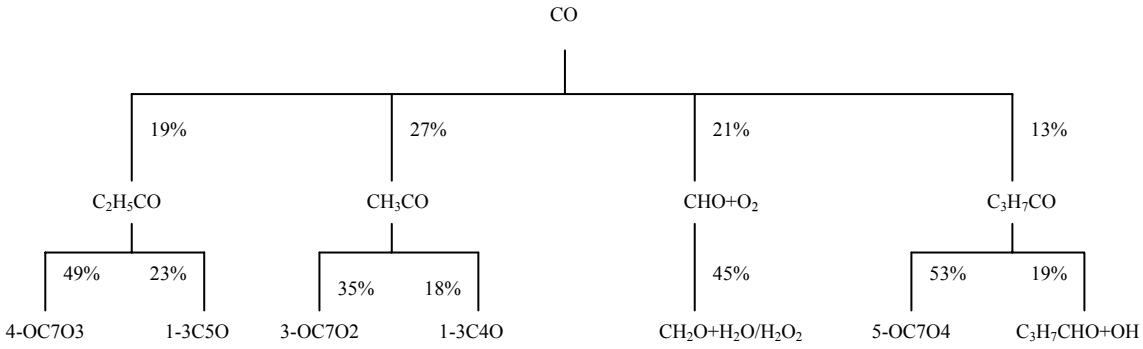

Fig. 6.8: The pathways of the carbon monoxide formation at 700 K.

At 1250 K the thermal decomposition of the formyl and acetyl radicals was found to account for about 61 % and 25 %, respectively, of the carbon monoxide formation. The thermal decomposition of the propionyl and butyryl radicals, which was found to be important at low temperatures, is not important anymore,

CHO + M → CO + H + M	61 %
CH_3CO + M → CH_3 + CO + M.	25 %

The formation of the formyl radical (CHO) primarily proceeds via the oxidation of vinyl radicals. H-atom abstraction from formaldehydes via H and OH attack as well as O-atom addition to a double-bond of ethylene followed by C-C rupture were found to be also important. They account for 32 % and 14 %, respectively, of the formyl radical formation,

O_2 + C_2H_3 → CH_2O + CHO	34 %
CH_2O + H → H_2 + CHO	19 %
C_2H_4 + O → CHO + CH_3	14 %
CH_2O + OH → H_2O + CHO.	13 %

The formation of the vinyl radical (C_2H_3) was found to occur via the reaction of formaldehydes with formyl radicals and H and OH attack on acetylenes,

$CH_2O + CHO \rightarrow O_2 + C_2H_3$	46 %
$C_2H_4 + H \rightarrow H_2 + C_2H_3$	25 %
$C_2H_4 + OH \rightarrow H_2O + C_2H_3$.	13 %

Another precursor to carbon monoxide, i.e. the acetyl radical (CH_3CO), is produced via the isomerization reaction $CH_2CHO \rightarrow CH_3CO$, where CH_2CHO is yielded primarily through the oxidation of the vinyl radical, with O-atom addition to a double-bond of ethylene being also important,

$O_2 + C_2H_3 \rightarrow O + CH_2CHO$	62 %
$C_2H_4 + O \rightarrow H + CH_2CHO$.	31 %

Figure 6.9 shows schematically the pathways of the carbon monoxide formation at 1250 K.

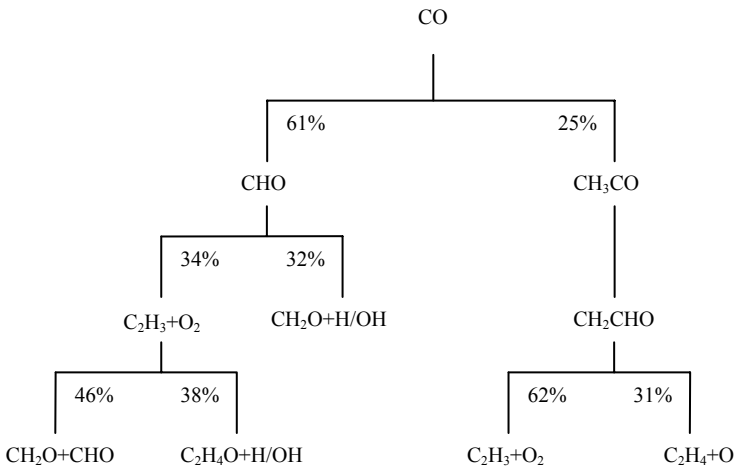

Fig. 6.9: The pathways of the carbon monoxide formation at 1250 K.

6.2.3 Carbon dioxide

Carbon dioxide is exclusively formed through the reaction between ketenes and OH radicals at 600 and 700 K. This reaction possesses a negative influence on the overall reactivity by exchanging a very reactive OH radical for a methyl radical,

$$OH + CH_2CO \rightarrow CO_2 + CH_3.$$

Ketene is formed via the decomposition of ketyl radicals, i.e. an isomer of ethyl methyl ketone radical (1-2C_4O), an isomer of acetone radical (CH_3COCH_2) and an isomer of methyl propyl ketone radical (1-2C_5O),

$$1\text{-}2C_4O \rightarrow CH_2CO + C_2H_5$$
$$CH_3COCH_2 \rightarrow CH_3 + CH_2CO$$
$$1\text{-}2C_5O \rightarrow CH_2CO + N\text{-}C_3H_7.$$

The decomposition of the 1-2C_4O radical shows the largest contribution at 600 K, while that of the CH_3COCH_2 radical shows the largest contribution at 700 K.

These ketyl radicals are the products of the decomposition of carbonyl radicals (5-OC_7O3, 6-OC_7O4, 4-OC_7O2),

$$5\text{-}OC_7O3 \rightarrow C_2H_5CHO + 1\text{-}2C_4O$$
$$6\text{-}OC_7O4 \rightarrow CH_3CHO + 1\text{-}2C_5O$$
$$4\text{-}OC_7O2 \rightarrow CH_3COCH_2 + C_3H_7CHO.$$

The pathways of the carbon dioxide formation at 600 K and 700 K are shown schematically in Fig. 6.10 and 6.11, respectively.

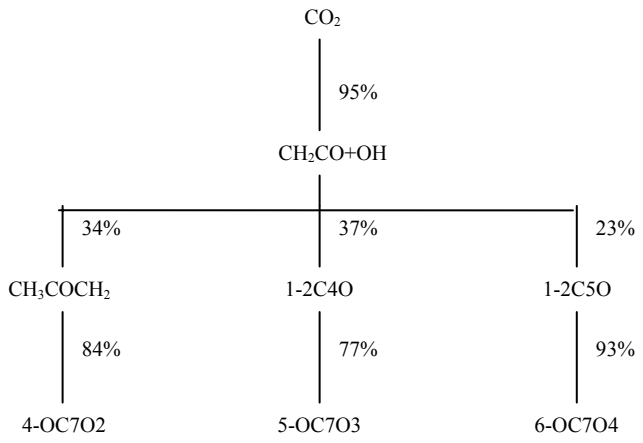

Fig. 6.10: The pathways of the carbon dioxide formation at 600 K.

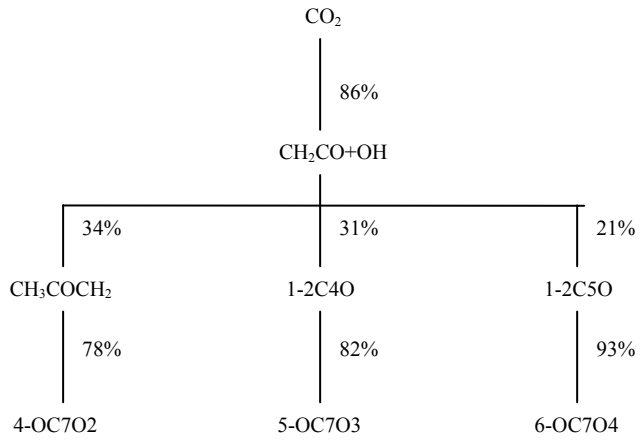

Fig. 6.11: The pathways of the carbon dioxide formation at 700 K.

At 1250 K the origin of carbon dioxide is directly from carbon monoxide, which reacts with OH and HO_2 radical,

$CO + OH \rightarrow CO_2 + H$	67 %
$CO + HO_2 \rightarrow CO_2 + OH.$	26 %

The first reaction has a negative effect on the overall rate of the reaction since it exchanges an OH radical for a hydrogen atom, while the second reaction possesses a positive influence because it exchanges a HO_2 radical for an OH radical.

6.2.4 Formaldehyde

The oxidation of methoxy radicals and the reactions of OH radicals with ketenes or propenes are major contributors to the formation of formaldehydes at 600 K,

$CH_3O + O_2 \rightarrow CH_2O + HO_2$	20 %
$CH_2CO + OH \rightarrow CH_2O + CHO$	34 %
$C_3H_6 + OH \rightarrow C_2H_5 + CH_2O.$	13 %

The two last reactions have a very negative effect on the overall reactivity by exchanging OH radicals for CHO and C_2H_5 radical.

The formation of ketenes has been described above. The formation of the methoxy radicals was found to mainly occur through the decomposition of methyl peroxides (CH_3OOH), with the reaction between two methyl peroxy radicals being also important,

$CH_3OOH \rightarrow OH + CH_3O$ 55 %
$CH_3O_2 + CH_3O_2 \rightarrow O_2 + CH_3O + CH_3O.$ 31 %

Methyl peroxide is exclusively formed through the reaction of hydroperoxy radicals with methyl peroxy radicals,

$HO_2 + CH_3O_2 \rightarrow O_2 + CH_3OOH.$ 98 %

The methyl peroxy radical is mainly produced via addition of methyl radicals to molecular oxygen,

$O_2 + CH_3 + M \rightarrow CH_3O_2 + M.$ 85 %

Figure 6.12 shows schematically the pathways of the formaldehyde formation at 600 K.

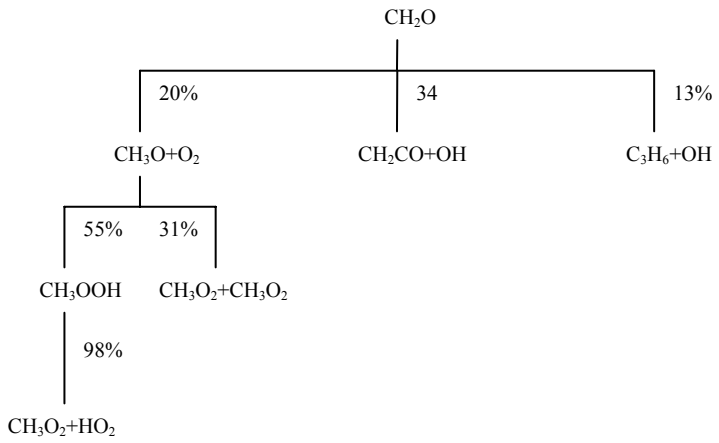

Fig. 6.12: The pathways of the formaldehyde formation at 600 K.

At 700 K the formation of formaldehydes was found to primarily occur via the oxidation of methoxy radicals, which are formed through the route $CH_3 \rightarrow CH_3O_2 \rightarrow CH_3OOH \rightarrow CH_3O \rightarrow CH_2O$.

At 1250 K the pathway of the formaldehyde formation is rather different. The major pathways are via oxidation processes, with the decomposition of the methoxy radicals being also important,

$O_2 + C_2H_3 \rightarrow CH_2O + CHO$	46 %
$O_2 + CH_2OH \rightarrow CH_2O + HO_2$	17 %
$O_2 + CH_3 \rightarrow CH_2O + OH$	9 %
$CH_3O + M \rightarrow CH_2O + H + M$	12 %

The first reaction is reversible, which transforms back formaldehydes to vinyl radicals (C_2H_3). Thus, the formation of the vinyl radical was found to primarily occur through H-atom abstraction from ethylenes via H and OH attack,

$CH_2O + CHO \rightarrow O_2 + C_2H_3$	46 %
$C_2H_4 + H \rightarrow H_2 + C_2H_3$	25 %
$C_2H_4 + OH \rightarrow H_2O + C_2H_3$.	13 %

6.2.5 Ethylene

Ethylene, overestimated in our simulation at low temperatures, is mainly formed via the oxidation of ethyl radicals at 600 and 700 K,

$$C_2H_5 + O_2 \rightarrow C_2H_4 + HO_2.$$

The formation of the ethyl radical was found to mainly occur via the decomposition of propionyl radicals, with the decomposition of 1-2C4O radicals being also important at 600 K,

$C_2H_5CO \rightarrow CO + C_2H_5$	52 %
1-2C4O $\rightarrow CH_2CO + C_2H_5$.	30 %

At 700 K the decomposition of 4-heptyl radicals was found to be the main contributor to the formation of the ethyl radical, with the decomposition of the propionyl radical being still important,

4-$C_7H_{15} \rightarrow$ 1-$C_5H_{10} + C_2H_5$	46 %
$C_2H_5CO \rightarrow CO + C_2H_5$.	25 %

At 1250 K ethylene is mainly yielded from the thermal decomposition of ethyl radicals, with minor contribution coming from the decomposition of n-propyl and 1-butyl radicals,

$C_2H_5 + M \rightarrow C_2H_4 + H + M$	56 %
$n\text{-}C_3H_7 \rightarrow C_2H_4 + CH_3$	17 %
$p\text{-}C_4H_9 \rightarrow C_2H_4 + C_2H_5$.	11 %

The formation of the ethyl radical was found to primarily occur through OH and H attack on ethanes, with the decomposition of the 1-butyl radical being also important,

$C_2H_6 + OH \rightarrow H_2O + C_2H_5$	26 %
$p\text{-}C_4H_9 \rightarrow C_2H_4 + C_2H_5$	18 %
$C_2H_6 + H \rightarrow H_2 + C_2H_5$.	14 %

Ethane is exclusively formed via the termination step,

$CH_3 + CH_3 + M \rightarrow C_2H_6 + M$,	99 %

and the 1-propyl radical is yielded through the decomposition of 2-heptyl radicals,

$2\text{-}C_7H_{15} \rightarrow C_3H_6 + P\text{-}C_4H_9$.	62 %

6.2.6 Methane

Methane, which is only significant at high temperatures, is produced through reactions of methyl radicals with formaldehydes, ethylenes and hydrogen atoms,

$CH_2O + CH_3 \rightarrow CH_4 + CHO$	37 %
$H + CH_3 + M \rightarrow CH_4 + M$	23 %
$C_2H_4 + CH_3 \rightarrow CH_4 + C_2H_3$.	17 %

The formation of the methyl radical was found to primary occur via the decomposition of acetyl radicals, with O-atom addition to ethylenes and the decomposition of n-propyl radicals being found also important,

$CH_3CO + M \rightarrow CO + CH_3 + M$	34 %
$C_2H_4 + O \rightarrow CHO + CH_3$	16 %
$n\text{-}C_3H_7 \rightarrow C_2H_4 + CH_3$.	11 %

Chapter 7

CONCLUSIONS

A mechanism generator code to automatically generate reaction mechanisms for the oxidation and combustion of large hydrocarbons has been successfully modified in this work. In addition to simulate ignition delay times, detailed reaction mechanisms generated by the code can be used to simulate the formation of a wide spectrum of observed products of fuel oxidation.

The modification was through:

(1) improvement of the existing rules such as cyclic-ether reactions and aldehyde reactions,
(2) inclusion of some additional rules to the code, such as ketone reactions, hydroperoxy cyclic-ether formations and additional reactions of alkenes,
(3) inclusion of small oxygenates, produced by the code but not included in the handwritten C_1-C_4 sub-mechanism yet, to the handwritten C_1-C_4 sub-mechanism.

In order to evaluate mechanisms generated by the code, simulation of observed results in different experimental environments has been carried out. The simulation of auto-ignition of n-pentane in a rapid-compression machine shows good agreement with experimental results. Two steps of ignition delays times, the lower ignition limit and the negative temperature coefficient are correctly reproduced.

Experimentally derived and numerically predicted ignition delays of n-heptane/air and n-decane/air mixtures in high-pressure shock tubes in a wide range of temperatures, pressures and equivalence ratios agree very well. The negative temperature coefficient region is shifted towards lower temperatures as pressure is increased. The overall reactivity of the mixtures increases with increasing pressure. The fuel-rich mixtures burn more easily than the fuel-lean mixtures in the low- and intermediate-temperature regimes. In the high temperature regime a contrary trend occurs. At a constant initial pressure of 13.5 bar and above 1250 K the fuel-lean mixtures autoignite more easily than the fuel-rich mixtures.

Concentration profiles of the main products and intermediates of n-heptane, iso-octane and n-decane oxidation in jet-stirred reactors at a wide range of temperatures and equivalence ratios are generally well reproduced by the kinetic models. The fuel-lean mixtures show a

higher overall reactivity than the stoichiometric and fuel-rich mixtures. The location of the NTC region does not change in practice with increase of the amount of oxygen in the initial mixtures. The NTC region of n-heptane oxidation spans from 640 K to 750 K at 10 bar. Simulation results show that carbon monoxide is a major intermediate in the low- and high-temperature regimes, formaldehyde is a major oxygenate intermediate following carbon monoxide, methane is a major paraffinic intermediate and ethylene is a major olefinic intermediate.

Sensitivity analysis for shock tube environment shows that the ignition of n-heptane is governed by fuel-specific processes at low temperatures and by rather fuel-unspecific processes at high temperatures. The chain-branching processes, i.e. the decomposition of hydroperoxyde and ketohydroperoxy molecules and the attack of alkylperoxy radicals to the fuel, control the overall rate of the fuel oxidation in shock tubes at 600 K and 13.5 bar. In the NTC region the decomposition of hydrogen peroxides to produce hydroxyl radicals is a major chain branching, which possesses a positive influence on the overall reactivity. At 1200 K the most positive sensitivity is shown by the chain-branching reaction $O_2 + H \rightarrow OH + O$.

From the simulation of ignition delays of various normal alkanes under high-pressure shock tube conditions we observe that the reactivity of normal alkanes increases as the carbon chain length increases at low temperatures. At intermediate temperatures the reactivity of n-pentane precedes that of other alkanes, with the reactivity of n-heptane being the lowest. At higher temperatures the reactivity of all normal alkenes is practically the same.

From reaction flow analysis for jet-stirred reactor environment we observe that the reactions directly consuming fuel are H-atom abstraction via hydroxyl radical attack at low temperatures and thermal decomposition of fuel and H-atom abstraction via hydrogen atom attack at high temperatures. Carbon monoxide is mainly produced through the decomposition and oxidation of small ketyl radicals at low temperatures, while at high temperatures it mostly comes from the thermal decomposition of formyl radicals.

At low temperatures the reaction of ketenes with hydroxyl radicals has a major contribution to the formation of carbon dioxide. At high temperature the origin of carbon dioxide is directly from carbon monoxide, which reacts with hydroxyl and hydroperoxyl radicals. The oxidation of methoxy radicals and the reactions of hydroxyl radicals with ketenes or propenes are major contributors to the formation of formaldehyde at 600 K. At 1250 K the major pathways of the formaldehyde formation are via the oxidation of vinyl methyl and hydroxymethyl radicals as well as the metoxy decomposition.

REFERENCES

1. Ribaucour, M., Minetti, R. and Sochet, L.R. (1998). Autoignition of n-Pentane and l-Pentane: Experimental Data and Kinetic Modelling. *Twenty-Seventh Symposium (International) on Combustion.* The Combustion Institute, Pittsburgh, 345.
2. Westbrook, C.K., Curran, H.J., Pitz, W.J., Griffiths, J.F., Mohamed, C. and Wo, S.K. (1998). The Effects of Pressure, Temperature and Concentration of the Reactivity of Alkanes: Experiments and Modelling in a Rapid-compression Machine. *Twenty-Seventh Symposium (International) on Combustion.* The Combustion Institute, Pittsburgh, 371.
3. Ribaucour, M., Minetti, R., Sochet, L.R., Curran, H.J., Pitz, W.J. and Westbrook, C.K. (2000). Ignition of Isomers of Pentane: an Experimental and Kinetic Modelling Study. *Twenty-Eight Symposium (International) on Combustion.* The Combustion Institute, Pittsburgh, 1671.
4. Curran, H.J., Pitz, W.J., Hisham, M.W.M. and Walker, R.W. (1996). An Intermediate Temperature Modeling Study of the Combustion of Neopentane. *Twenty-Sixth Symposium (International) on Combustion.* The Combustion Institute, Pittsburgh, 641.
5. Wang, S.Q., Miller, D.L., Cernansky, N.P., Curran, H.J., Pitz, W.J. and Westbrook, C.K. (1999). A Flow Reactor Study of Neopentane Oxidation at 8 Atmospheres: Experiments and Modeling. *Combust. Flame*, **118**, 415.
6. Dagaut, P. and Cathonnet, M. (1999). Oxidation of Neopentane in a Jet-Stirred Reactor from 1 to 10 atm: Experimental and Detailed Kinetic Modeling Study. *Combust. Flame,* **118**, 191.
7. Taconnet, S., Simon, Y., Scacchi, G. and Baronnet, F. (1999). Experimental Study and Modeling of the Oxidation Reaction of Neopentane and Isopentane. *Can. J. Chem.*, **77**, 1177.
8. Curran, H.J., Gaffuri, P., Pitz, W.J., Westbrook, C.K. and Leppard, W.R. (1995). Autoignition Chemistry of the Hexane Isomers: an Experimental and Kinetic Modelling Study. SAE-952406.
9. Burcat, A., Olchanski, E. and Sokolinski, C. (1996). Kinetics of Hexane Combustion in a Shock Tube. *Israel J. Chem.*, **36**, 313.
10. Burcat, A., Olchanski, E. and Sokolinski, C. (1999). 2-Mathyl-pentane Ignition Kinetics in a Shock Tube. *Combust. Sci. Technol*., **147**, 1.
11. Westbrook, C.K., Warnatz, J. and Pitz, W.J. (1988). A Detailed Chemical Kinetic Reaction Mechanism for the Oxidation of Iso-octane and n-Heptane over an

Extended Temperature Range and Its Application to Analysis of Engine Knock. *Twenty-Second Symposium (International) on Combustion.* The Combustion Institute, Pittsburgh, 893.

12. Chevalier, C., Pitz., W.J., Warnatz, J., Westbrook, C.K. and Melenk, H. (1992). Hydrocarbon Ignition: Automatic Generation of Reaction Mechanisms and Applications to Modeling of Engine Knock. *Twenty-Forth Symposium (International) on Combustion.* The Combustion Institute, Pittsburgh, 93.
13. Chakir, A., Bellman, M., Boettner, J.C. and Cathonnet, M. (1992). Kinetic Study of n-Heptane Oxidation. *Int. J. Chem. Kinet*., **24**, 385.
14. Lindstedt, R.P. and Maurice, L.Q. (1995). Detailed Kinetic Modelling of n-Heptane Combustion. *Combust. Sci. Technol.,* **107**, 317.
15. Hamins, A. and Seshadri, K. (1987). The Structures of Diffusion Flames Burning Pure, Binary and Ternary Solutions of Methanol, Heptane and Toluene. *Combust. Flame*, **68**, 295.
16. Gibbs, G.J. and Calcote., H.F. (1959). Effect of Molecular Structure on Burning Velocity. *J. Chem. Engng. Data,* **4**, 226.
17. Ranzi, E., Gaffuri, P., Faravelli, T., Gaffuri P. and Sogaro, A. (1995). Low Temperature Combustion: Automatic Generation of Primary Oxidation Reactions and Lumping Procedures. *Combust. Flame,* **102**, 179.
18. Nehse, M., Warnatz, J. and Chevalier, C. (1996). Kinetic Modeling of the Oxidation of Large Aliphatic Hydrocarbons. *Twenty-Sixth Symposium (International) on Combustion.* The Combustion Institute, Pittsburgh, 773.
19. Ciezki, H.K. and Adomeit, G. (1993). Shock-tube Investigation of Self-Ignition of n-Heptane-Air Mixtures under Engine Relevant Conditions. *Combust. Flame* **93**, 421.
20. Pfahl, U., Fieweger, K., and Adomeit, G. (1996). Self-Ignition of Diesel-Relevant Hydrocarbon-Air Mixtures under Engine Conditions. *Twenty-Sixth Symposium (International) on Combustion.* The Combustion Institute, Pittsburgh, 781.
21. Come, G.M., Warth, V., Glaude, P.A., Fournet, R., Battin-Leclerc, F. and Scacchi, G. (1996). Computer-aided Design of Gas-Phase Oxidation Mechanisms-Application to the Modeling of n-Heptane and Iso-Octane Oxidation. *Twenty-Sixth Symposium (International) on Combustion.* The Combustion Institute, Pittsburgh, 755.
22. Simon, Y., Scacchi, G. and Baronnet, F. (1996). Studies on the Oxidation Reactions of n-Heptane and Isooctane. *Can. J. Chem.*, **74**, 1391.
23. Dagaut, P., Reuillon, M. and Cathonnet, M.(1994). High Pressure Oxidation of Liquid Fuels from Low to High Temperature. 1. n-Heptane and Iso-octane. *Combust. Sci. Technol*., **95**, 233.

24. Curran, H.J., Gaffuri, P., Pitz, W.J. and Westbrook, C.K. (1998). A comprehensive Modelling Study of n-Heptane Oxidation. *Combust. Flame*, **114**, 149.
25. Vermeersch, M.L., Held, T.J., Stein, Y.S. and Dryer, F.L. (1991). *SAE Trans.*, **100**, 645.
26. Callahan, H.J., Held, T.J., Dryer, F.L., Minetti, R., Ribaucour, M., Sochet, L.R., Faravelli, T., Gaffuri, P. and Ranzi, E. (1996). Experimental Data and Kinetic Modelling of Primary Reference Fuel Mixtures. *Twenty-Sixth Symposium (International) on Combustion.* The Combustion Institute, Pittsburgh, 739.
27. Dagaut, P., Reuillon, M. and Cathonnet, M. (1995). Experimental Study of the Oxidation of n-Heptane in a Jet-Stirred Reactor from Low to High Temperature and Pressures up to 40 atm. *Combust. Flame*, **101**, 132.
28. Vermeer, D.J., Meyer, J.W. and Oppenheim, A.K. (1972). Auto-Ignition of Hydrocarbons behind Reflected Shock Waves. *Combust. Flame,* **18**, 327.
29. Coats, C.M. and Williams, A. (1978). Investigation of the Ignition and Combustion of n-Heptane-Oxygen Mixtures. *Seventieth Symposium (International) on Combustion.* The Combustion Institute, Pittsburgh, 611.
30. Minetti, R., Carlier, R., Ribaucour, M., Therssen, E. and Sochet, L.R. (1995). A Rapid Compression Machine Investigation of Oxidation and Auto-Ignition of n-Heptane: Measurements and Modeling. *Combust. Flame,* **102**, 298.
31. Doute, C., Delfau, J.L. and Vovelle, C. (1999). Detailed Reaction Mechanisms for Low-pressure Premixed n-Heptane Flames. *Combust. Sci. Technol.,* **147**, 61.
32. Doute, C., Delfau, J.L., Akrich, R. and Vovelle, C. (1997). Experimental Study of the Chemical Structure of Low-pressure Premixed n-Heptane /O_2/Ar and Iso-octane/O_2/Ar Flames. *Combust. Sci. Technol.,* **124**, 249.
33. El Bakali, A., Delfau, J.L. and Vovelle, C. (1999). Kinetic Modeling of a Rich, Atmospheric Pressure, Premixed n-Heptane/O_2/N_2 Flame. *Combust. Flame,* **118**, 381.
34. Seiser, R., Pitsch, H., Seshadri, K., Pitz, W.J. and Curran, H.J. (2000). Extinction and Auto-ignition of n-Heptane in Counterflow Configuration. *Twenty-Eighth Symposium (International) on Combustion.* The Combustion Institute, Pittsburgh, 2029.
35. Westbrook, C.K., Pitz, W.J., Curran, H.C., Boercker, J. and Kunrath, E. (2001). Chemical Kinetic Modelling Study of Shock Tube Ignition of Heptane Isomers. *Int. J. Chem. Kinet.,* **33**, 868.
36. Davidson, D.F., Horning, D.C., Hanson, R.K. and Hitch, B. (1999). Shock Tube Ignition Time Measurements for n-Heptane/O_2/Ar Mixtures with and without Additives. *Twenty-Second International Symposium on Shock Waves*.
37. Ranzi, E., Faravelli, T., Gaffuri, P., Sogaro, A., Danna, A. and Ciajolo, A. (1997). A Wide-range Modelling Study of Iso-octane Oxidation. *Combust. Flame,* **108**, 24.

38. Dryer, F.L. and Brezinsky, K. (1986). A Flow Reactor Study of the Oxidation of n-Octane and Isooctane. *Combust. Sci. Technol.,* **45**, 199.
39. Fieweger, K., Blumenthal, R. and Adomeit, G. (1994). Shock Tube Investigations on the Self-ignition of Hydrocarbon/air Mixtures at High Pressures. *Twenty-Fifth Symposium (International) on Combustion.* The Combustion Institute, Pittsburgh, 1579.
40. Curran, H.J., Gaffuri, P., Pitz, W.J. and Westbrook, C.K. (2002). A Comprehensive Modeling Study of Iso-octane Oxidation. *Combust. Flame,* **129**, 253.
41. Chen, J.S., Litzinger, T.A. and Curran, H.J. (2000). The Lean Oxidation of Isooctane in the Intermediate Temperature Regime at Elevated Pressures. *Combust. Sci. Technol.,* **156**, 49.
42. Fieweger, K., Blumenthal, R. and Adomeit, G. (1997). Self-ignition of SI Engine Model Fuels: a Shock Tube Investigation at High Pressure. *Combust. Flame,* **109**, 599.
43. Leppard, A. (1992). Comparison of Olefin and Paraffin Autoignition Chemistries: A Motored-engine Study. W.R., SAE-9223.
44. Glaude, P.A., Warth, V., Fournet, R., Battin-Leclerc, F., Scacchi, G. and Come, G.M. (1998). Modelling of the Oxidation of n-Octane and n-Decane Using an Automatic Generation of Mechanisms. *Int. J. Chem. Kinet.,* **30**, 949.
45. Dagaut, P., Reuillon, M., and Cathonnet, M. (1994). High Pressure Oxidation of Liquid Fuels from Low to High Temperature. 3. n-Decane. *Combust. Sci. Technol.,* **103**, 349.
46. Doute C., Delfau, J.L. and Vovelle, C. (1997), Modeling of the Structure of a Premixed n-Decane Flame. *Combust. Sci. Technol.,* **130**, 269.
47. Bales-Gueret, C., Cathonnet, M., Boettner, J.C. and Gaillard, F. (1997). Experimental Study and Kinetic Modeling of Higher Hydrocarbons Oxidation in a Jet-stirred Flow Reactor. *Energy & Fuels*, **6**, 189.
48. Battin-Leclerc, F., Fournet, R., Glaude, P.A., Judenherc, B., Warth, V., Come, G.M. and Scacchi, G. (2000). Modeling of the Gas-phase Oxidation of n-Decane from 550 to 1,600 K. *Twenty-Eight Symposium (International) on Combustion.* The Combustion Institute, Pittsburgh, 1597.
49. Delfau, J.L., Bouhria, M., Reuillon, M., Sanogo, O., Akrich, R. and Vovelle, C. (1990). Experimental and Computational Investigation of the Structure of a Decane/O_2/Ar Flame. *Twenty-Third Symposium (International) on Combustion.* The Combustion Institute, Pittsburgh, 1567.
50. Zeppieri, S.P., Klotz, S.D. and Dryer, F.L. (2000). Modeling Concepts for Larger Carbon Number Alkanes: a Partially Reduced Skeletal Mechanism for n-Decane Oxidation and Pyrolysis. *Twenty-Eighth Symposium (International) on Combustion.* The Combustion Institute, Pittsburgh, 1587.

51. Bikas, G. and Peters, N. (2001). Kinetic Modeling of n-Decane Combustion and Autoignition. *Combust. Flame*, **126**, 1456.
52. Bradley, D., El-Din Habik, S. and El-Sharif, S.A. (1991). A Generalization of Laminar Burning Velocities and Volumetric Heat Release Rates. *Combust. Flame*, **87**, 336.
53. Ristori, A., Dagaut, P., and Cathonnet, M. (2001). The Oxidation of n-Hexadecane: Experimental and Detailed Kinetic Modeling. *Combust. Flame*, **125**, 1128.
54. Fournet R., Battin-Leclerc, F., Glaude, P.A., Judenherg, B., Warth, V., Come, G.M., Scacchi, G., Ristori, A., Pengloan, G., Dagaut, P., and Cathonnet, M. (2001). The Gas-Phase Oxidation of n-Hexadecane. *Int. J. Chem. Kinet.*, **33**, 574.
55. Tomlin, A.S., Turanyi, T. and Pilling, M.J. (1997). Comprehensive Chemical Kinetics. In *Low Temperature Combustion and Autoignition* (Pilling, M.J. and Hancock, G., Eds.). Elsevier, Amsterdam, p. 293.
56. Green, W.H., Barton, P.I., Bhattacharjee, B., Matheu, D.M., Schwer, D.A., Song, J., Sumathi, R., Carstensen, H.-H., Dean, A.M. and Grenda, J.M. (2001). Computer Construction of Detailed Chemical Kinetic Models for Gas-phase Reactors. *Ind. Engng. Chem. Res*., **40**, 5362.
57. Nehse, M., Warnatz, J., Chevalier, C., Louessard, P. and Melenk, H. (1996). MOLEC: A Program for the Generation of Chemical Reaction Equations. User's Manual. Interdisziplinäres Zentrum für Wissenschaftliches Rechnen, Universität Heidelberg.
58. http://www-g.eng.cam.ac.uk/energy/NondasTeaching/345.
59. Warnatz, J., Maas, U. and Dibble, R.W. (1999). *Combustion. Physical and Chemical Fundamentals, Modeling and Simulation, Experiments, Pollutant Formation* (2nd edn). Springer, Heidelberg.
60. Warnatz, J. (1984). Chemistry of High Temperature Combustion of Alkanes up to Octane. *Twentieth Symposium (International) on Combustion.* The Combustion Institute, Pittsburgh, 845.
61. Glassman, I. (1996). Combustion (3rd edn.). Academic Press, New York.
62. Pilling, M.J., and Seakins, P.W. (1995). *Reaction Kinetics* (1st edn). Oxford Science Publications.
63. Richard, C., Scacchi, G. and Back, M.H. (1978). *Int. J. Chem. Kin.*, **10**, 307.
64. Chevalier, C., Warnatz, J. and Melenk, H. (1990). Automatic Generation of Reaction Mechanisms for the Description of the Oxidation of Higher Hydrocarbons. *Ber. Bunsenges. Phys. Chem.*, **94**, 1362.
65. Warnatz, J. (2002). HOMREA: User Guide, Version 2.5. Interdisziplinäres Zentrum für Wissenschaftliches Rechnen, Universität Heidelberg.

66. Walker, R.W. (1998). Reactions of HO_2 Radicals in Combustion Chemistry. *Twenty-Second Symposium (International) on Combustion*. The Combustion Institute, Pittsburgh, 883.
67. Tsang, W. (1988). Chemical Kinetic Data Base for Combustion Chemistry. Part 3. Propane. *J. Phys. Chem. Ref. Data,* **17**, 887.
68. Ingham T., Walker, R.W. and Woolford, R.E. (1994). Kinetic Parameters for the Initiation Reaction RH + O_2 → R + HO_2. *Twenty-Fifth Symposium (International) on Combustion.* The Combustion Institute, Pittsburgh, 767.
69. Allara, D.L. and Shaw, R. (1980). A Compilation of Kinetic Parameters for the Thermal Degradation of n-Alkane Molecules. *J. Phys. Chem. Ref. Data*, **9**(3), 523.
70. Sundaram, K. M. and Froment, G. F. (1978). *Ind. Eng. Chem. Fundam.*, **17**, 174.
71. Ranzi, E., Sogaro, A., Gaffuri, P., Pennati G., Westbrook, C.K. and Pitz, W.J. (1994). *Combust. Sci. Technol*., **100**, 299.
72. Heyberger, B., Belmekki, N., Conraud, V., Glaude, P.A., Fournet, R. and Battin-Leclerc, F. (2002). Oxidation of Small Alkenes at High Temperature. *Int. J. Chem. Kinet.* **34**, 666.
73. Tsang, W. (1991). Chemical Kinetic Data Base for Combustion Chemistry Part V. Propene. *J. Phys. Chem. Ref. Data,* **20**(2), 221.
74. Baldwin, R.R., Stout, D.R. and Walker, R.W. (1991). Arrhenius Parameters for the Addition of HO_2 Radicals to Ethene between 400-degrees-C and 500-degrees-C. *J. Chem. Soc. Faraday Trans.,* **87**(4), 2147.
75. Benson, S.W. (1982). The Kinetics and Thermochemisty of Chemical Oxidation with Application to Combustion and Flames. *Prog. Energy Combust. Sci*., **7**, 125.
76. Fish, A. (1970). Rearrangement and Cyclization Reactions of Organic Peroxy Radicals. In *Organic Peroxyde* (Swern, D., Ed.), Vol. 1. Willey-Interscience, NewYork, pp. 141, 198.
77. http://www-cms.llnl.gov/combustion/combustion_home.html.
78. Tsang, W., and Hampson, R.F. (1987). Chemical Kinetic Data Base for Combustion Chemistry. Part 1. Methane and Related Compounds. *J. Phys. Chem. Ref. Data*, **15**, 1087.
79. Battin-Leclerc, F., Glaude, P.A., Warth, V., Fournet, R., Scacchi G. and Come, G. M. (2000). Computer Tools for Modelling the Chemical Phenomena Related to Combustion. *Chem. Eng. Sci.,* **55**, 2883.
80. Chevalier, C. (1993). Entwicklung eines detaillierten Reaktionsmechanismus zur Modellierung der Verbrennungsprozesse von Kohlenwasserstoffen bei Hoch- und Niedertemperaturbedingungen. Dissertation. Universität Stuttgart.
81. Pollard, R.T. (1977). Comprehensive Chemical Kinetics. In *Gas-Phase Combustion* (Bamford, C.H. and Tipper, C.F.H., Eds.) Vol. 17. Elsevier, New York, pp. 249-367.

82. Baulch, D.L., Cobos, C.J., Cox, R.A., Esser, C., Frank, P., Just, Th., Kerr, J.A., Pilling, M. J., Troe, J., Walker, R. W. and Warnatz, J. (1992). Evaluated Kinetic Data for Combustion Modeling. *J. Phys.Chem. Ref. Data,* **21**(3), 411.
83. Baulch, D.L., Cobos, C.J., Cox, R.A., Frank, P., Haymann, G., Just, Th., Kerr, J.A., Murrels, T., Pilling, M.J., Troe, J., Walker, R.W. and Warnatz, J. (1994). Evaluated Kinetic Data for Combustion Modeling Suplement I. *J. Phys.Chem. Ref. Data,* **23**(6), 847.
84. Benson, S.W. (1976). *Thermochemical Kinetics* (2nd edn.). John Wiley & Sons, New York.
85. Bird, R.B., Stewart, W.E. and Lighfoot, E.N. (1960). *Transport Phenomena*. John Wiley and Sons, New York.
86. Bui-Pham, M. and Seshadri, K. (1991). Comparison between Experimental Measurements and Numerical Calculations of the Structure of Heptane-Air Diffusion Flames. *Combust. Sci. Technol*., **79**, 293.
87. Cathonnet, M., Boettner, J.C. and James, H. (1981). Experimental Study and Numerical Modeling of High Temperature Oxidation of Propane and n-Butane. *Eighteenth Symposium (International) on Combustion*. The Combustion Institute, Pittsburgh, 903.
88. Chakir, A., Cathonnet, M., Boettner, J.C. and Gaillard, F. (1988). Kinetic Study of n-Butane Oxidation. *Combust. Sci. Technol*., **65**, 207.
89. Chakir, A., Cathonnet, M., Boettner, J.C. and Gailard, F. (1988). Kinetic Study of 1-Butene Oxidation in a Jet-Stirred Reactor Flow. *Twenty-Second Symposium (International) on Combustion.* The Combustion Institute, Pittsburgh, 873.
90. Chakir, A., Bellman, M., Boettner, J.C. and Cathonnet, M. (1991). Kinetic Study of n-Pentane Oxidation. *Int. J. Chem. Kinet*., **77**, 239.
91. Cohen, N. (1982). The Use of Transition-State Theory to Extrapolate Rate Coefficients for Reations of OH with Alkanes. *Intl. J. Chem. Kinet.*, **14**, 1339.
92. Colket, M.B. and Spadaccini. L.J. (2001) Scramjet Fuels Autoignition Study. *J. Propul. Power,* **17**, 315.
93. Cox, R.A. and Cole, J.A. (1985). Chemical Aspects of the Autoignition of Hydrocarbon-Air Mixtures. *Combust. Flame*, **60**, 109.
94. Curran, H.J., Pitz, W.J., Westbrook, C.K., Callahan, C.V. and Dryer, F.L. (1998). Oxidation of Automotive Primary Reference Fuels at Elevated Pressures. *Twenty-Seventh Symposium (International) on Combustion.* The Combustion Institute, Pittsburgh, 379.
95. D'Anna, A., Mercogliano, R., Barbella, R. and Ciajolo, A. (1992). Low Temperature Oxidation Chemistry of Iso-octane under High-Pressure Conditions. *Combust. Sci. Technol*., **83**, 217.

96. Dagaut, P., Cathonnet, M. and Boettner, J.C. (1988). Experimental Study and Kinetic Modeling of Propene Oxidation in a Jet-Stirred Flow Reactor. *J. Phys. Chem.*, **92**, 661.
97. Dagaut, P., Reuillon, M. and Cathonnet, M.(1994). High Pressure Oxidation of Liquid Fuels from Low to High Temperature. 2. Mixtures of n-Heptane and Iso-octane. *Combust. Sci. Technol*., **103**, 315.
98. Dagaut, P., Reuillon, M., Boettner, J.C. and Cathonnet, M. (1994). Kerosene Combustion at Pressure up to 40 atm: Experimental Study and Detailed Chemical Kinetic Modeling. *Twenty-Fifth Symposium (International) on Combustion.* The Combustion Institute, Pittsburgh, 919.
99. Dagaut, P., Reuillon, M., Cathonnet, M. and Voisin, D. (1995). High Pressure Oxidation of Normal Decane and Kerosene in Dilute Conditions from Low to High Temperatures. *J. Chim. Phys. Physico-Chim. Biol.*, **92**, 47.
100. Davidson, D.F., Herbon, J.T., Horning, D.C. and Hanson, R.K. (2001) OH Concentration Time Histories in n-Alkane Oxidation. *Int. J. Chem. Kinet.*, **33**, 775.
101. Davidson, D.F., Oelschlaeger, M.A., Herbon, J.T. and Hanson, R.K. (2002). Shock Tube Measurements of Iso-octane Ignition Times and OH Concentration Histories. *Twenty-Ninth Symposium (International) on Combustion.* The Combustion Institute, Pittsburgh, 1295.
102. Davis, S.G., Law, C.K. and Wang, H. (1999). Propene Pyrolysis and Oxidation Kinetics in a Flow Reactor and Laminar Flames. *Combust. Flame*, **119**, 375.
103. Eiteneer, B. and Frenklach, M. (2003). Experimental and Modeling Study of Shock-Tube Oxidation of Acetylene. *Int. J. Chem. Kinet*., **35**, 414.
104. El Bakali, A., Delfau, J.L. and Vovelle. C. (1998). Experimental Study of 1 Atmosphere, Rich, Premixed n-Heptane and Iso-octane Flames. *Combust. Sci. Technol.*, **140**, 69.
105. El Bakali A., Dagaut, P., Pillier, L., Desgroux, P., Pauwels, J.-F., Rida, A. and Meunier, P. (2004). Experimental and Modeling Study of the Oxidation of Natural Gas in a Premixed Flame, Shock Tube, and Jet-Stirred Reactor. *Combust. Flame*, **137**, 109.
106. Encyclopedia Britannica 2003 Deluxe Edition CD-ROM. (2003). Encyclopedia Britannica, Inc.
107. Faravelli, T., Gaffuri, P. Ranzi, E. and Griffths, J.F. (1998). Detailed Thermokinetic Modelling of Alkane Autoignition as a Tool for the Optimization of Performance of Internal Combustion Engines. *Fuel*, **77**(3), 147.
108. Fournet, R., Bauge, J.C. and Battin-Leclerc, F. (1999). Experimental and Modeling of Oxidation of Acetylene, Propyne, Allene and 1,3-Butadiene. *Int. J. Chem. Kinet*., **31**, 379.

109. Fournet R., Warth, V., Glaude, P.A., Battin-Leclerc, F., Scacchi, G. and Come, G.M. (1999). Automatic Reduction of Detailed Mechanisms of Combustion of Alkanes by Chemical Lumping. *Int. J. Chem. Kinet.*, **32**, 36.
110. Gardiner, Jr., W.C. (2000). Introduction to Combustion Modeling. In *Gas-Phase Combustion Chemistry* (Gardiner, Jr., W.C., Ed.). Springer, New York.
111. Gardiner, Jr., W.C. and Troe, J. (2000). Rate Coefficients of Thermal Dissociation, Isomerization, and Recombination Reactions. In *Gas-Phase Combustion Chemistry* (Gardiner, Jr., W.C., Ed.). Springer, New York.
112. Glaude, P.A., Battin-Leclerc, F., Fournet, R., Warth, V., Come, G.M. and Scacchi, G. (2000). Construction and Simplification of a Model for the Oxidation of Alkanes. *Combust. Flame*, **122**, 451.
113. Griffiths, J.F., Halford-Maw, P.A. and Mohamed, C. (1997). Spontaneous Ignition Delays as a Diagnostic of the Propensity of Alkanes to Cause Engine Knock. *Combust. Flame*, **111**, 327.
114. Held, T.J., Marchese, A.J. and Dryer, F.L. (1997). A Semi-empirical Reaction Mechanism for n-Heptane Oxidation and Pyrolysis. *Combust. Sci. Technol.*, **123**, 107.
115. Heyberger, B., Battin-Leclerc, F., Warth, V., Fournet, R., Come, G.M. and Scacchi, G. (2001). Comprehensive Mechanism for the Gas-Phase Oxidation of Propene. *Combust. Flame*, **126**, 1780.
116. Horning, D.C., Davidson, D.F. and Hanson, R.K. (2001). Ignition Time Correlations for n-Alkane/Oxygen/Argon Mixtures. *Twenty-Third International Symposium Shock Waves*.
117. Horning, D.C., Davidson, D.F. and Hanson, R.K. (2002). Study of the High Temperature Autoignition of n-Alkane/Oxygen/Argon Mixtures. *J. Propul. Power*, **18**, 363.
118. http://www.ensic.u-nancy.fr/ENSIC/DCPR.
119. Ingemarsson, A.T., Pedersen, J.R. and Olsson, J.O. (1999). Oxidation of n-Heptane in a Premixed Laminar Flame. *J. Phys. Chem. A*, **103**, 8222.
120. Just, Th. (1994). Multichannel Reactions in Combustion. *Twenty-Fifth Symposium (International) on Combustion.* The Combustion Institute, Pittsburgh, 687.
121. Kiefer, J. (1998). Some Unusual Aspects of Unimolecular Falloff of Importance in Combustion Modeling. *Twenty-Seventh Symposium (International) on Combustion.* The Combustion Institute, Pittsburgh, 113.
122. Laskin, A., Wang, H. and Law, C.K. (2000). Detailed Kinetic Modeling of 1,3-Butadiene Oxidation at High Temperatures. *Int. J. Chem. Kinet*., **32**, 614.
123. Lay, T. H., Bozzelli, J. W., Dean, A. M. and Ritter, E. R. (1995). Hydrogen Atom Bond Increments for Calculation of Thermodynamic Properties of Hydrogen Radical Species. *J. Phys. Chem*., **99**, 15054.

124. Leung, K.M. and Lindstedt, R.P. (1995). Detailed Kinetic Modeling of C_1-C_3 Alkane Diffusion Flames. *Combust. Flame*, **102**, 129.
125. Lignola, P.G. and Reverchon, E. (1987). Cool Flame. *Prog. Energy Combust. Sci*., **13**, 75.
126. Maas, U. (1988). Mathematische Modellierung instationärer Vebrennungsprozesse unter Verwendung detaillierter Reaktionsmechanismen. Dissertation. Universität Heidelberg.
127. Mallard, W.G., Westley, F., Herron, J.T., Hampson, R.F. and Frizzell, D.H. (1994). NIST Chemical Kinetic Database: Version 6.0. National Institute of Standards and Technology, Gaithersburg, MD.
128. Miller, J.A. (1996). Theory and Modeling in Combustion Chemistry. *Twenty-Sixth Symposium (International) on Combustion.* The Combustion Institute, Pittsburgh, 461.
129. Minetti, R., Carlier, M., Ribaucour, M., Therssen, E. and Sochet, L.R. (1996). Comparison of Oxidation and Autoignition of the Two Reference Fuels by Rapid Compression. *Twenty-Sixth Symposium (International) on Combustion.* The Combustion Institute, Pittsburgh, 747.
130. Mirokhin, Y., Mallard, W. G., Westley, F., Herron, J. T., Frizzell, D. and Hampson, R. (1998). NIST Standard Reference Database 17-2Q98, Gaithersburg, MD.
131. Pfahl, U., Fieweger, K. and Adomeit, G. (1996). Final Report, Subprogramme FK4, EDEA-EFFECT.
132. Poutsma, M.L. (2000). Fundamental Reactions of Free Radicals Relevant to Pyrolysis Reactions. *J. Anal. App. Pyrol*., **54**, 5.
133. Ranzi, E., Gaffuri, P., Faravelli, T. and Dagaut, P. (1995). A Wide Range Modeling Study of n-Heptane Oxidation. *Combust. Flame*, **103**, 91.
134. Ranzi, E., Dente, M., Goldaniga, A., Bozzano, G. and Faravelli, T. (2001). Lumping Procedures in Detailed Chemical Kinetics Modeling of Gasification, Pyrolysis, Partial Oxidation and Combustion. *Prog. Energy Combust. Sci*., **27**, 99.
135. Ritter E.R. and Bozzelli, J.W. (1991). THERM: Thermodynamic Property Estimation for Gas Phase Radicals and Molecules. *Int. J. Chem. Kinet*., **23**, 767.
136. Savage, E.P. (2000). Mechanisms and Kinetics Models for Hydrocarbon Pyrolysis. *J. Anal. App. Pyrol*., **54**, 109.
137. Simmie, J.M. (2003). Detailed Chemical Kinetic Models for the Combustion of Hydrocarbon Fuels. *Prog. Energy Combust. Sci*. **29**, 599.
138. Simon, V., Simon, Y., Scacchi, G. and Baronnet, F. (1997). Experimental Study and Modeling of Oxidation of n-Pentane and Cyclopentane. *Can. J. Chem*., **75**, 575.

139. Tsang, W. (1990). Chemical Kinetic Data Base for Combustion Chemistry. Part 4. Isobutane. *J. Phys. Chem. Ref. Data*, **19**, 1.
140. Warnatz, J. (1977). Berechnung der Flammengeschwindigkeit und der Struktur von laminaren flachen Flammen, Habilitationsschrift, Universität Darmstadt.
141. Warnatz, J. (1981). The Structure of Laminar Alkane, Alkene and Acetylene Flames. *Eighteenth Symposium (International) on Combustion.* The Combustion Institute, Pittsburgh, 369.
142. Warnatz, J. (1992). Resolution of Gas Phase and Surface Combustion Chemistry into Elementary Reactions. *Twenty-Forth Symposium (International) on Combustion.* The Combustion Institute, Pittsburgh, 553.
143. Warnatz, J. (2000). Rate Coefficients in the C/H/O System. In *Gas-Phase Combustion Chemistry* (Gardiner, Jr., W.C., Ed.). Springer, New York.
144. Warth, V., Stef. S., Glaude, P.A., Battin-Leclerc, F., Scacchi, G. and Come, G.M. (1998). Computer-Aided Derivation of Gas-Phase Oxidation Mechanisms: Application to the Modeling of the Oxidation of n-Butane. *Combust. Flame*, **114**, 81.
145. Warth, V., Battin-Leclerc, F., Fournet, R., Glaude, P.A., Come, G.M. and Scacchi, G. (2000). Computer-based Generation of Reaction Mechanisms for Gas Phase Oxidation. *Comput. Chem.*, **24**, 541.
146. Westbrook, C.K. and Pitz, W.J. (1987). Kinetic Modeling of Autoignition of Higher hydrocarbons: n-Heptane, n-Octane and Iso-octane. In *Complex Chemical Reaction Systems* (Warnatz, J. and Jager, W., Eds.). Springer-Verlag, Berlin-Heidelberg, 39.
147. Westbrook, C.K., Pitz, W.J., Curran, H.C., Boercker, J., Griffiths, J.F., Mohamed, C. and Ribaucour, M. (2002). Detailed Chemical Kinetic Reaction Mechanisms for Autoignition of Isomers of Heptane under Rapid Compression. *Twenty-Ninth Symposium (International) on Combustion.* The Combustion Institute, Pittsburgh, 1311.
148. Zellner, R. (2000). Bimolecular Reaction Rate Coefficients. In *Gas-Phase Combustion Chemistry* (Gardiner, Jr., W.C., Ed.). Springer, New York.

Appendix 1
TABLE OF KINETIC PARAMETERS

$k = AT^b \exp(-E_a/RT)$; ***A*** **in s^{-1}/b/E_a in kJ/mol**

Reaction rules	*k*			Ref.
HIGH TEMPERATURE				
Alkane reactions				
3.1.1 Unimolecular decomposition of alkanes				
a. C-C breaking				
$C_{primary}$-$C_{secondary}$	1.750E+19	-0.86	364.38	24
$C_{primary}$-$C_{tertiary}$	6.040E+17	-0.55	353.51	40
$C_{primary}$-$C_{quaternary}$	1.740E+22	-1.62	351.54	5
$C_{secondary}$-$C_{secondary}$	4.150E+22	-1.60	369.32	24
$C_{secondary}$-$C_{tertiary}$	3.090E+21	-1.41	358.65	40
$C_{secondary}$-$C_{quaternary}$	2.000E+16	0.00	326.35	40
b. C-H breaking				
Primary H	2.790E+21	-1.71	434.30	5
Secondary H	1.290E+18	-0.82	415.64	5
Tertiary H	1.450E+20	-1.42	406.39	5
3.1.2 Abstraction of H atoms from alkanes				
H				
Primary	9.350E+06	2.00	32.20	18
Secondary	4.500E+06	2.00	20.90	18
Tertiary	1.260E+14	0.00	30.60	18
O				
Primary	1.670E+13	0.00	32.90	18
Secondary	1.400E+13	0.00	21.80	18
Tertiary	1.000E+13	0.00	13.70	18
OH				
Primary	1.430E+09	1.10	7.58	18
Secondary	6.500E+08	1.30	2.94	18
Tertiary	4.000E+12	0.00	1.85	18
HO_2				
Primary	1.870E+12	0.00	81.20	18
Secondary	1.680E+12	0.00	71.20	18
Tertiary	1.000E+12	0.00	60.30	18
CH_3				
Primary	2.200E+11	0.00	48.60	18
Secondary	2.000E+04	0.00	39.80	18
Tertiary	1.000E+11	0.00	33.10	18

Reaction rules	*k*			Ref.
O_2				
Primary	4.200E+12	0.00	205.2	18
Secondary	1.000E+13	0.00	199.3	18
Tertiary	2.000E+12	0.00	192.6	18
CH_3O_2				
Primary	4.200E+12	0.00	87.5	18
Secondary	1.500E+12	0.00	71.2	18
Tertiary	3.000E+12	0.00	62.8	18
Peroxy radical				
Primary	1.000E+12	0.00	58.6	66
Secondary	1.000E+12	0.00	46.1	66
Tertiary	1.000E+12	0.00	33.5	66
CHO				
Primary	3.390E+04	2.50	77.30	67
Secondary	5.370E+06	1.90	71.10	67
Tertiary	3.390E+03	2.53	56.40	67
CH_2OH				
Primary	3.310E+01	2.90	58.50	67
Secondary	3.020E+01	2.90	50.20	67
Tertiary	1.200E+02	2.70	45.10	67
CH_3O				
Primary	3.200E+11	0.00	29.29	68
Secondary	1.100E+11	0.00	20.92	68
Tertiary	1.900E+10	0.00	11.72	68
C_2H_5				
Primary	1.667E+10	0.00	56.07	69
Secondary	2.500E+10	0.00	43.51	69
Tertiary	1.000E+11	0.00	33.05	69
I-C_3H_7				
Primary	1.410E-03	4.20	36.40	54
Secondary	1.410E-03	4.20	33.40	54
Tertiary	1.410E-03	4.20	25.10	54
C_2H_3				
Primary	1.667E+11	0.00	75.31	70
Secondary	2.000E+11	0.00	70.29	70
Tertiary	2.000E+11	0.00	59.83	70
Primary alkyl radical				
Primary	1.000E+11	0.00	56.40	71
Secondary	1.000E+11	0.00	46.80	71
Tertiary	1.000E+11	0.00	37.60	71
Secondary alkyl radical				
Primary	1.000E+11	0.00	60.60	71
Secondary	1.000E+11	0.00	51.00	71
Tertiary	1.000E+11	0.00	41.80	71

Reaction rules	*k*			Ref.
Tertiary alkyl radical				
Primary	1.000E+11	0.00	62.70	71
Secondary	1.000E+11	0.00	53.10	71
Tertiary	1.000E+11	0.00	43.90	71
Alkyl radical reactions				
3.1.3 Decomposition of alkyl radicals				
a. C-C scission				
$C_{primary}$-$C_{secondary}$	8.000E+12	0.00	138.2	18
$C_{primary}$-$C_{tertiary}$	1.000E+13	0.00	108.9	18
$C_{primary}$-$C_{quaternary}$	1.000E+13	0.00	124.7	18
$C_{secondary}$-$C_{secondary}$	2.000E+13	0.00	119.6	18
$C_{secondary}$-$C_{tertiary}$	1.300E+13	0.00	123.5	18
$C_{secondary}$-$C_{quaternary}$	1.300E+13	0.00	123.5	18
a. C-H scission				
Primary H	8.394E+17	-1.30	173.64	24
Secondary H	2.397E+18	-1.55	168.36	24
Tertiary H	2.709E+20	-2.14	160.37	40
3.1.4 Isomerization of alkyl radicals				
a. 5-membered ring				
Primary H	1.000E+11	0.00	88.30	18
Secondary H	1.000E+11	0.00	75.66	18
Tertiary H	1.000E+11	0.00	67.40	18
b. 6-membered ring				
Primary H	1.000E+11	0.00	58.94	18
Secondary H	1.000E+11	0.00	46.40	18
c. 7-membered ring				
Primary H	1.000E+11	0.00	88.30	18
Secondary H	1.000E+11	0.00	75.66	18
3.1.5 Oxidation of alkyl radicals to form alkenes				
Primary H	2.500E+08	0.00	25.94	18
Secondary H	2.500E+08	0.00	16.32	18
Tertiary H	2.500E+08	0.00	10.26	18
Alkene reactions				
3.1.6 Decomposition of alkenes	2.500E+16	0.00	297.06	69
3.1.7 Abstraction of allylic H atoms				
H				
Primary	2.820E+04	2.50	0.6	18
Secondary	1.320E+04	2.50	-10.7	18
Tertiary	1.230E+04	2.50	-21.6	estimation

Reaction rules	*k*			Ref.
O				
Primary	3.160E+10	0.70	15.3	72
Secondary	2.400E+10	0.70	4.2	72
Tertiary	1.860E+10	0.70	-8.6	estimation
OH				
Primary	1.480E+06	2.00	3.0	72
Secondary	2.140E+06	2.00	-2.08	72
Tertiary	1.910E+06	2.00	-6.68	estimation
HO_2				
Primary	3.160E+03	2.60	27.8	72
Secondary	3.160E+03	2.60	21.5	72
Tertiary	1.580E+04	2.60	15.2	estimation
CH_3				
Primary	6.310E-01	3.50	7.1	72
Secondary	2.880E+05	3.50	9.1	72
Tertiary	9.550E+04	3.50	4.3	estimation
O_2				
Primary	7.940E+11	0.00	164	72
Secondary	2.000E+12	0.00	160	72
Tertiary	3.980E+12	0.00	151	estimation
3.1.8 Abstraction of vinylic H atoms				
H				
Secondary	8.130E+05	2.50	51.3	54
Tertiary	4.070E+05	2.50	40.9	54
O				
Secondary	5.010E+10	0.70	36.0	72
Tertiary	6.310E+10	0.70	32.0	72
OH				
Secondary	2.190E+06	2.00	11.6	54
Tertiary	1.100E+06	2.00	6.1	54
CH_3				
Secondary	1.350E+00	3.50	53.9	54
Tertiary	9.800E-01	3.50	48.9	54
O_2				
Secondary	1.000E+13	0.00	241	72
Tertiary	2.000E+12	0.00	232	72
3.1.9 Abstraction of alkylic H atoms				
- gama position				
H				
Primary	1.830E+13	0.00	16.3	18
Secondary	2.750E+13	0.00	16.3	18
Tertiary	5.500E+13	0.00	16.3	18

Reaction rules	*k*			Ref.
O				
Primary	4.330E+12	0.00	18.8	18
Secondary	6.500E+12	0.00	18.8	18
Tertiary	1.300E+13	0.00	18.8	18
OH				
Primary	6.000E+13	0.00	29.1	18
Secondary	9.000E+13	0.00	29.1	18
Tertiary	1.800E+14	0 00	29.1	18
HO_2				
Primary	3.330E+10	0.00	71.4	18
Secondary	5.000E+10	0.00	71.4	18
Tertiary	1.000E+11	0.00	71.4	18
CH_3				
Primary	3.330E+10	0.00	30.6	18
Secondary	5.000E+10	0.00	30.6	18
Tertiary	1.000E+11	0.00	30.6	18
O_2				
Primary	1.330E+12	0.00	167.4	18
Secondary	2.000E+12	0.00	167.4	18
Tertiary	4.000E+12	0.00	167.4	18
- other positions	Same as abstraction of H atoms from alkanes			
3.1.10 Addition of H atoms to double bonds				
Primary	1.000E+13	0.00	5.02	69
Secondary	1.000E+13	0.00	12.13	69
Tertiary	1.000E+13	0.00	13.39	69
3.1.11 Addition of CH_3 radicals to double bonds	2.000E+11	0.00	30.2	73
3.1.12 Addition of O atoms to double bonds	3.390E+07	1.83	1.1	73
3.1.13 Addition of OH radicals to double bonds	1.260E+12	0.00	-2.1	73
3.1.14 Addition of HO_2 radicals to double bonds	1.000E+12	0.00	28.8	74
3.1.15 Retro-ene reactions	8.000E+12	0.00	236	63
Alkenyl radical reactions				
3.1.16 Isomerization of alkenyl radicals				
5-membered ring	2.510E+14	0.00	125.5	22 (x16)
6-membered ring	2.510E+14	0.00	125.5	22 (x16)
3.1.17 Decomposition of allylic radicals	2.510E+13	0.00	125.5	18

Reaction rules	*k*	Ref.
3.1.18 Decomposition of vinylic radicals		
dialkene formation	2.510E+13 0.00 125.5	18
alkyne formation	1.000E+13 0.00 125.5	18
3.1.19 Decomposition of alkenyl radicals	2.510E+13 0.00 125.5	18
LOW TEMPERATURE		
Alkyl radical reactions		
3.2.1 Addition of alkyl radicals to molecular oxygen		
primary C	2.000E+12 0.00 0.0 k_{inf}: 2.000E+15 0.00 117.30	75
secondary C	2.000E+12 0.00 0.0 k_{inf}: 2.000E+15 0.00 117.30	75
tertiary C	2.000E+12 0.00 0.0 k_{inf}: 1.200E+16 0.00 117.30	75
Alkyl peroxy radical reactions		
3.2.2 Isomerization of alkylperoxy radicals		
5-membered ring		
primary H	2.980E+12 0.00 124.26 k_{inf}: 1.000E+11 0.00 52.3	24 76
secondary H	2.980E+12 0.00 116.73 k_{inf}: 1.000E+11 0.00 52.3	24 76
tertiary H	2.590E+12 0.00 106.27 k_{inf}: 1.000E+11 0.00 43.4	24 76
6-membered ring		
primary H	2.470E+11 0.00 100.0 k_{inf}: 1.000E+11 0.00 27.6	24 76
secondary H	2.480E+11 0.00 92.68 k_{inf}: 1.000E+11 0.00 27.6	24 76
tertiary H	2.160E+11 0.00 82.42 k_{inf}: 1.000E+11 0.00 26.8	24 76
7-membered ring		
primary H	2.060E+10 0.00 88.28 k_{inf}: 1.000E+11 0.00 29.3	24 76
secondary H	2.060E+10 0.00 80.96 k_{inf}: 1.000E+11 0.00 31.4	24 76
tertiary H	1.800E+10 0.00 68.62 k_{inf}: 1.000E+11 0.00 30.6	24 76

Reaction rules	*k*	Ref.
8-membered ring		
primary H	1.720E+09 0.00 100.0	24
	k_{inf}: 1.000E+11 0.00 66.9	76
secondary H	1.720E+09 0.00 92.68	24
	k_{inf}: 1.000E+11 0.00 67.0	76
tertiary H	1.500E+09 0.00 82.42	24
	k_{inf}: 1.000E+11 0.00 67.0	76
3.2.4 Reaction of alkylperoxy radicals with HO_2	1.750E+10 0.00 -13.7	77
3.2.5 Reaction of alkylperoxy radicals with H_2O_2	2.410E+12 0.00 41.59	78
Hydroperoxide reactions		
3.2.6 Homolytic O-O scission of hydroperoxides		
Secondary C	1.500E+16 0.00 177.8	77
Tertiary C	1.250E+16 0.00 174.1	77
Quartery C	7.500E+15 0.00 173.8	77
Alkoxy reactions		
3.2.7 Decomposition of alkoxy radicals	4.000E+14 0.00 72.0	18
Hydroperoxy radical reactions		
3.2.8 Addition of hydroperoxy alkyl radicals to molecular oxygen	1.000E+13 0.00 0.0 k_{inf}: 5.000E+12 0.00 117.0	18
3.2.9 β scission of hydroperoxy alkyl radicals formed by the (1,4) isomerization	2.000E+13 0.00 83.8	80
3.2.10 Homolytic C-C scission of hydroperoxy alkyl radicals formed by the (1,5) isomerization	2.000E+13 0.00 120.0	79
3.2.11 Homolytic C-C scission of hydroperoxy alkyl radicals formed by the (1,6) and (1,7) isomerization	2.000E+13 0.00 120.0	79
3.2.12 Homolytic O-O scission of hydroperoxy alkyl radicals with the radical site at a carbon atom linked to oxygen atom	1.000E+09 0.00 31.3	79
3.2.13 Oxidation of hydroperoxy alkyl radicals		
primary H	2.340E+11 0.00 20.9	54
secondary H	7.940E+11 0.00 20.9	54
tertiary H	4.470E+11 0.00 20.9	54

Reaction rules	*k*	Ref.
3.2.14 Formation of cyclic ethers from hydroperoxy alkyl radicals		
3-membered ring	6.000E+11 0.00 92.05	77
4-membered ring	7.500E+10 0.00 63.81	77
5-membered ring	9.375E+09 0.00 29.29	77
6-membered ring	1.172E+09 0.00 7.531	77
Peroxy hydroperoxy alkyl reactions		
3.2.15 Isomerization of peroxy hydroperoxy alkyl radicals		
5-membered ring		
secondary H	1.490E+12 0.00 111.7	24
	k_{inf}: 1.000E+11 0.00 52.3	76
tertiary H	1.490E+12 0.00 104.2	24
	k_{inf}: 1.000E+11 0.00 43.4	76
6-membered ring		
secondary H	1.240E+11 0.00 87.44	24
	k_{inf}: 1.000E+11 0.00 27.6	76
tertiary H	1.240E+11 0.00 80.12	24
	k_{inf}: 1.000E+11 0.00 26.8	76
7-membered ring		
secondary H	1.030E+10 0.00 75.73	24
	k_{inf}: 1.000E+11 0.00 31.4	76
tertiary H	1.030E+10 0.00 68.41	24
	k_{inf}: 1.000E+11 0.00 30.6	76
8-membered ring		
secondary H	8.600E+08 0.00 87.44	24
	k_{inf}: 1.000E+11 0.00 67.0	76
tertiary H	8.600E+08 0.00 80.12	24
	k_{inf}: 1.000E+11 0.00 67.0	76
Dihydroperoxy alkyl radical reactions		
3.2.16 Homolytic O-O scission of dihydroperoxy alkyl radicals	1.000E+09 0.00 31.4	80
3.2.17 Formation of hydroperoxy cyclic ethers from dihydroperoxy radicals		
3-membered ring	6.000E+11 0.00 92.05	77
4-membered ring	7.500E+10 0.00 63.81	77
5-membered ring	9.375E+09 0.00 29.29	77
6-membered ring	1.172E+09 0.00 7.531	77

Reaction rules	*k*			Ref.
Ketohydroperoxyde reactions				
3.2.18 Decomposition of ketohydroperoxides				
primary H	1.260E+16	0.00	182.0	81
secondary H	7.940E+15	0.00	174.0	81
tertiary H	4.470E+15	0.00	177.5	81
O=R"O$^{\bullet}$ radical reactions				
3.2.19 Decomposition of O=R"O$^{\bullet}$	2.000E+13	0.00	62.8	18
Cyclic ether reactions				
3.2.20 Abstraction of H atoms from cyclic ethers				
a. H abstraction at H-C-C position				
OH				
primary H	3.830E+07	1.53	3.24	24
secondary H	2.340E+07	1.61	-0.146	24
tertiary H	5.730E+10	0.51	0.27	24
HO_2				
primary H	3.330E+03	2.55	64.85	24
secondary H	7.400E+03	2.60	58.20	24
tertiary H	3.610E+03	2.55	44.07	24
b. H abstraction at H-C-O position				
OH				
secondary H	9.500E+07	1.61	-0.146	24
tertiary H	8.840E+09	1.00	-0.623	24
HO_2				
secondary H	3.000E+04	2.60	58.20	24
tertiary H	1.080E+04	2.55	44.07	24
Hydroperoxy cyclic ether reactions				
3.2.21 Decomposition of hydroperoxy cyclic ethers	7.000E+14	0.00	175.7	18
Aldehyde and ketone reactions				
3.2.22 Abstraction of H atoms from aldehydes or ketones				
a. aldehydes				
OH				
primary H	1.757E+09	0.97	6.636	77
secondary H	2.335E+07	1.61	-0.146	77
tertiary H	1.684E+12	0.00	-3.268	77
H-C=O position	2.690E+10	0.76	-1.423	77

Reaction rules	*k*			Ref.
HO_2				
primary H	9.200E+03	2.55	68.95	77
secondary H	7.375E+03	2.60	58.20	77
tertiary H	8.000E+10	0.00	49.87	77
H-C=O position	2.800E+12	0.00	56.9	77
CH_3O_2				
primary H	2.010E+12	0.00	81.09	77
secondary H	9.950E+11	0.00	71.34	77
tertiary H	3.610E+03	2.55	33.61	77
H-C=O position	1.000E+12	0.00	39.75	77
O_2				
H-C=O position	2.000E+13	0.50	176.6	77
H				
H-C=O position	4.000E+13	0.00	17.57	77
O				
H-C=O position	5.000E+12	0.00	7.489	77
CH_3				
H-C=O position	1.700E+12	0.00	35.31	77
CH_3O				
H-C=O position	1.150E+11	0.00	5.356	77
b. ketones				
OH				
primary H	6.883E+06	1.73	3.151	77
primary H-C-C=O	1.700E+11	0.00	4.987	77
secondary H	1.808E+07	1.64	-1.033	77
secondary H-C-C=O	4.225E+11	0.00	-0.954	77
tertiary H	5.730E+10	0.51	0.264	77
tertiary H-C-C=O	1.684E+12	0.00	-3.268	77
HO_2				
primary H	7.933E+03	2.55	68.99	77
primary H-C-C=O	7.933E+03	2.55	61.46	77
secondary H	2.800E+12	0.00	74.06	77
secondary H-C-C=O	1.000E+11	0.00	36.39	77
tertiary H	2.800E+12	0.00	66.94	77
tertiary H-C-C=O	8.000E+10	0.00	49.87	77
CH_3O_2				
primary H	1.003E+12	0.00	81.09	77
primary H-C-C=O	1.003E+12	0.00	73.55	77
secondary H	9.950E+11	0.00	71.33	77
secondary H-C-C=O	1.000E+12	0.00	63.81	77
tertiary H	3.610E+03	2.55	44.06	77
tertiary H-C-C=O	3.610E+03	2.55	33.61	77

Reaction rules	*k*			Ref.
Ketyl radical reactions				
3.2.23 Decomposition of ketyl radicals				
a. to produce CO	1.580E+13	0.00	72.0	77
b. to produce alkenal/alkenon	2.000E+13	0.00	57.4	77
c. to produce small ketyl radical or alkenal/alkenon	3.700E+13	0.00	120	77

Appendix 2

MOLEC USER'S MANUAL

MOLEC: A Program for the Generation of Chemical Reaction Equations

This document is the user's manual for the MOLEC package. MOLEC is a software package to generate chemical reaction equations. These equations are used for modelling and simulating a chemical combustion process. Starting from elementary reaction rules between hydrocarbon molecules and radicals, and from an initial mixture of species, the decompositions and rearrangements are automatically evaluated in order to generate new species with their equations. The method is based on a representation of molecules as binary trees (using the abilities of the programming language LISP), and on pattern matching. It has been developed in a cooperation of the Konrad-Zuse-Zentrum and the group of Prof. Warnatz.

M. Nehse and J. Warnatz
Interdisziplinäres Zentrum für Wissenschaftliches Rechnen (IWR),
Universität Heidelberg, Im Neuenheimer Feld 368, D-69120 Heidelberg

C. Chevalier and P. Louessard
Institut für technische Verbrennung (ITV),
Universität Stuttgart, Pfaffenwaldring 12, D-70569 Stuttgart

H. Melenk
Konrad-Zuse-Zentrum für Informationstechnik Berlin (ZIB),
Takustr. 7, D-14195 Berlin

Contents

1 Introduction

In the last decade numerical modelling has rapidly become an essential part of many combustion research and development programs, and there has been an accelerating evolution from the use of single-step empirical representations to the use of lumped (overall) multistep models, and finally to the inclusion of full detailed chemical kinetic mechanisms to better simulate chemistry interactions. The chemical reactions converting fuel to combustion products are complex, because the directly observed phenomena of flame propagation, explosions, cool flames, critical fuel/oxidizer ratio, and so forth depend in subtle ways on the conditions under which combustion takes place. Detailed reaction schemes of higher hydrocarbons (components of commercial fuels) describing such phenomena typically involve several hundred chemical species taking part in thousands of elementary reactions. Nevertheless, only a very limited number of different reaction types appear. The most important reaction types of the mechanism of hydrocarbons are [6, 10, 11]

- decomposition of hydrocarbons (e.g. alkanes, alkenes),
- H-atom abstraction by small reactive species (O, OH, H, HO_2, CH_3),
- β-scission of radicals,
- internal H-atom abstraction,
- addition of molecular oxygen,
- O-O bond scission.

The rate coefficients of these reactions for hydrocarbons with more than four carbon atoms can be classified. They depend on [6, 10, 11]

- the radical abstracting a H-atom from an alkane or alkene (O, OH, H, HO_2, CH_3),
- the type of the H-atom being abstracted (primary, secondary or tertiary),
- the number of available equivalent H-atoms,
- the size of the intermediate ring structure (5-, 6-, 7- or 8-members).

It is possible to formulate these reactions and their rate expressions using simple rules. There are two compelling reasons for the development of automatic generation procedures of large kinetic schemes, namely (a) that manual routes are exceedingly laborious and prone to many errors, and (b) that it is a logical, symbolic transformation that is readily achieved algorithmically.
Starting from elementary reaction rules between hydrocarbon molecules and radicals, and from an initial mixture of species, the decompositions and rearrangements are automatically evaluated generating new species with their equations. As mentioned, the code considers only the decomposition of carbon chains larger than C_4, due to the fact that the reaction mechanism for the C_1 to C_4 hydrocarbons already exists [5] and the rate coefficients of the small species strongly depend on the chain length. The method of the

MOLEC program is based on a representation of molecules as binary trees (using the facilities of the programming language LISP) and on pattern matching.
The first section of this report describes the details of the chemical reaction equation building in this program. The next section presents the structure of the MOLEC program and its important parts. Afterwards, it is explained how to use the program itself and which keyword inputs are needed to define a special problem.

2 Details of Chemical Reaction Equations

The combustion reactions can be described at the molecular level by giving the elementary reactions that comprise the combustion mechanism of the fuel of interest. Elementary reactions are described by writing chemical symbols for the reactants and the products connected by an > (irreversible reaction) or = (reversible reaction):

$$\mathrm{A} + \mathrm{B} > \mathrm{C} + \mathrm{D} \quad \text{or} \quad \mathrm{A} + \mathrm{B} = \mathrm{C} + \mathrm{D}\,. \tag{2.1}$$

To determine how fast elementary reactions proceed one has to define the rate r of a chemical reaction as the derivative of the concentration of a product species with respect to time due to the reactions involved. A mass action rate law connects the rate of reaction to the reactant concentrations. Thus, for the H + O_2 > OH + O elementary reaction we have

$$\text{forward rate} = k_f[\mathrm{H}][\mathrm{O}_2]\,, \tag{2.2}$$
$$\text{reverse rate} = k_r[\mathrm{OH}][\mathrm{O}]\,, \tag{2.3}$$
$$r = k_f[\mathrm{H}][\mathrm{O}_2] - k_r[\mathrm{OH}][\mathrm{O}]\,, \tag{2.4}$$

where the proportionality constants k_f and k_r are called the rate coefficients in forward and reverse directions and the brackets are used to denote concentrations. For gas-phase reactions, the latter may be expressed in mol/cm^3 units, with the rate coefficients then having (cm^3/mol)$^{n-1}$s^{-1} units depending on the reaction order n. The rate coefficients are mostly a function of temperature and sometimes also of pressure. It is a common – and largely justified – practice to express the temperature dependence of the rate coefficient in the modified Arrhenius form

$$k = AT^{\beta} \exp\left(-\frac{E_\mathrm{a}}{RT}\right)\,, \tag{2.5}$$

where A denotes the preexponential factor, β the dimensionless temperature exponent, E_a the activation energy, and R the molar gas constant (8.314 J/(K·mol)). The three parameters A, β, and E_a are input values to describe a chemical reaction. They can be taken from experimental measurements, theoretical computations [2, 3, 8, 1] or estimated with the help of group additiv methods [4]. In this program, the rate coefficients are expressed as shown in equation (2.5).

3 Program Structure

For the implementation of rule-oriented programming, techniques from several areas of computer science are used, mainly from artificial intelligence (rule paradigm, tree technique) and computer algebra (canonical form technique). LISP is used as support system, as here the best flexibility regarding the data structure, the algorithm development and the user interface design is available. One problem to be considered is a unique representation of the molecules considered to allow unambiguous identification of equal ones and distinction of different ones. A second problem is the representation of rules describing the reaction types occurring. A third point is the production of a computer code which generates a reaction mechanism by recursive methods, taking into account reactions of products, generated on level n, in a level $n + 1$.
Details are reported in the following subsection. First, the organization of the program is presented. Afterwards the representation of species, the representation of rules and the generation of reaction mechanism is described.

3.1 Organization of this Program

For the program system two layers has to be distinguished:

- the basic layer includes the support of molecule representation, pattern matching, interference engine, end-user language (rules format ect.) and
- the application layer includes the rules modelling a specific area of investigation.

The modules and their special functions are described in the Table 3.1. To make changes in the algorithmic part and execution part, one should be familiar with LISP internals. Only the routines of the last group have to be modified according to changing tasks of the program. The last three files can be modified by the user without in-depth knowledge of LISP. Be careful with the brackets ("unexpected EOF" hints to unpaired brackets). After each change, a compilation of the respective module has to be done (see Chapter 4.3). How to make changes and which key functions can be used is presented in the following sections.

3.2 Representation of Species

To generate chemical reactions it is nessary to specify the initial composition of species, identify the structure of species and their properties, make easy decompositions and rearrangements and get a output which can be used for numerical modelling of combustion processes. Therefore, tools have been developed to read chemical species, get information about their structure and properties and print species in chemical reaction. The input of species is done by 2-dimensional drawings – the usual way to define chemical structures in chemistry. This presentation is not efficient for the determination of species properties, rearrangements and output in reaction mechanisms. Thus, for the internal use we take the canonically sorted tree. This allows a completley unique representation of species and

function	file	description
control of execution	*molmain*	driver program (inference machine), i/o handling
algorithmic part	*molcons*	selectors, constructors and other special algorithms for keeping the molecules in internal (canonical) graph-structure
	molpatt	pattern matcher and 2d input of structural formular
	moltree	graphical printing of struture trees (a 2 dimensional plot is converted into a molecule tree)
	molcyk	graphical printing of struture trees (cyclic molecules are represented as binary tree)
	molnomen	nomenclature related stuff; support of generic names of molecules
	molread	convert a molecule from an input list
	patch	patch for IRIS floating point arithmetic
	hash	data bases with hash coded retrieval
chemical knowledge	*molpreds*	elementary routines for checking of properties of molecules or parts of them; counting of atoms and bonds
	mstdnames	list of molecules known to the program by name and structure (used in output instead of internal names)
	*molrules**	sets of rules used for generation of mechanisms
	molrates	rates to be applied to generated reactions

Table 3.1: Modules of MOLEC

an easy description of rearrangements of them. But for the output of the complete reaction mechanism it would be better to convert the canonically tree representation through names. Here an internal nomenclature exists and short names for special species are being used. Details will be presented in the next subsections.

3.2.1 Input of Species

The input of species is done by 2-dimensional plots being used normally in chemistry to denote the chemical structure of species. As examples here the 2-dimensional plots of isobutane and methyl radical are shown:

```
                                    "      H       "
"      C      "                     "      |       "
"      |      "          or         "    H-C-@     "   .
"    C-C-C    "                     "      |       "
                                    "      H       "
   isobutane                       methyl radical
```

You can specify the molecule with all links or omit the H atoms as shown for isobutane. Missing links are filled by H atoms automatically. Atoms are presented by there symbols

(C, H, O, N), radicals by @, single bonds by — or | (vertical) and double bonds through = or : (vertical). Also cyclic species can be denoted. Tetrahydrofuran can be expressed as follows:

```
"   C-----C   "
"   |     |   "    tetrahydrofuran
"   C--C--O   " .
```

This form of input can be used as long as no atom has a valence higher than four, and it has the advantage that it is easily understood by a human reader.

3.2.2 Mapping Molecules to Trees

In chemistry, the atomic structure of a molecule usually is represented as a graph where the atoms are the nodes and the arcs represent the molecular linkage structure, e.g. pentane:

```
      H  H  H  H  H
      |  |  |  |  |
   H--C--C--C--C--C--H
      |  |  |  |  |
      H  H  H  H  H
```

This representation is not unique; there is a certain freedom for the arrangent of the atoms, and the above form emphasizes the linear chain of carbon atoms.
It is a quasi-natural approach, to use a linked structure as an internal data model for an information system processing molecular structures, too. There are several possibilities to do that mapping. In the current approach, a tree representation is selected. The tree is a well-established structure in information processing, and various techniques for the manipualtion of trees are known, e.g., in the areas of artificial intelligence and in computer algebra. So we can adopt concepts developed there for the manipulation of molecular structures. Among these are the canonical normal form and the pattern matching technique.
A molecule (more exact: the linkage structure of a molecule type) is represented by a molecular tree ("MT"). The MT is defined by a set of recursive axioms:

(MT0) An atom is an element from the list H, O, C, N,...

(MT1) A MT is an atom together with zero or more links to other MTs (subtrees).

(MT2) Each link (l) has a label (n) which represents the valence of the link; standard links are labelled by "1", double bounds by "2" etc. The label "1" is the default and so omitted in external representations (see Fig. 3.1).

The uppermost element in a tree is called the root; each link to a subtree is a branch. The recursive definition of the MT at the same time shows, how these objects are handled. The two basic operations are

- combination: make a MT out of an atom and 0 to n sub MTs,
- decomposition: split a MT into the atom and the subtrees.

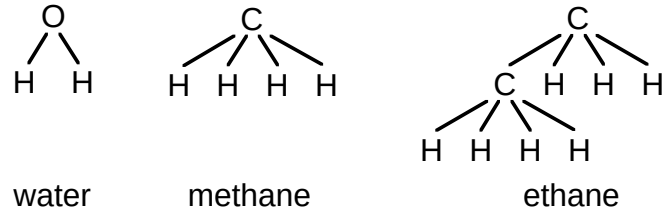

Figure 3.1: Example of molecular tree representations

For the processing it is extremely important to recognize, if two structures from different origin are chemically identical or not. It is well known in computer science, that the ability to decide on the "equivalence" of two structures by an algorithm is equivalent to the existence of a canonical normal form operator ("CN") for the concept of equivalence. This operator has the property that two objects a and b are only "equivalent", if CN(a) is equal to CN(b), while for all non-equivalent pairs the corresponding values are different. Up to now we have two choices when constructing a MT: the selection of the root and the ordering of the branches to each node. These have to be fixed in order to get a CN. First we introduce an ordering for the MTs and their components, denoted by ">>" and defined by the recursive axioms:

(L1) For atoms a_1,a_2: $a_1 >> a_2$ if $\mathrm{mass}(a_1) > \mathrm{mass}(a_2)$.

(L2) For links to subtrees $l_1=(n_1,MT_1)$, $l_2=(n_2,MT_2)$
$l_1 >> l_2$ if $n_1 < n_2$
or $n_1 = n_2$ and $MT_1 >> MT_2$.

(L3) For trees $MT_1=(a_1,l_{11},l_{12},...)$, $MT_2=(a_2,l_{21},l_{22},...)$:
$MT_1 >> MT_2$ if $a_1 >> a_2$
or $a_1=a_2$ and $l_{11} >> l_{21}$
or $l_{11} = l_{21}$ and $l_{12} >> l_{22}$
or ...

e.g. C >> H :

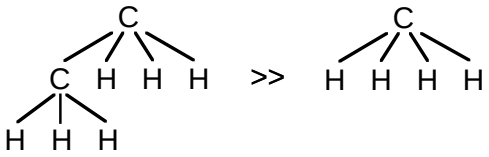

and we complete the definition of the MT by

(MT3) At each node the links are ordered "descending" by ">>".

In algebraic terms, the order given by (L1)-(L3) is a complete one. It is a "lexicographical" one due to the following properties:

- It is based on an elementary comparison (lexicon: the alphabetic order of letters; here: atomic weight, linkage valence),
- it proceeds "from left to right",
- the first structural difference found gives the final decision already.

With the MT we still are completely free to select an arbitrary atom of a molecule as a root. If the root is selected, the rest of the tree is fixed; there are no two trees with different shapes starting from the same atom. Furthermore, if two atoms in a molecule are chemically equivalent (e.g. the H-atoms in a methyl branch), the trees with them as roots will be equal too. So we need only one more step to define the CN operator:

(MT4) A MT for a molecule m is normal,

- if its root atom is the heaviest one in the molecule,
- if there is more than one atom with that property, that atom among with the "largest" MT wrt ">>"is selected.

The algorithm for calculating the normal form of a given MT is simple and effective:

- select the heaviest element,
- create all possible trees with atoms from that element as a root,
- sort them wrt ">>",
- choose the biggest one.

At first, this normal form definitions seem to be a bit arbitrary. But at least for the hydrocarbons, it is closely related to the "usual view". An example of a MT is shown in Fig. 3.2. There the central C chain systematically appears as the leftmost path down in the tree. It is obvious, that the rightmost C in the molecule generates the same MT; so does the C in the methyl appendix; and the central C as root generates a "smaller" MT because its leftmost branch has only 1 C element.

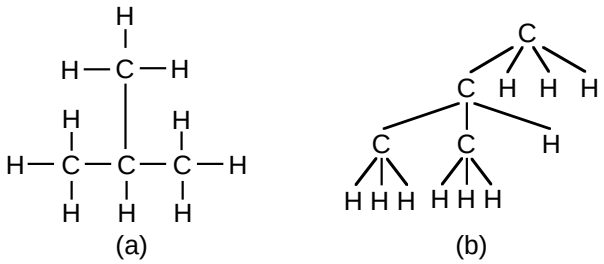

Figure 3.2: Representation of isobutane: a) molecular structure, b) unnormalized tree.

Normalized vs. Unormalized Trees Axioms MT0 - MT3 together with L1 - L3 are the complete definition of the MT, while MT4 defines the property "normal" for a MT. The normal form CF(m) of a given molecule m has the primary purpose of comparing m with other molecules and to find equivalent ones. For the computation, unnormalized representations will be used too. It is an advantage of the tree representation, that it is easy to rearrange a tree for other root elements. So the "interesting" part of the molecule becomes the root, and it can be decomposed immediately.

E.g., if we are interested to see a C-atom which has only one H attached, we simply invert the left link of the root in

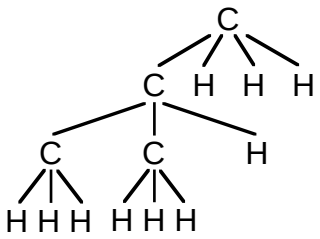

to receive

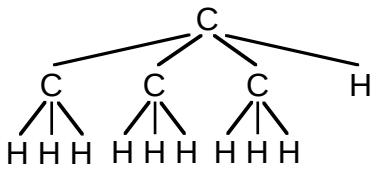

.

Note that for that rearrangement only two links have to be modified. This rearrangement plays an important part of the manipulation of molecules: If a molecule is investigated for a given property, it is rearranged so that the structures playing a role in that property are situated near to the root. So the interesting part of the molecule is quasi focussed for the operation.

3.2.3 Representation of Radicals

In saturated molecules, for each atom in the MT the number of incoming and outgoing links is equal to the valence (more exact: the number of link labels). Looking at radicals, we have to deal with unsaturated links. One way would be to simply omit them. However, we have selected another approach:

- MT(5) A radical position in a molecule is represented as a link to an artificial atom "@" with valence 1 and mass 0.

There are several reasons for this choice:

- Now all molecules are formally saturated and therefore the number of links must correspond to the valence; this allows a dynamic data control and prevents the construction of meaningless objects by programming errors.
- The "<<" alorithm has not to be changed in the case of unsaturated links.
- There is a simple classification: A molecule is a radical only if the element @ is present.
- It is possible to select the "@" as root of a MT for the radical; so the most interesting chemical portion of the molecule can be selected as center of representation.

Of course, the last statement is most important.

3.2.4 Representation of Cyclic Species

Cyclic molecules are represented as binary tree (as usual), where special "labels" represent the closed loops:

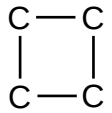

will be represented as

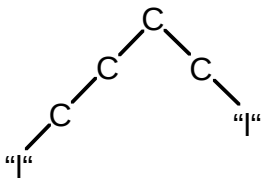

,

where "l" (label) represents the link. If a graph is reformed for processing, every time the result is re-balanced such that the label is as far away from the root as possible such that during pattern matching for local properties the cyclic structure is invisible. Multiple cycles are supported by different labels. Here we take the advantage of the difference between EQUALity and EQality in LISP: All labels are coded as string "l", such that two congurent graphs are EQUAL in LISP sense, but each closed loop has its own instance of the string "l" (a copy) such that only fitting labels are identical (EQ in LISP). For external printing, the labels are renamed by lower case characters.

3.2.5 Algorithmic Nomenclature for Arbitary Molecules

To print a chemical reaction mechanism, it is better to give a name to each species presented by trees. Therefore, we define the following rules to make a unique nomenclature:

- The molecule is ordered canonically: The heaviest atom is the root of the structure.
- A chain is given by the name of the central atom(s), followed by a repetition number, (if >1).
- The subchains follow the chain, each in brackets; in the bracket the leading numbers denominate the number of the atom where the chain is attached to; the rest is represented as a chain, which can have subchains itself.
- Radical positions are denoted by the "artificial atom" @, which is treated as an ordinary atom with lowest mass.
- H atoms are generally omitted with the only exception that pure H molecules are denoted explicitly as H and H_2.
- A double link is represented as a special connection to a subchain, where a "=" preceeds the subchain name.

Examples:

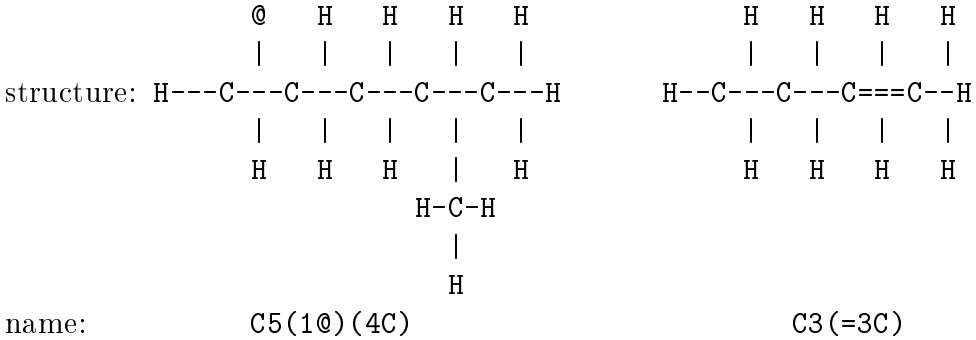

Note, that in contrast to IUPAC notation rules

- the lexicographical order, which is the basis for the canonical representation, tends to place "heavy" branches in the "right" portion of the molecule graph,
- a "parallel" chain will be viewed as two separate branches.

As example, the molecule

```
C--C--C--C--C--C--C--C--C     will be      C--C--C--C--C--C--C--C--C
            |                  represented                 |
         C--C--C               internally as               C--C
                                                              |
                                                              C
```

which generates a name nested twice: `C9(5C2(1C))`.

3.2.6 External Representation of Species

The writing of chemical reaction mechanisms with MT is unusual and hard to understand. Therefore, a special name would be desired for each species. This relationship has to be a unique representation and, if possible, easy to understand by the user. The algorihmic nomenclature presented in the last subsection 3.2.5 is one possibility. But the best way for easy understanding of the mechanism would be to use short names. We orientate our nomenclature to the computation programs used to simulate special combustion problems like HOMREA [7] or MIXFLA [9]. There the name of the species is limited to 8 characters without any blanks in it. For the task to develop a transformation of the algorithmic nomenclature to small names, three features are possible:

(1) Define a special name for a species giving in a 2-dimensional form (in file *mstdnames*),

(2) define special name through an internal transformation of an algorithmic nomenclature for a group of species (in file *molnomen*), or

(3) use a variable (Z1,Z2,...), which represents a special algorithmic nomenclature in this case.

Preference is given to (1) and (2), whereas (3) is only used, if no other denomination is found. The first method defines a name for a graphically drawing of the species, e.g.,

```
(molname IC4H10    "  C--C--C "
                   "     |    "
                   "     C    " )  .
```

`molname` is the name of this function, and the whole definition has to be in brackets. The structure of this function is `(molname <short name> <graphically structure>)`. All such transformations are summarised in the file *mstdnames*.
The second method makes a conversion of the algorithmic nomenclature to a short name. For example here the conversion of alcanes is shown:

```
(setq namepatterns* '(
   ( C                      T   `(C H 4))
   ( (C &x)                 T   `(C ,&x H ,(plus (times 2 &x) 2))) )).
```

All characters beginning with `&` are variables, whose values can be any positive number. This transformation is efficient and time-saving, due to the conversion of a group of species like here all alcanes. The definitions can be seen in the module *molnomen*. If for one species a both transformations (1) and (2) are defined, the first one will have the priority. The last method (3) is only used if the two mentioned before give no result. For these species the names are `Z1`,`Z2`,...,`Zn`. In the ouput of the mechanism is a list of the transformations:

```
----    Z1  represents  C5(=1C2)(4@)
----    Z2  represents  C5(=1C2)(3@)
----   .... represents  ...
```

3.3 Pattern Matching

When mechanisms of reactions classes are modelled, properties of the reacting molecules have to be described. Besides of properties of a simple enumerating type, e.g. alcane = atoms from C,H and special links, the important properties are described by relations of atoms in the molecular structure, easiest described by patterns for parts of the molecule. E.g.,

```
        H
        |
   <---C--->
        |
        H
```

describes the general pattern for a carbone atom with secondary H atoms "somewhere" in a hydrocarbone. Many reactions are described by this type of prerequisit information. On the other hand, pattern matching is a well known technique in information processing, and so here it is a natural approach to use it as a central tool.
The above pattern has two indefinite parts, the links to the rests of the molecule. When used in a programming environment, these parts are caught by pattern variables, denominated by `&1` to `&9` (so they cannot be mixed with atoms). And, of course, we use the two-dimensional input for the representation of patterns, which here gains its most important benefit. So the above pattern looks like

```
"          H         "
"          |         "
"    &1---C---&2     "
"          |         "
"          H         " .
```

During compilation, a pattern is tranformed into a corresponding MT (the `&1`,..,`&n` ordered below all other elements), with the most discriminating element as root (that will often be the "`@`"). If now a molecule `m` is investigated under this pattern, the following

steps are executed:

- `m` is tested, whether it has at least the atoms which are mentioned explicitly in the pattern (here one C and two H).
- `m` is reordered such that it has the same root element as the pattern; in general, there will be more than one such form. If one form appears more than once in the reordering, all but one are deleted, but the multiplicity is preserved and will be available later in a variable `&n`.
- For each reordering of `m` `&2` is compared with the pattern node by node, branch by branch; explicit atoms and links from the pattern match their identical correspondents in `m`, while the pattern variables match any subtree; it is possible that the match has no result, (the pattern does not fit at all), has a unique result, or that it has more than one result. Multiplicities which arise by simply interchanging the roles of the variables are suppressed automatically.
- Additional explicit restrictions for the pattern variables are evaluated; e.g., one can exclude pure H atoms as values for `&1` and `&2` from the above pattern, because they belong to sites with primary H atoms.
- The match acts as a loop over all positive match results: The dependent part of the program is performed for each match once, where the pattern variables are set to their corresponding values from the match.

These steps can be illustrated by the following simple example (decomposition of a H-atom from a secondary C-atom). The above pattern is applied to propane:

```
          H  H  H
          |  |  |
m  =   H--C--C--C--H
          |  |  |
          H  H  H
```

- (1): `m` has more than one C and two H atoms.
- (2): There are three C atoms as possible roots for compatible trees; two of them (the "outer" ones) generate the same MT. So we get two trees, one (Fig. 3.3a) with multiplicity 2 and one (Fig. 3.3b) with multiplicity 1.
- (3): The matching of pattern and trees is a one-to-one comparsion branchwise:
- (4) In the first match, `&2` is bound to a pure H (Fig. 3.4); so this case will be rejected by the additional test. In the second case, both pattern variables are bound to a methyl group; so this case passes the test and the further processing takes place.
- (5) We generate new molecules with the graph:

```
"          @          "
"          |          "
"    &1---C---&2      "
"          |          "
"          H          "
```

In tree form this is

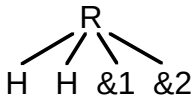

and with the two methyl groups bound to `&1` and `&2` plugged in we get

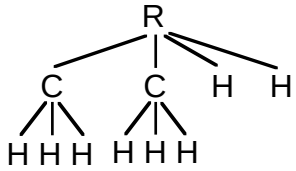

which is a (not yet normalized) MT for propyle

```
   H  @  H
   |  |  |
H--C--C--C--H      .
   |  |  |
   H  H  H
```

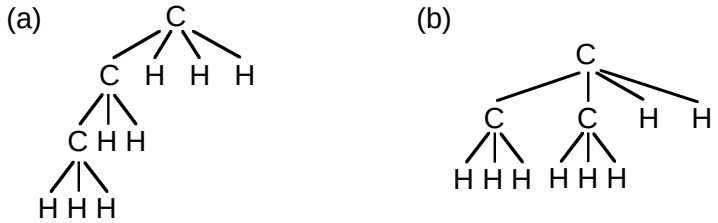

Figure 3.3: Example: (a) multiplicity = 2, (b) multiplicity = 1

Note, that during construction the branches with origin in `@` are reordered automatically, because the replacement is done with the elementary operations decomposition - (replacement) - construction, which is governed by (MT3).
Of course, the pattern matching technique is much more important for more complicated cases. The above example still can be programmed "by hand", which is not so easy for more complicated contexts. As LISP allows to do reasoning on programs, the conversion of the pattern and the generation of the code for the steps (1)-(4) is done automatically during compilation. So the complete source code for the above given procedure is (written in generic LISP style):

```
(mrule secondary_H_abstraction (m)
       (prog (p1 p2)
       (mpmatch ALL m
             "                  *H                    "
             "                   |                    "
             "            &1----C----&2               "
             "                   |                    "
             "                   H                    "

          % none of each a pure H
          (test (not (equal &1 H))(not (equal &2 H)))

          (setq p1 (mpgen     % the alkyl
             "                  @                     "
             "                   |                    "
             "            &1----C----&2               "
             "                   |                    "
             "                   H                    "))
          (setq p2 (H)) )))
```

where `secondary_H_abstraction` is the name of the routine, `m` is the formal parameter, `mpmatch` opens the control structure, `all` tells that all matches should be inspected, the `test` excludes all simple H matches and, `setq p1` and `setq p2` define the products and `mpgen` generate a product through a molecular tree.

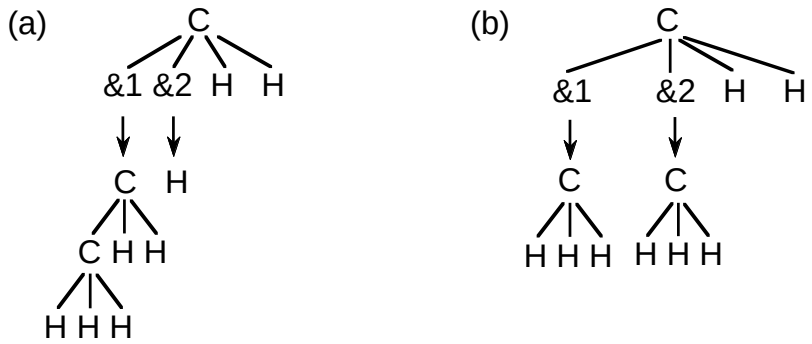

Figure 3.4: Example: (a) multiplicity = 2, (b) multiplicity = 1

3.4 Generation of Elementary Reactions

The pattern matching technique is used to describe the decompositions and rearrangements of species. The rules are described in the following manner: `(rule name (<set of premises>) (<conclusions>) (reaction (<reactants>) (<products>) (<rate coefficients>)))`. Every rule has a name which later will be used for identification. A set of premises is linked by logical conjunctions (`or`, `and`, `not`) to test `m` for certain properties. These tests include the pattern matching as well as test functions like `m` is an alcane. If all tests are positive, the conclusions are activated and the resulting reaction is listed with

its rate coefficients.
Premises are special test functions and pattern. The pattern is already describe in subsection 3.3. Test functions which are defined in the program check, whether the species fulfil the condition. For example, `(alkane? m)` checks, if `m` contains only H- and C-atoms, which are linked with single bonds. In the conclusion mostly patterns of the products are described like `(setq p1 (mgen " &1--@ "))`. At last the reaction with its rate coefficients is stored. The syntax of this command is `(reaction (list <reactants>) (list <products>) (<rate>))`. The keywords `reaction` and `invreaction` specify, whether this reaction is a forward reaction or the reverse reaction. `<reactants>` and `<products>` is a list of all species involved in this reaction. The `<rate>` is described through the three arrhenius parameter (see Section 2). They can be given explicitly as three number `(1.00E+13  0.0  130.0)` or as a function `(rate_radical_abstraction 2 &n rad)` (Fig. 3.5).

```
(reaction (list m rad) (list p1 p2)
          (rate_radical_abstraction 2 &n rad))

(de rate_radical_abstraction(n mult rad)
  % n = index of the H atom (1,2,3)
  % mult =  the multiplicity of the equivalent cases
  % rad = the abstracting radical
  (prog (m)
    (setq m
       (cond ((equal rad H)
              (cdr (assoc n '((1  9.38E6   2 32.2)
                              (2  4.40E6   2 20.9)
                              (3  1.26E14  0 30.6)))))
             ((equal rad OH)
              (cdr (assoc n '((1  1.43E9   1.05 7.58)
                              (2  6.50E8   1.25 2.94)
                              (3  4.00E12  0 1.85)))))
       ))
      (when (null m)(prin2 "##### constants unknown for radical")
                    (print (nomen rad))(setq m '(0 0 0)))
      (return (cons (times mult (car m)) (cdr m)))))
```

Figure 3.5: Function rate_radical_abstraction

`Rate_radical_abstraction` is the name of the function and `2 &n rad` are parameters. `&n` is always the multiplicity. `2` and `rad` are special parameters. In this example, `2` means a H-atom abstraction from a secondary C-atom and `rad` is the radical which gets the H-atom (e.g. OH). Please don't enter numbers with a dot in the beginning or insert a blanc in the number.
An example of a complete generation rule is shown in Fig. 3.6, e.g., an alkyl radical decomposes in β-position to the radical. `Alkyl_decomposition` is the name of the rule. `m` is the formal parameter and `alkyl?` tests, whether `m` is an alkyl. If the tests are positive, `prog` is the entry for the further processing. `remark` is the command which is listed above the reaction in the output. `mpmatch` opens the control structure, `all` tells that all matches should be inspected. `setq p1` and `setq p2` defines the pattern of the resulting products.

Finally, the reaction is stored: the reactants, products and the rate coefficients for this reaction.

```
(mrule alkyl_decomposition (m)
    (when (alkyl? m)
     (prog (p1 p2)

        (remark "alkyl_decomposition: ALKYL BETA SCISSION")

        (mpmatch ALL m
             "            &6 &7 @                    "
             "            |  |  |                    "
             "   &1------C--C--C----&5                "
             "            |  |  |                    "
             "            &8 &9 &4                   "

          (setq p1 (mpgen
            "               &7                      "
            "               |                       "
            "               C==C----&5              "
            "               |  |                    "
            "               &9 &4                   "))

          (setq p2 (mpgen
            "            &6                         "
            "            |                          "
            "   &1------C--@                        "
            "            |                          "
            "            &8                         "))

          (reaction (list m) (list p1 p2)
                    (rate_alkyl_beta_scission
                    (C_order &1 &6 &8) &n (C_sec_order &7 &9)) )
          (invreaction (list p1 p2) (list m)
                       (invrate_alkyl_beta_scission
                       (C_order &1 &6 &8) &n (C_sec_order &7
&9)))
 ))))
```

Figure 3.6: β-decomposition of an alkyl radical

At the moment, the rules act on three semantic levels:

- On the production level, reactions are deduced from new or generated species; a general interface machine activates each production rule for any relevant object or combination of objects exactly once.
- On a reformation level, each new generated species is investigated for necessary reformations; here, e.g., two neighboured radical positions are converted into a double bound.

- Rule `rule1` should be activated only if rule `rule2` did not yet fire. This meta-rule defines a unique sequence of dependency and facilitate sometimes the description. But it creates an additional dependency among the rules, which reduces the flexibiltiy. In generic LISP style this procedure is described through `(precedence 'rule1 'rule2)`.

The description of rule types is done by ordering the rules in lists. The rules on the reformation level contain the list named `bg_rules`. The other rules are sorted in `rs_rules` (list of rules which connect species and radicals) and `s_rules` (list of rules which apply to all species). The special LISP command for this ordering is `(push 'rule1 s_rules)`. If the meta-rules are avoided, every rule can be switched on or off easily.

4 Use of MOLEC

The program can be used interactively as well as in batch. Due to the large volume of output, the batch mode is preferable. In the following subsection the input and output are described. At last, the commands are presented for compiling the module if changes were made.

4.1 Program Input

The shell scripts for execution can be found in */molec/exec*. An example is shown in Fig. 4.1. The command sequence `source pslenv` sets the invirement variables like the directory of binaries `$go/bin`. The command `bare-psl` opens the lisp monitor and `EOF` closes it. All statements between this command must be LISP commands. In LISP, all statements must be fully bracket-balanced (careful counting is strongly recommended). Outside of strings, a single blank or a new line act as separator. Additional blanks and blank lines are permitted. Anything between a `%` and `eol` is interpreted as comment and ignored. First, a file for output is opened: `(wrs (setq file (open "$mech/name.report" 'output)))`. There are statements written which occure during the compilation. The command `(load molmain)` loads the driver program. The report which occurs between the two commands `(on echo)` and `(off echo)` is written on the standard output file. With the command `(setq min_C 5)`, a lower limit for the molecule size is given. Molecules with less than 5 C atoms are discarded from the rule processing. `min_C` is initially set to 4. The set of initial species is defined through two sequences. The initial radical pool is given by `(setq initial_radicals (list H O OH CH3 O2 HO2))` and the fuel by `(setq Testfuel (mpmol " C-C-C-C-C-C-C "))`. The initial radicals are used, e.g., for the H-atom abstraction from an alkane. The structure of the fuel is the same as described in Subsection 3.2. The names of the fuels can include characters and numbers like a,b,c,$\cdots$,z,0,1,2,$\cdots$,9 and -.

If a mixture of fuels should be treated the sequence has to be repeated. The command `(molreset)` clears the used memory and variables and accepts the above named radicals. The inference machine is started for the fuel through the sequence `(addspecies Testfuel)`. All relevant rules are applied for the fuel and the new products. During this process

```
#! /bin/csh
source pslenv         % set-up of enviromental variables
cd $go/bin
bare-psl <<EOF

(wrs (setq file (open "$mech/name.report" 'output)))

(load molmain)
(on echo)
(setq min_C 5)
(output-case 'raise)
(setq initial_radicals (list H O OH CH3 O2 HO2))

(setq Testfuel (mpmol   " C-C-C-C-C-C-C     "))

(molreset)
(addspecies Testfuel)

(off echo)
(printreactions_report)
(wrs nil)
(close file)

(wrs (setq myfile (open "$mech/name.mech" 'output)))
(printreactions_data)
(wrs nil)
(close myfile)

EOF
```

Figure 4.1: Example of a shell script to execute the program

warnings about duplicate reactions and other problems may appear. All these comments are listed in report (`(printreactions_report)`). Additionally, a list of reactions and their arrhenius parameters is printed out. Afterwards the file for the report is closed (`(close file)`). The reaction mechanism which can be used for combustion computations is written in the file *name.mech* (`(wrs (setq myfile (open "$mech/name.mech" 'output))) (printreactions_data) (wrs nil) (close myfile)`). The report and the mechanism are Unix files which are in the directory */genrea/molec/mech*. All above named commands can be also read from a file, especially useful for predefined structures of fuels. The content of these files can be read by `(dskin <filename>)`.
In the directory */genrea/molec/exec* you find two shell scripts: *exec_one* and *exec_two*. The first should be used for the generation of a mechanism for only one fuel. Type the command `exec_one <fuelname> <outputname>` and the execution will start. The `<fuelname>` which is used in this command have to be an Unix file in the directory */genrea/molec/fuels* which includes the structure of the fuel. The output files have the name *<outputname>.mech* and *<outputname>.report*. For fuel mixtures only a second fuels have to define: command `exec_two <fuelname1> <fuelname2> <outputname>`. Additional commands are:

function	description
(ruleon <rulename>)	add this rule to the list which includes all rules for execution
(ruleoff <rulename>)	delete this rule to the list which includes all rules for execution
(off invreactions)	delete all inverse reactions
(on moltrace)	additional information is given during the execution. Should be used for diagnoistics.

4.2 Output of the Reaction Mechanism

For presentation of the mechanism there are two steps: Molecules (of reactants or products) classification and reactions classification. Molecules of products or reactants are classified with respect to increasing numbers of carbon atoms (ex: C1, C2, C3, ...). If the number of the carbon atoms is the same for two or more molecules, the classification is done with respect to the increasing numbers of hydrogen atoms (ex: C, CH, CH_2, CH_3, CH_4, C_2, CH_2, ...). If the number of H atoms is also same for two or more molecules then increasing number of oxygen molecules is considered for classififcation (ex: C, CH, CH_2, CH_3, CH_2OOH, CH_3OO, CH_4, CH_3OOH, ...). According to this classification, the molecules CH_4, CH_3, CH_3OO can be classified as:

```
*****************************
1.       CH3 REACTIONS
*****************************
*****************************
2.       CH3OO REACTIONS
*****************************
*****************************
3.       CH4 REACTIONS
***************************** .
```

For each product or reactant, a list of all the possible reactions of the products alone, or with the smaller species in the mechanism, is reported. The priority order for reactions is: decomposition, radical H-abstraction, internal H-abstraction, β-scission, addition of molecular oxygen, O-O bond homolitic scission. Reactions are written in the following shape: $\text{reactant}_1 + \text{reactant}_2 > \text{product}_1 + \text{product}_2$. Each name of species consist of 8 characters. An example is shown in Fig. 4.2.

4.3 Application of Modification

Normally, reaction mechanisms for different fuels can be generated without any change in the lisp modules. The definition of the structure of a fuel is done separatly, and the rules can switch on and off.
If any change is made in a LISP file (*/genrea/molec/src/*.sl*), a compilation of the respective module has to be done. Type the command `make`, and the preparation of modified binaries will be done automatically. The only environmental variables have to point to (`source pslenv`).

```
!*********************************************************************
!****   1.            C2H5 REACTIONS
!*********************************************************************
!----     - INVERSE: R3 ALKYL BETA SCISSION -
C2H5    +C3H6    >2C5H11                      6.300E+10 0.0       29.3
!*********************************************************************
!****   2.            C3H7 REACTIONS
!*********************************************************************
!----     - INVERSE: R3 ALKYL BETA SCISSION -
N-C3H7  +C2H4    >1C5H11                      6.300E+10 0.0       29.3
!*********************************************************************
!****   3.            C4H8 REACTIONS
!*********************************************************************
!----     - INVERSE: R3 ALKYL BETA SCISSION -
1-C4H8  +CH3     >3C5H11                      6.300E+10 0.0       29.3
!*********************************************************************
!****   4.            C5H11 REACTIONS
!*********************************************************************
!----     - R3 ALKYL BETA SCISSION -
2C5H11  >C2H5    +C3H6                        2.000E+13 0.0       119.6
3C5H11  >1-C4H8  +CH3                         8.000E+13 0.0       138.2
1C5H11  >N-C3H7  +C2H4                        2.000E+13 0.0       119.6
!----     - R4 INTERNAL H ABSTRACTION (izomerization of alkyl radicals) -
2C5H11  >1C5H11                               3.000E+11 0.0       88.2
1C5H11  >2C5H11                               2.000E+11 0.0       75.66
!----     - INVERSE: R2 EXTERNAL H ATOM ABSTRACTION FROM ALKANE -
1C5H11  +HO2     >C5H12   +O2                 1.200E+13 0.0       0.0
3C5H11  +HO2     >C5H12   +O2                 1.000E+13 0.0       0.0
2C5H11  +HO2     >C5H12   +O2                 2.000E+13 0.0       0.0
!*********************************************************************
!****   5.            C5H12 REACTIONS
!*********************************************************************
!----     - R1 ALKANE DECOMPOSITION -
C5H12   >N-C3H7  +C2H5                        3.200E+16 0.0       339.2
!----     - R2 EXTERNAL H ATOM ABSTRACTION FROM ALKANE -
C5H12   +HO2     >1C5H11  +H2O2               1.122E+13 0.0       81.2
C5H12   +HO2     >3C5H11  +H2O2               3.360E+12 0.0       71.2
C5H12   +HO2     >2C5H11  +H2O2               6.720E+12 0.0       71.2
!*********************************************************************
!**** number of equations: 57
!*********************************************************************
END
```

Figure 4.2: Part of the reaction mechanism for n-pentane at high-temperature conditions

References

[1] Allara, D. L. und Shaw, R.: *A Compilation of Kinetic Parameters for the Thermal Degradation of n-Alkane Molecules.* J. Phys. Chem. Ref. Data **9**(3):523–59 (1980).

[2] Baulch, D.L., Cobos, C.J., Cox, R.A., Esser, C., Frank, P., Just, Th., Kerr, J.A., Pilling, M.J., Troe, J., Walker, R.W. und Warnatz, J.: *Evaluated Kinetic Data for Combustion Modelling.* J. Phys. Chem. Ref. Data **21**(3):411–734 (1992).

[3] Baulch, D.L., Cobos, C.J., Cox, R.A., Frank, P., Haymann, G., Just, Th., Kerr, J.A., Murells, T., Pilling, M.J., Troe, J., Walker, R.W. und Warnatz, J.: *Evaluated Kinetic Data for Combustion Modelling Supplement I.* J. Phys. Chem. Ref. Data **23**(6):847–1033 (1994).

[4] Benson, S.W.: *Thermochemical Kinetics.* John Wiley & Sons, New York, 2nd edition, 1976.

[5] Chevalier, C.: *Entwicklung eines detaillierten Reaktionsmechanismus zur Modellierung der Verbrennungsprozesse von Kohlenwasserstoffen bei Hoch- und Niedertemperaturbedingungen.* Dissertation, Universität Stuttgart, 1993.

[6] Chevalier, C., Pitz, W.J., Warnatz, J., Westbrook, C.K. und Melenk, H.: *Hydrocarbon Ignition: Automatic Generatoin of Reaction Mechanisms and Applications to Modeling of Engine Knock.* In: Twenty–Fourth Symposium (International) on Combustion, 93–101, Pittsburgh, 1992. The Combustion Institute.

[7] Maas, U.: *Mathematische Modellierung instationärer Verbrennungsprozesse unter Verwendung detaillierter Reaktionsmechanismen.* Dissertation, Universität Heidelberg, 1988.

[8] Mallard, W.G., Westley, F., Herron, J.T., Hampson, R.F. und Frizzell, D.H.: *NIST Chemical Kinetic Database: Version 6.0.* National Institute of Standards and Technology, Gaithersburg, MD, 1994.

[9] Warnatz, J.: *Berechnung der Flammengeschwindigkeit und der Struktur von laminaren flachen Flammen.* Habilitationsschrift, Universität Darmstadt, 1977.

[10] Warnatz, J.: *Resolution of Gas Phase and Surface Combustion Chemistry into Elementary Reactions.* In: Twenty–Fourth Symposium (International) on Combustion, 553–579, Pittsburgh, 1992. The Combustion Institute.

[11] Westbrook, C.K., Warnatz, J. und Pitz, W.J.: *A Detailed Chemical Kinetic Reaction Mechanism for the Oxidation of iso–Octane and n–Heptane over an Extended Temperature Range and Its Application to Analysis of Engine Knock.* In: Twenty–Second Symposium (International) on Combustion, 893–901, Pittsburgh, 1988. The Combustion Institute.